WARWICK
THE UNIVERSITY OF WARWICK

Engineering a synthetic gut model to explore microbial infections

by

Jack Hassall

Doctoral Thesis

Submitted to the University of Warwick

for the degree of

Doctor of Philosophy

Supervisor: Dr Meera Unnikrishnan

Synthetic Biology Centre for Doctoral Training

School of Life Sciences

University of Warwick

Submitted: Sept 2019

EPSRC Engineering and Physical Sciences Research Council
BBSRC bioscience for the future
University of BRISTOL
UNIVERSITY OF OXFORD
WARWICK THE UNIVERSITY OF WARWICK

SYNBIO CDT
EPSRC & BBSRC Centre for Doctoral Training in Synthetic Biology

Table of Contents

i. List of figures

ii. List of Tables

iii. Acknowledgements

Firstly, I would like to thank my supervisor Dr Meera Unnikrishnan, for being a fantastic mentor and teacher. Throughout my PhD journey, her advice and support were invaluable.

I would like to show my heartiest gratitude to Dr Arnaud Kengmo Tchoupa and Dr Blessing Anonye for their help and expertise in the lab, and for ensuring not a single day went by without laughter. I wish to thank my advisory panel, Dr Yin Chen and Dr Marco Polin, for their expert advice on my project. A special thanks goes to Kate Watkins for her keen interest, endless help and support, from troubleshooting experiments to presentation feedback, she always offered kind and supportive feedback.

Finally, I would like to thank my parents for their continued generosity and support. Mum, thank you for taking the time and patience to teach me how to read, I don't think any of this would have been possible without you.

iv. Declaration

This thesis is submitted to the University of Warwick in support of my application for the degree of Doctor of Philosophy. It has been composed by myself and has not been submitted in any previous application for any Degree.

The work presented (including data generated and data analysis) was carried out by the author.

Signed: 

Date: 3/3/2020

v. Summary

Our intestines are home to over one thousand bacterial species, often referred to as the gut microbiota. This microbiota is profoundly beneficial to our bodies, with disturbances to this community associated with pathogenic infection and diseases such as diabetes, obesity and inflammatory bowel disease. In this project we aimed to engineer a representative microbiota, with an emphasis on tracking individual species. Utilising propidium monoazide (PMA)-qPCR, we were able to track the nine individual species of our representative gut microbiota within a mixed biofilm setup for 72 hours. *Clostridioides difficile* is an opportunistic pathogen, which targets the gut during times of microbiota dysbiosis. We have used our tracking technology to see how a representative microbiota reacts to a *C. difficile* invasion. We found that the representative gut microbiota could inhibit *C. difficile* colonisation, with a pre-established microbiota biofilm creating the most significant effect. Given the strong links between antibiotic-associated microbiota disturbance and the increased risk of *C. difficile* infection, we tested the impact of vancomycin treatment on the nine species mix. Surprisingly, we found that the microbiota in biofilm conditions could withstand high doses of vancomycin (20 μg/ml).

We developed a gut epithelial model, the E-VDC, that supports the growth of strictly anaerobic bacteria. We used this model to investigate *C. difficile* infections in the presence of the gut commensal, *Bacteroides dorei*. In dual biofilm conditions, we found *B. dorei* to have an inhibitory effect on *C. difficile*. This effect carries over into the adherent community within our gut model, however we found the inhibition was less pronounced. To investigate how *B. dorei* was inhibiting *C. difficile* we performed mass-spectrometry based proteomics. A total of 39 proteins were found to be differentially expressed between single and cocultures of *C. difficile* and *B. dorei*. For *C. difficile* we found that the majority of the proteins affected by the presence of *B. dorei* were stress related. Interestingly, when with *B. dorei*, *C. difficile* was producing more of the protein HpdB, an enzyme needed for the production of p-cresol a highly bacteriostatic compound thought to influence the gut microbiota.

vi. List of Abbreviations

ABC	Ammonium bicarbonate
AI-2	Autoinducer-2
AMPs	antimicrobial peptides
ANOVA	Analysis of variance
AP-1	Activator protein 1
ASD	Autism spectrum disorder
BHI	Brain-heart infusion
BHIS	Brain-heart infusion supplemented with yeast and l-cysteine
BLAST	Basic local alignment search tool
bp	base pair
BSH	Bile salt hydrolase
CAA	2-chloroacetamide
CDAD	Clostridioides difficile associated disease
CDI	*C. difficile* infection
CFU	Colony forming unit
Ct	Cycle threshold
CTAB	Cetyl Trimethyl Ammonium Bromide
CVB1	Coxsackievirus B1
DCA	Deoxycholic acid
DMEM	Dulbecco's Modified Eagle's Medium
DMEM-10	Dulbecco's Modified Eagle's Medium with 10% fetal bovine serum
DNA	Deoxyribonucleic acid
E-VDC	Epithelial Vertical Diffusion chamber
ECM	Extracellular matrix
ELISA	Enzyme-linked immunosorbent assay
FBS	Fetal bovine serum
FDA	Food and Drug Administration
FMT	Faecal microbiota transplants
GI	Gastrointestinal

G_{Length}	Genome length
HDPs	Host defense peptides
HuMiX	Human–microbial crosstalk
IBD	Inflammatory bowel disease
IBS	Irritable bowel syndrome
KEGG	Kyoto Encyclopedia of Genes and Genomes
LCA	Lithocholic acid
M-VDC	Multilayered Vertical diffusion chamber
M_{DNA}	Starting mass of DNA
MIC	Minimum inhibitory concentration
N_A	Avogadro's number
OD	Optical density
OOC	Organ-on-a-chip
PBS	Phosphate-buffered saline
PCA	Principal component analyses
PCI	Phenol chloroform:isoamyl alcohol
PET	Polyethylene terephthalate
PMA	Propidium Monoazide
PPI	proton pump inhibitors
qPCR	Quantitative polymerase chain reaction
RPM	Rotations per minute
SAB	Schaedler anaerobe broth
SAB+	Schaedler anaerobe broth with l-cysteine and vitamin k
SCFA	Short-chain fatty acids
SDS	Sodium dodecyl sulfate
SHIME	Simulator of the Human Intestinal Microbial Ecosystem
TCEP	Tris(2-carboxyethyl)phosphine
TEER	Transepithelial electrical resistance
TFA	Trifluoroacetic acid
VDC	Vertical Diffusion chamber
W_{Base}	Average weight of 1M nucleotides

1 Introduction

1.1 Microbiota

Our bodies are not solely made up of human cells, we play host to an extraordinary microbial ecosystem made up of vast numbers of bacteria, fungi, archaea and viruses (Proctor, 2011; Morgan and Huttenhower, 2012). An ecological community of microorganisms that survive off a multicellular organism is referred to as a 'microbiota' (Rosenberg and Zilber-Rosenberg 2016). These microbiota communities greatly influence their host (Hacquard *et al.,* 2015; McFall-Ngai, 1999; Li *et al.,* 2016a; Jandhyala, 2015; Yissachar *et al.,* 2017; Chung *et al.,* 2012; Li *et al.,* 2016b), with individual microorganisms interacting with their host in a variety of ways; commensal, symbiotic and pathogenic (Lukeš *et al.,* 2015). Our skin, gut, lungs, genital tract, nasal and oral cavities are all home to distinct microbiotas (Opazo *et al.*, 2018), which appear to be essential for body functions.

A commensal bacterial-host interaction is a positive relationship during which either the microbe or the host gains advantage without providing benefit or harm to the other (Hooper and Gordon, 2001; Sousa *et al.,* 2017). This dynamic often works in favour of the microbe, for example, the microbe could take an unused biproduct from the host and absorb it as a nutrient. In rare cases, a commensal interaction refers to a neutral relationship, where neither experience a gain or loss (Lukeš *et al.,* 2015). However, it can be argued that with further study a net positive or negative would be found. A symbiotic interaction is a similar positive relationship but where both the host and microbe benefit, the classical example being the *Euprymna scolopes* and *Vibrio fischeri* (McFall-Ngai, 1999; Thompson *et al.,* 2017; Bongrand *et al.,* 2016). The Hawian Bobtail Squid (*E. scolopes*) is a nocturnal feeder that uses bioluminescence, provided by *V. fischeri,* to hide itself. When moonlight hits a *V. fischeri* deficient squid, it casts a silhouette into the water below, revealing its location to any predators beneath. The bioluminescence of the bacteria counteracts this by matching the intensity of the moonlight enabling the squid to cancel out its silhouette. In return for providing this life-saving

bioluminescence, the squid provides both a habitat for *V. fischeri*, as well as a sugar and amino acid feed solution (McFall-Ngai, 1999). The final type of relationship is parasitic which involves a negative interaction. Parasites take host resources in a detrimental fashion which ensures the host gains no benefit from housing the microorganism. In the worst cases these relationships are pathogenic, either because of severity or the chronic nature of the infection.

The species present in a microbiota not only interact with the host, but amongst themselves (Lustri *et al.,* 2017; Longford *et al.,* 2019). These interactions are poorly studied but are speculated to have an impact on the makeup of the microbiota, especially in the context of invading species attempting to colonise (Rolhion and Chassaing, 2016). Imbalances and shifts in the makeup of a microbiota can have detrimental effects on the host, for example, the gut microbiota in humans when disturbed can have a major influence on; chronic gastrointestinal diseases (irritable bowel syndrome (IBS) & inflammatory bowel disease (IBD)) (Guinane and Cotter, 2013; Harris and Chang, 2018) and systemic metabolic diseases (diabetes & obesity) (Qin *et al.,* 2012; devi Devaraj *et al.,* 2013; Tremaroli and Bäckhed, 2012; Haro *et al.,* 2016; Marchesi *et al.,* 2016).

1.2 Gut microbiota

The human gut, or gastrointestinal tract (GI tract) is the collection of organs leading from the mouth to the anus. Each region of the GI tract is home to its own microbiota, each containing a remarkably different species composition (Donaldson *et al.,* 2015; Hacquard *et al.,* 2015). The differing environmental conditions of the GI tract have a large impact on the makeup of the microbiota. The pH of early gut regions is far more acidic, compared to that of the hindgut (specifically large intestine), where the pH is relatively neutral (Ridlon *et al.,* 2014; Booijink *et al.,* 2007; Gerritsen *et al.,* 2011; Donaldson *et al.,* 2015).

The largest microbial community found in the human body is in the intestines, specifically the distal gut, which is often referred to as the gut microbiota (Gill *et al* 2006). Here bacterial cell densities reach 10^{11} - 10^{12} cells/ml, compared to regions such as the oesophagus or stomach which only reach 10 cells/ml (Jandhyala, 2015; O'Hara and Shanahan, 2006; Pilato *et al* 2017, Sender *et al.,* 2016; dos Santos *et al.,* 2010). This complex ecosystem consists of thousands of bacterial species, with the majority being strict anaerobes (Morgan and Huttenhower, 2012; Qin *et al.,* 2010; D'Argenio and Salvatore, 2015; Vacharaksa and Finlay, 2010; Amrane *et al.,* 2018). 16S based sequencing has given great insights into the species present in the distal gut, showing that it is dominated by *Firmicutes* and *Bacteroidetes* (Qin *et al.,* 2010; Eckburg *et al.,* 2005).

Compositions of the microbiota associated with our body are not only site-specific but vary dramatically across individuals and with time (non-static in nature) (Proctor, 2011; Bäckhed *et al.,* 2012; Almeida *et al.,* 2019; Qin *et al* 2012). A person's location and lifestyle choices impact their microbiota, creating variation across individuals (Yatsunenko *et al.,* 2012; Filippo *et al* 2010). The western high fat and sugar content diet rich in animal products such as meat, milk and eggs lead to a different microbiota makeup when compared to that of a typical eastern (Chinese) rice and noodle-based diet (Senghor *et al.*, 2018). Twin studies have shown a hereditary component to the composition of the gut microbiota, however environmental factors are thought to be a larger determinant (Goodrich *et al* 2014, Rothschild *et al* 2018, Valdes

et al 2018). For healthy individuals, it has been found that although the gut microbiota is variable, essential genes found in the microbiome (genomes found in the microbiota) are conserved, this is termed the 'core microbiome' (de Cárcer 2018, Qin *et al* 2010, Turnbaugh *et al* 2008, Gill *et al* 2006). Unhealthy individuals such as those suffering from obesity and diabetes are found to have differing microbiotas, with essential genes predicted missing from their core microbiome (Qin *et al* 2012, Haro *et al* 2016, Lloyd-Price *et al* 2016, Breen *et al* 2013, Turnbaugh *et al* 2008).

1.3 How does the gut microbiota impact human health?

Our gut microbiota plays a key role in an array of essential physiological processes, from the immune system to metabolism and nutrient absorption (Table 1) (Maslowski *et al.,* 2009; Round and Mazmanian, 2010; Clarke *et al.,* 2010; Kau *et al.,* 2011; Round and Mazmanian, 2009; Li *et al.,* 2016b; Valdes *et al.,* 2018; Yadav *et al.,* 2018; Sommer and Bäckhed, 2013). Bacterial cells are able to utilize matter we are unable to break down, this provides a source of nutrients for themselves, and in doing so they produce by-products that aid our bodies (Krajmalnik-Brown *et al.,* 2012; Yadav *et al.,* 2018). Vitamin K, which is required to produce the clotting factors in blood is synthesized from menaquinone made by intestinal bacteria (Lloyd-Price *et al.,* 2016; Okumura and Takeda, 2017). The exact bacteria in the gut which contribute to Vitamin K synthesis are unknown at present.

Table 1: The gut microbiota affects multiple processes in the body and provides numerous benefits, this table provides references to some of those key interactions.

Benefits/Influences	**Reference**
Colonization resistance, prevention of the pathogenic invasion	Lawley *et al.,* 2012; Karjalainen 2009; Petrof *et al* 2012
Regulation of Short Chain Fatty Acids (SCFAs)	Chen *et al.*, 2015; Roediger, 1980, Valdes *et al.,* 2018
Stimulation of host antimicrobial peptides (AMPs)	Hooper *et al.*, 2003; Cash *et al.*, 2006; Jandhyala, 2015
Gut epithelium mucus production	Deplancke and Gaskins, 2001; Hatayama *et al.*, 2007; Jakobsson *et al.*, 2015
Immune system homeostasis and regulation	Clarke *et al.,* 2010; Round and Mazmanian, 2009; Maslowski *et al.*, 2009; Sommer and Bäckhed, 2013; Valdes *et al.,* 2018; Wu and Wu, 2012
Metabolism and nutrient absorption	Kau *et al.,* 2011; Krajmalnik-Brown et al., 2012; Yadav *et al.,* 2018

1.3.1 Colonisation resistance

During food intake, exogenous microorganisms enter the gut. While a selection of these will inhabit the intestine and add to the gut microbiota, others will be pathogenic invaders. The microbiota acts as a protective barrier, helping to prevent colonisation by pathogens (Lawley *et al* 2012, Petrof *et al* 2012). This defensive property is called colonisation resistance and the microbiota conveys this resistance through an array of bacterial and host interactions (Karjalainen 2009). These interactions can be either be direct, through the use of secreted compounds, or indirect, through competition for nutrients, host metabolites and space with the pathogen. An example of indirect inhibition, through competition, is the interaction between the pathogen *Citrobacter rodentium* and the commensal *Bacteroidetes thetaiotaomicron*. *B. thetaiotaomicron* consumes carbohydrates essential to *C. rodentium* causing it to be excluded (Kamada *et al* 2012). There are a variety of secreted compounds released by the microbiota which directly affect an invading pathogen. These compounds broadly fall into two categories; those that are bacteriocin-related and those that are not. Bacteriocins are peptidic, ribosome synthesised antimicrobial compounds found throughout nature, they can be both broad and narrow in range (Garcia-Gutierrez *et al* 2018). The gut microbiota contains a large number of bacteriocins (Drissi *et al.*, 2015; Garcia-Gutierrez *et al.*, 2018),

predominantly made up of class I inhibitors such as microcins (Gaillard-Gendron *et al.*, 2000; Patzer *et al.*, 2003) and sactibiotics (Rea *et al.*, 2010), lantibiotics (Dabard *et al.*, 2001) etc. The non-bacteriocin-related compounds are mainly non-peptides such as hydrogen peroxide (Hertzberger *et al.*, 2014). For example, Bacteroides were shown to inhibit Salmonela Typhimurium through the production of the short-chain fatty acid propionate (Jacobson *et al.*, 2018).

1.3.2 Short Chain Fatty Acids (SCFAs)

The microbiota not only functions as a barrier but also importantly regulates both local and systemic immune responses. It does this through the secretion of short-chain fatty acids (SCFAs) such as acetate, butyrate and propionate (Chen *et al.*, 2015). These microbial SCFAs impact epithelial barrier function (Peng *et al.*, 2009; Yan and Ajuwon, 2017), production of antimicrobial peptides (AMPs) (Schauber *et al.*, 2003), the secretion of pro-inflammatory mediators (Li *et al.*, 2018) and T cell differentiation (Luu *et al.*, 2018).

The maintenance of a healthy relationship between our cells and the microbiota relies on physical segregation. The gut epithelial layer, containing epithelial and mucus-producing goblet cells is a key barrier separating the lumen from the body. Epithelial cells are held together by desmosomes, tight and adheren junctions (Niessen, 2007). Tight junctions dictate the permeability of the membrane, regulating what solutes and fluids are able to pass through the epithelial cells (Choi, Yeruva and Turner, 2017). Butyrate from the gut microbiota is the main energy source for these cells providing 80% of their daily supply (Roediger, 1980), facilitating tight junction assembly which protects the body (Peng *et al.*, 2009).

Goblet cells produce mucin glycoproteins, namely Mucin 2, the main building block for the double layered protective mucus barrier. The inner layer, closest to the epithelial cells is firmly adherent, with a tight stratified structure, while the larger outer layer is far less organised with a looser net of mucin (Luu *et al.*, 2018). The makeup of the two layers dictate their roles. The inner layer is dense and protective preventing bacteria from touching the epithelial layer.

The secondary layer, in contrast, is a looser structure allowing it to harbour many of the adherent gut bacteria that make up the microbiota (Johansson, Larsson and Hansson, 2011). SCFAs from the microbiota have been shown to upregulate the production of mucin 2 (Deplancke and Gaskins, 2001; Hatayama *et al.*, 2007; Jakobsson *et al.*, 2015), this stimulation has been shown to prevent pathogenic bacteria from adhering to the epithelial layer (Jung *et al.*, 2015). Butyrate was originally shown to induce MUC2 (gene coding mucin 2 protein) expression via the mitogen activated protein kinase (MEK) (Hatayama *et al.*, 2007). However, later it was found that acetate, butyrate and propionate are all able to induce MUC2 expression through the promotor region AP1 (Activator protein 1) (Burger-van Paassen *et al.*, 2009). Interestingly, a fibre-deprived dietary disruption to the microbiota was shown to cause the microbiota to degrade the mucus layer and worsen pathogenic susceptibility (Desai *et al.*, 2016).

1.3.3 Host Antimicrobial peptides (AMPs) and Immune modulation

The microbiota stimulates the host to produce AMPs (also called host defence peptides (HDPs)) as well as mucin. AMPs produced by the host form part of the innate immune response, and a healthy microbiota is needed for their production, with *Bacteroides thetaiotaomicron* and *Lactobacillus innocua* speculated as being key drivers (Hooper *et al.*, 2003; Cash *et al.*, 2006; Jandhyala, 2015). In Caco-2 and HT29 cell lines it was shown that butyrate increases levels of the AMP, LL-37 (Schauber *et al.*, 2003). LL-37 has been shown to be active against numerous pathogens such as *Pseudomonas aeruginosa* and *Staphylococcus aureus* and is reported to have biofilm dispersing properties (Duplantier and van Hoek, 2013).

Effector and regulatory CD4+ T cells are highly abundant in intestinal tissues and like the innate immune system, they have been shown to be affected by the microbiota. Specifically, the microbiota drives cellular differentiation and physiological changes of CD4+ T at epithelial barrier sites (Sorini *et al.*, 2018). The immune system needs to achieve a stable balance between effectively eliminating an invading pathogen and avoiding autoimmunity. The gut microbiota aids in this balancing act, by regulating immune homeostasis

(Round and Mazmanian, 2009; Maslowski *et al.*, 2009; Wu and Wu, 2012). This is evident in germ-free mice as they often develop a variety of autoimmune problems, which can be corrected with the introduction of bacteria into the gut (Mazmanian *et al.*, 2005; Round and Mazmanian, 2009; Reading and Kasper, 2011).

1.3.4 Gut microbiota and diseases

Numerous diseases have been associated with disturbances in our gut microbiota. Commonly reported are the correlations between diabetes, IBD, IBS and obesity with alterations to the general makeup of our gut microbiota (Turnbaugh *et al.*, 2008; Qin *et al.*, 2012; Breen *et al.*, 2013; Haro *et al.*, 2016; Lloyd-Price, Abu-Ali and Huttenhower, 2016). More recently, there have been growing arguments for links between the gut microbiota and the brain. As one might guess, the gut microbiota has an effect on satiety. Gut bacteria depend on their host to provide nutrients which gives them great incentive to control food intake (Tremaroli and Bäckhed, 2012; Fetissov, 2016). The more surprising effect is the impact the gut microbiota is thought to have on anxiety, depression, cognition, and autism spectrum disorder (ASD) (Sharon *et al.*, 2016). Earlier this year the Krajmalnik-Brown lab published in Nature outlining the benefits a microbiota transplant has on autism (Kang *et al.*, 2019).

The gut microbiota, although hugely beneficial, can itself be detrimental to the body. A comprehensive study of patients with bloodstream infection revealed that the gut microbiota was a potential reservoir or the starting point of infection, especially for cases involving *Escherichia coli* and *Klebsiella pneumoniae* (Tamburini *et al.*, 2018). *Bacteroides fragilis,* a common member of a healthy gut microbiota and general commensal, becomes highly pathogenic when in the bloodstream or surrounding tissue of the gut following trauma. Despite the low numbers of *B. fragilis* found in the gut, it is a commonly isolated anaerobic pathogen which could be attributed to its numerous virulence factors (Polk and Kasper, 1977; Wexler, 2007). Enterococcus faecalis similarly is a gut commensal that can cause life-

threatening diseases such as endocarditis and sepsis (Megran, 1992). *E. faecalis* multidrug nature makes it especially dangerous (Paulsen *et al.*, 2003).

1.3.5 Microbiota dysbiosis and microbial infections

The dysbiosis of the gut microbiota by antibiotic treatment has long been documented, with broad-spectrum antibiotics causing adverse effects to their target pathogens and the bacteria that compose the microbiota. Less, however, is known about the effects of non-antibiotic drugs on the gut microbiota. Long-term use of proton pump inhibitors (PPI) is found to alter the microbiota composition and increase the risk of bacterial enteric infections (Freedberg *et al.*, 2015). The associated pH increase from PPI has been shown to reduce the bactericidal effect of the stomach, resulting in small intestinal bacterial outgrowth and lowered colonisation resistance (Yasutomi *et al.*, 2018). The antidiabetic drug, Metformin, is another example of a non-antibiotic drug causing a disturbance in the gut microbiota. Metformin causes a depletion of butyrate producing bacteria although the exact mechanism is unknown (Forslund *et al.*, 2015). Disturbed microbiota and the loss of colonisation resistance is associated with many pathogen infections; *Clostridioides difficile* (Pérez-Cobas *et al.*, 2015), *Salmonella typhimurium* (Bratburd *et al.*, 2018), *Enterohemorrhagic E. coli* (Saito *et al.*, 2019), *Shingella flexneri* (Anderson, Sansonetti and Marteyn, 2016), *Campylobacter jejuni* (O'Loughlin *et al.*, 2015) *and Vibrio cholerae* (Freter, 1955). More research needs to be carried out to truly understand how the microbiota might protect us, how we benefit from its presence, and what we can do to improve it.

1.4 Clostridioides difficile

Clostridioides difficile (previously known as *Clostridium difficile*) is a Gram-positive, spore-forming, opportunistic gut pathogen (Lawson *et al.*, 2016). Originally described by Ivan Hall and Elizabeth O'Toole, the bacterium was given the name *Bacillus difficiles* (Hall and O'Toole, 1935). With new nomenclature techniques introduced in the 1970s, *Bacillus* was replaced with *Clostridium* (Bartlett *et al.*, 1978). In 2013, *Clostridium* was changed to

Peptoclostridium difficile (Lawson *et al.*, 2016) in order to emphasise differences between it and other members of the *Clostridium* genus. A further taxonomic change was done to allow for previous acronyms (*C. diff*, *C. difficile* etc.) to be used whilst maintaining a taxonomic difference to *Clostridium*.

C. difficile has a broad host range, shown to infect bovine, canine, equine, swine, and humans (Keel *et al.*, 2007). Spores enable *C. difficile* to persist in the environment (Lawley *et al.*, 2009). They are highly resistant to environmental stresses and are able to withstand hospital grade cleaning detergents and some disinfectants (Đapa *et al.*, 2013; Peng *et al.*, 2017). Soil, faeces (animals and humans), sewage, and meat are all reservoirs of *C. difficile* (Diaz, Seyboldt and Rupnik, 2018; Dharmasena and Jiang, 2018). *C. difficile* is transmitted via the faecal – oral route, shed into the environment by colonised individuals (Surawicz *et al.*, 2013). Once taken into the digestive system spores are key to *C. difficile*'s ability to survive through the acidic pH of the stomach (Vonberg *et al.*, 2008; Rodriguez-Palacios and LeJeune, 2011; Isidro *et al.*, 2017; Kochan *et al.*, 2018).

1.4.1 *C. difficile* Infection (CDI)

C. difficile is highly contagious with half a million new cases each year in the United States (U.S.) alone (Lessa *et al.*, 2015). *C. difficile* infection (CDI) (also known as *C. difficile* associated disease CDAD) is the leading cause of gastroenteritis-associated death in the U.S. (Lessa *et al.*, 2015). The disease symptoms include abdominal pain, diarrhoea, fever and nausea. Severe cases lead to pseudomembranous colitis, toxic megacolon, perforation of the colon, and sepsis (Yasunaga *et al.*, 2013). The majority of CDI cases (65%) are health care-associated, making CDI the leading cause of health care-associated diarrhoea (Rupnik, Wilcox and Gerding, 2009; Leffler and Lamont, 2015). The spore-forming and antibiotic resistant nature of the bacteria means a staggering 15% to 35% patients will have repeat infections (McFarland, 2005; Marsh *et al.*, 2012; DePestel and Aronoff, 2013).

In the UK the average cost to treat a patient with *C. difficile* in 2017 was £6294, recurrent infection cost £7539/CDI and the average length of hospital stay was

7.2 days (van Kleef *et al.*, 2014; Wilcox *et al.*, 2017). Across Europe the average stay was 15 days, and recently got as high as 26 days in Spain and Italy (Wiegand *et al.*, 2012; Asensio *et al.*, 2015; Ramírez and Bouza, 2018). The estimated cost of CDI across Europe is around €3 billion/year and is expected to double over the next 40 years (Kuijper, Coignard and Tüll, 2006; Wiegand *et al.*, 2012).

C. difficile is transported into the body by the faecal-oral route. Those infected with *C. difficile* are thought to shed spores which acts as a mode of bacterial transmission. If ingested these highly resistant spores pass through the stomach and once in the small intestine *C. difficile* spores begin to germinate into vegetative cells. There are major gaps in the understanding of the germination process of *C. difficile*. It has, however, been established that there is a requirement for primary bile acids such as taurocholic acid (Sorg and Sonenshein, 2008; 2010; Giel *et al.*, 2010). More recent work suggests quorum sensing is equally important (Darkoh, Odo and DuPont, 2016). Once germinated, vegetative cells begin to colonise the gut. Bacteria are able to penetrate through the mucus layer and embed themselves on and between epithelial cells (Engevik *et al.*, 2014). McKee *et al.*, 2018 demonstrated that the type IV pili is essential for *C. difficile* adherence and persistence within the gut. To aid colonisation *C. difficile* produces two large, glucosylating enterotoxins TcdA and TcdB (Toxins A and B), these are key virulence factors needed for infection (Kuehne *et al.*, 2010). These two toxins cause the onset of CDI associated symptoms such as fluid secretion, immune cell influx and tissue damage (LaFrance *et al.*, 2015).

C. difficile is an opportunistic pathogen that is able to establish itself after prolonged or frequent antibiotic treatments. Spore formation and inherent antibiotic resistance allow *C. difficile* to survive many antibiotics and take advantage of the body's weakened gut microbiota defences. Antibiotics affect both pathogens and the gut microbiota, therefore antibiotic treatment leads to disruption of the gut microbiota. As a consequence, colonisation resistance is lost. Fluoroquinolones such as gatifloxacin and moxifloxacin are a predominant risk factor for CDI (Pepin *et al.*, 2005). CDI commonly affects the

elderly as they require repeat or frequent broad-spectrum antibiotic treatments. Within one month of a *C. difficile* diagnosis 1 in 11 people over the age of 65 are expected to die (Lessa *et al.*, 2015; Asempa and Nicolau, 2017).

Combating *C. difficile* infections is difficult due to its intrinsic antibiotic resistance and tendency to cause recurrent infections (Peng *et al.*, 2017). A case of recurrent CDI refers to a patient initially responding well to the treatment administered, but at a later stage reacquires the infection. Initial antibiotic treatments will reduce *C. difficile* numbers leading to a false recovery, but as the gut microbiota is also altered it leaves the patient vulnerable to reinfection either through re-exposure or more likely, germination of remaining spores (Marsh *et al.*, 2012). Seekatz *et al.*, 2018 reported that recurrent infections often (78.6% in a sample size of 61 patients) contain a mixed *C. difficile* population. This implies that recurrent infection comes from antibiotic resistant sub-species. Recurrent *C. difficile* has most effectively been treated with vancomycin and fidaxomicin, however, vancomycin resistant strains are now frequently occurring (Peng *et al.*, 2017). Once a patient has recurrent CDI, the chances of treatment success are low (Hopkins and Wilson, 2017). With limited availability of effective therapeutics against *C. difficile*, it poses a serious public health challenge (Lessa *et al.*, 2015).

1.4.2 The role of the microbiota in *C. difficile* colonisation

A healthy gut microbiota has been shown to prevent *C. difficile* colonisation (Figure 1). The increased susceptibility of CDI after antibiotic dysbiosis of the gut microbiota is well documented (Dethlefsen *et al.*, 2008; Theriot and Young, 2015). This dysbiosis significantly reduces the number of beneficial Bacteroidetes and Firmicutes present and increases Proteobacteria in the gut (Peterfreund *et al.*, 2012).

The microbiota in a healthy state consumes/converts primary bile acid into secondary, depleting the number of *C. difficile* able to germinate (Weingarden *et al.*, 2013; Yoon *et al.*, 2017). Secondary bile acids, deoxycholic acid (DCA) and lithocholic acid (LCA), are toxic to vegetative *C. difficile* (Weingarden *et al.*, 2013; J. D. Kang *et al.*, 2019). The bacteria *Clostridium scindens* and

Bacteroides ovatus have both been shown to inhibit *C. difficile* solely through this mechanism *in vitro* (Yoon *et al.*, 2017; J. D. Kang *et al.*, 2019). A depletion in the abundance of the gut microbiota also results in an abundance of available nutrients e.g., monosaccharides which can be utilized by *C. difficile* (Wilson and Perini, 1988). The microbiota not only competes for resources but actively inhibits *C. difficile*. A notable example is the bacteriocin "thuricin CD", produced by *Bacteroides thuringiensis,* which has been shown to be highly targeted towards *C. difficile* spores (Rea *et al.*, 2010; Rolhion and Chassaing, 2016). Bacteriocins from Bacillus, Enterococcus and Lactococcus strains, have all been shown to inhibit *C. difficile* in *in vitro* conditions (Rea *et al.*, 2007; Trzasko *et al.*, 2012; Bartoloni *et al.*, 2013).

The microbiota influences the epithelial cells creating an environment less favourable to a *C. difficile* invasion – through general upregulation of antimicrobial peptides, mucus production, and cell shedding (Jakobsson *et al.*, 2015; Buonomo and Petri, 2016). The gut epithelial layers, much like the skin, are produced in a bottom up fashion, where the top layer is shed to make way for new cells. If the rate of this shedding is too slow it allows for a significant build-up of pathogen infected/associated cells and gaps can form in the epithelial barrier ruining the protective properties (Williams *et al.*, 2015). The microbiota influence on the shedding process may help to prevent *C. difficile* colonisation, as *C. difficile* toxins induce increased cell shedding as part of its infection strategy (Williams *et al.*, 2015).

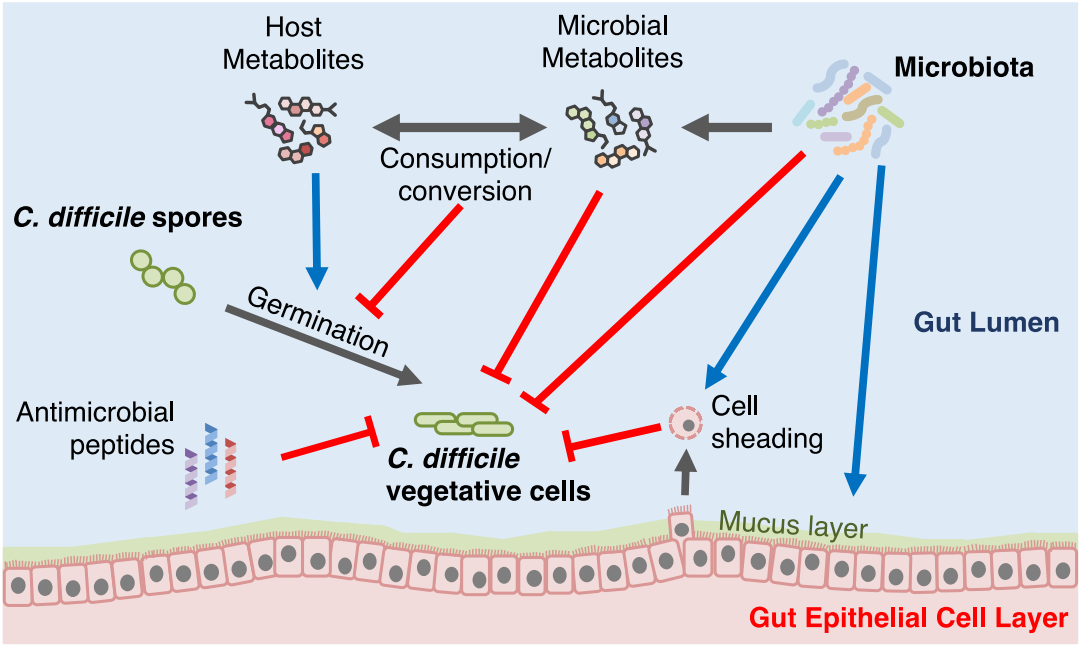

Figure 1: **Schematic overview of how the microbiota helps to impede *C. difficile* infections**. Blue arrows indicate areas of beneficial interaction, and red arrows indicate areas of inhibition.

1.4.3 Use of microbiota as a treatment for *C. difficile*

To combat severe cases, where patients are unable to recover with antibiotic treatment, clinicians are resorting to faecal microbiota transplants (FMT) to restore the microbiota (Petrof *et al.*, 2012). FMT is the process of transferring stool from a healthy donor into the GI tract of an unhealthy patient using either an enema, colonoscopy, oral capsules, nasogastric, nasoenteric tube, or endoscopy (Surawicz, Bowman and Broussard, 2015). The first documented use of FMT to treat *C. difficile* in modern medicine was in 1958 when Dr Eiseman reported the prompt cure of four pseudomembranous enterocolitis patients with a faecal enema (Eiseman *et al.*, 1958; Surawicz, Bowman and Broussard, 2015). Faecal transplants come with their own associated risks and burdens therefore they are currently only used as a final treatment option. The Food and Drug Administration (FDA) this year released a safety alert regarding the transmission of multi-drug resistant bacteria via faecal transplants. The alert was a response to reports of the first death of an immunocompromised patient who had undergone FMT (FDA, 2019).

1.5 Models of *C. difficile* infection and the human gastrointestinal tract

The impact of the microbiota is extensive, *C. difficile* is a great example of this. The majority of gut epithelial–microbiota research has been carried out using genomics and metagenomics. Omics research can provide rich insights into bacterial species present but only at discrete timepoints. These snapshots of information are not sufficient to understand the highly dynamic gut microbiota, providing no information on the mechanisms underlying the bacterium- bacterium interactions. Models of the gut including the microbiota are essential for our knowledge of their interactions to progress, especially given the complexity of the system and the difficulties in sampling humans.

1.5.1 *In vivo* infection models

Up until the last decade models of the gut microbiota have mainly been carried out under *in vivo* conditions with mice frequently chosen as the host (Hugenholtz and de Vos, 2018). Gnotobiotic mice models have revealed numerous insights into how the microbiota influences autoimmunity (Mazmanian *et al.*, 2005; Wu and Wu, 2012; Opazo *et al.*, 2018). The use of murine models led to the discovery of the profound effect the gut microbiota has on obesity (Muscogiuri *et al.*, 2019). When mice were transplanted with the microbiota from people possessing the obese phenotype, the hepatic transcriptional profile of lipid metabolism in mice was severely impacted, causing liver steatosis (Wang *et al.*, 2018). A large range of hosts have been utilised as *C. difficile* infection models including hamster, mouse, prairie dog, piglet, foal, hare, rabbit, guinea pig, rhesus monkeys and zebrafish (Best, Freeman and Wilcox, 2012). The gold standard model of CDI has historically been the Golden Syrian hamster as pathologically their infection reflected many clinical aspects of a human infection (Warn *et al.*, 2016). Since 2008, when the first viable mouse model was published, more labs began switching to the more conventional mouse models (Chen *et al.*, 2008; Hutton *et al.*, 2014). Mouse models are more widely used in the research community than hamster models, as a consequence there are far more mouse specific reagents and genetically modified animals to work with.

1.5.2 *In vitro* gut epithelium and microbiota models

There are several models of the gut which do not have a host components, for example models such as the SHIME (Simulator of the Human Intestinal Microbial Ecosystem) have focused on producing accurate microbiota culturing techniques but lack any epithelial representative (Marzorati *et al.*, 2014; de Wiele *et al.*, 2015). The SHIME model uses human faecal material, which it ferments in three or five interconnected vessels; each vessel is set up to simulate a different part of the GI tract. In the five-vessel setup, the SHIME models the stomach, small intestine and the ascending, transverse and descending colon, changing from a low pH 5.6 in the stomach to a higher pH of 6.9 as it goes through the different vessels (Van de Wiele *et al.*, 2015). Recently, the SHIME gained a new module allowing for host-microbiota interactions called the HMI. The module aims to mimic host surface colonization and signalling through simulation of a mucosal area which bacteria can adhere under relevant shear stress, host cells within the HMI were shown to be viable for 48 hours (Marzorati et al., 2014). Similar to the SHIME models are the TNO intestinal models (TIMs) (Venema, 2015). TIM models are computer-controlled, dynamic systems consisting of four connecting glass compartments with flexible membrane insides. Between the glass walls and the inner membrane, water is pumped to control the temperature and flexibility of the membrane, as well as to create peristatic motions similar to those found in the GI tract. The peristatic motion of the membrane moves the luminal content throughout the model (Venema, 2015).

We have recently published a new system for modelling the interactions between gut epithelial cells and *C. difficile* (Anonye *et al.*, 2019), based on the VDC system (Figure 2). This system was first described by George Grass and Stephanie Sweetana, it is a two-chambered environment system separated by a polyester Snapwell (Grass and Sweetana, 1988). Each chamber is pumped with differing gas compositions to create an aerobic and anaerobic environment. This allows the culturing of anaerobic bacteria alongside human tissue. The system has successfully been used to model the interactions

between epithelial cells and *Escherichia coli* (Schüller and Phillips, 2010; Tran *et al.*, 2014; 2018) and *Campylobacter jejuni* (Mills *et al.*, 2012).

Three setups of the VDC have been developed, the most simplistic being a Caco-2 and HT29-MTX epithelial representative with a standard polyester Snapwell insert, termed epithelial – VDC (E-VDC). Under the gut epithelium there is a myofibroblast layer, these cells play a crucial role in the repairing the epithelial layer (Powell *et al.*, 2005). The E-VDC was developed further through the incorporation of human CCD-18co myofibroblasts. These cells were grown on the basolateral side of the polyester Snapwell insert creating a new multilayered VDC (M-VDC). The polyester membrane of the Snapwell is a great platform for cell adhesion and growth, however it is not very representative of the extracellular matrix (ECM) that holds up the epithelial layer. To model the porous nature and 3D architecture of the ECM an electrospun nanofiber scaffold was generated using polyethylene terephthalate (PET) (Morris *et al.*, 2014). In the more complex models, *C. difficile* adheres more efficiently compared to the single epithelial monolayers, leading to a quicker destruction of the epithelium (Anonye *et al.*, 2019). The advantage of using a Snapwell system is that cells can be cultured separately using the common transwell tissue culture technique and then inserted into the VDC at a later date. The disadvantage of this system is the lack of flow, and hence the inability to follow infection beyond 48 hours.

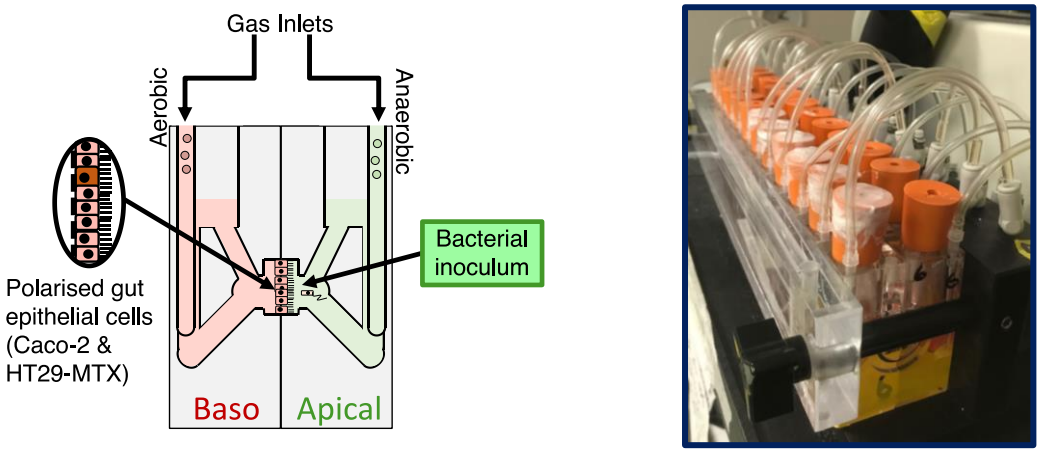

Figure 2: **Epithelial - Vertical diffusion chamber (E-VDC) A)** Illustration of the E-VDC, gut epithelial cells are grown on a Snapwell for 14 days before been introduced into model. The VDC consists of two chambers, that are fed with two different gas inlets; aerobic (5% O_2 and 95% N_2) and anaerobic (10% H_2, 10% CO_2 and 80% N_2). Bacteria are seeded on the apical side. **B)** A picture of twelve VDCs in use.

1.5.3 Microfluidic models

The advent of microfluidics has enabled the development of novel *in vitro* biomimetic models of human organs. These models know as 'Organ-on-a-chip' (OOC) platforms enable the modelling of critical aspects of living organs, and provide unique insights into their complex environments (Huh, Hamilton and Ingber, 2011; Kim *et al.*, 2012; Huh *et al.*, 2013; Lee and Sung, 2013; Caplin *et al.*, 2015; Zheng *et al.*, 2016). OOC's can mimic the physiological conditions of multiple organs simultaneously, with complex systems interconnecting to create closed loop systems, so called 'humans-on-a-chip' or 'body-on-a-chip' (Williamson *et al.*, 2013; Abaci and Shuler, 2015). The engineering of novel drugs is limited by expensive and time-consuming animal models, which frequently do not translate well to humans (Flint *et al.*, 2007; Kim and Ingber, 2013). With improved accuracy, OOC's are poised to be a viable complementation to animal testing (Kim *et al.*, 2012; Lee and Sung, 2013; Kim and Ingber, 2013; Selimović, Dokmeci and Khademhosseini, 2013; Bhatia and Ingber, 2014; Caplin *et al.*, 2015; Abaci and Shuler, 2015; Zheng *et al.*, 2016).

In 2012, the Wyss Institute created the 'Gut-on-a-chip' model (Kim *et al.*, 2012; Kim and Ingber, 2013; Kim *et al.*, 2016; Jalili-Firoozinezhad *et al.*, 2019), the chip consists of two aligned microchannels separated by a porus

membrane (Figure 3A). The top channel contains oxygenated media and supports the growth of epithelial cells grown on the porous membrane. The bottom channel is pumped with deoxygenated media and is aimed to mimic the gut lumen. Larger vacuum chambers run either side of the layered channels system, these are used to create peristatic motion. This peristatic motion was shown to aid the formation of micro-villi and crypts in the epithelial layer (Kim *et al.*, 2012). This model has been used in a variety of studies; from gut epithelial inflammation providing insights into irritable bowel syndrome (Kim *et al.*, 2016), to studying infections specifically of coxsackievirus B1 (CVB1). Enterovirus infection studies without a human gut cell mimic are difficult as animals express different virus receptors to humans (Villenave *et al.*, 2017). Recently, a microbiota study was performed using this model; the authors reported an extended coculture of epithelium cells with a stable gut community (Jalili-Firoozinezhad *et al.*, 2019). Initial testing of the chip was done with a single obligate anaerobe, *Bacteroides fragilis,* to ensure the anaerobic chamber sustained growth. They found that the barrier function of the epithelium improved with the presence of *B. fragilis*. To model a more complex and representative microbiota they chose to use faecal samples sustained in gnotobiotic mice for 30 generations and eventually they progressed to samples directly from humans. They found that their model was able to sustain a rich and abundant diversity of species, both with cell lines (Caco-2) and primary gut epithelial cells.

The 'gut-on-a-chip' model later inspired the larger capacity HuMiX (human–microbial crosstalk) model (Shah *et al.*, 2016) (Figure 3B). Both the 'HuMiX' and the 'Gut-on-a-chip' model successfully culture human epithelial cells alongside anaerobic bacteria. They achieve this by mimicking the anaerobic-aerobic barrier found in the human gut. Studying single species functions is insightful but overlooks any community-based effects. Investigating the microbiota as a complex community together with the host cell components would provide a unique perspective on microbiota function.

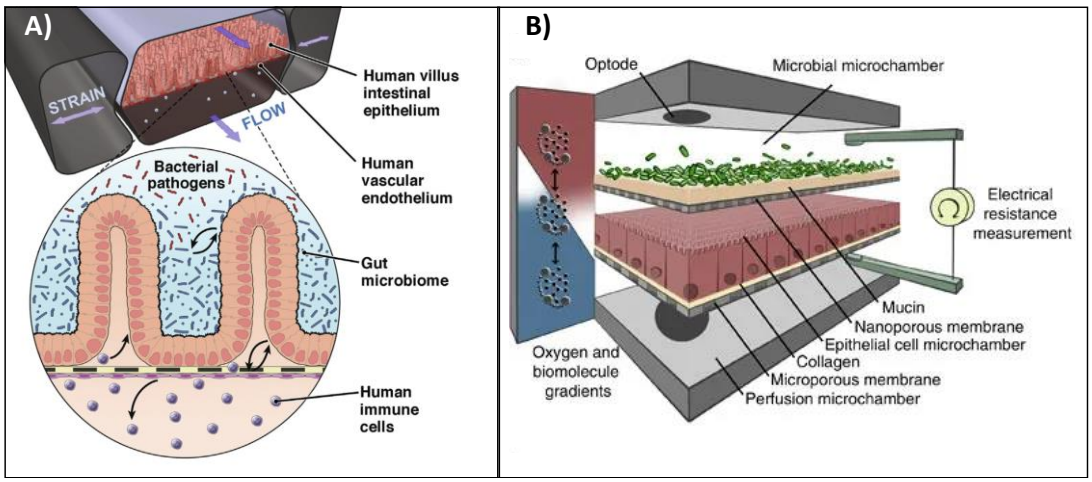

Figure 3: **Illustration of two microfluidic epithelial gut models. A)** Gut-on-a-chip, gut epithelium and vascular endothelium are seeded on opposite sides of a porous membrane. Peristatic motion from the vacuum sides creates strain across the porous membrane which encourages the formation of villi. Anaerobic media is pumped over the epithelial cells to support growth of anaerobic bacteria, with aerobic media is pumped on the endothelium to support the mammalian cells (Bein *et al* 2018). Reproduced from Open access journal, under creative common liscence CC BY-NC-ND 4.0. **B)** The HuMiX device is a similar two chamber system, however composed using two membranes, one seeded with epithelial cells separated by a second nanoporous membrane from the microbial community. Oxygen is perfused across the device to create a gradient, with microbial chamber (anaerobic bacteria) furthest from the oxygen source (Shah *et al* 2016). Reproduced with permission from Springer Nature.

2 Project Aims

The main goal of my PhD was to develop a trackable *in vitro* representative gut community which can be used to understand pathogen colonisation. Part of creating the community will be engineering techniques for quantification of each individual species. A trackable community will provide unparalleled insights into the microbiota, further, combining this with host cell components we can begin to get a picture of the interactions between invading pathogens (*C. difficile*), the host and the microbiota.

Specific aims:

- Study the interactions between *C. difficile* and a representative gut microbiota species (*B. dorei*) within a gut epithelial model (Chapter 4).
- To engineer a representative gut microbial community and develop single species quantification techniques (PMA-qPCR) (Chapter 5).
- To investigate *C. difficile* interactions with a representative gut microbiota community (Chapter 6).

3 Methods

3.1 Bacterial strains and growth media

To select the representative species that would make up our artificial microbiota community, we shortlisted using the following microbiota papers (Qin *et al.*, 2010; 2012; Schloissnig *et al.*, 2013; Li *et al.*, 2014). Any species which met the following criteria was chosen; high relative abundance, present across multiple regions (Europe, America and Asia), and has a sequenced genome. Culturing of all the strains was conducted at 37°C in anaerobic conditions using an anaerobic cabinet (Don Whitley), and unless stated otherwise cultures were grown in SAB (Schaelder Anaerobic Broth) (Oxoid) supplemented with 0.005 mg/ml Vitamin K (VWR) and 2 mg/ml L-cysteine (Sigma-Aldrich) (Refered to now as SAB+).

3.2 Propidium monoazide (PMA) treatment

PMA (Biotium) was added to samples prior to DNA extraction at a concentration of 160 μM. The samples were then incubated in the dark for 10 min (37°C in anaerobic cabinet). To photoactivate PMA, samples were exposed to blue light (465-475 nm) using the PhAST Blue (Geniul) light system for 15 min, following this DNA was extracted.

3.3 DNA extraction

DNA extraction was carried out using a phenol chloroform-based method. Cultures were centrifuged at 14,000 rpm for 5 min, after which the supernatant was discarded. The pelleted cells were re-suspended in 500 μl of 5 mg/ml lysozyme (VWR) and incubated for 20 min at 37°C. Following this; 20 μl RNase solution (20 mg/ml) (Fisher Scientific), 20 μl Proteinase K (20 mg/ml) (New England Biolabs) and 25 μl 10 Sodium dodecyl sulfate (SDS) (Fisher Scientific) were added. The samples were then incubated at 37°C for a further 10 min, following this 100 μl of NaCl (Fisher Scientific) and 80 μl Cetyl Trimethyl Ammonium Bromide (CTAB) (Sigma Aldrich) were added before a final incubation at 60°C for 45 min.

The lysed samples were treated with 750 µl of phenol chloroform IAA (PCI) (Sigma Aldrich), vortexed (2-3 sec) and centrifuged for 10 min at 14,000 rpm. The upper phase was transferred to a fresh Eppendorf tube, and the PCI centrifuge steps were repeated until a clear boundary could be seen between the two phases. Next, 75 µl of 3M NaAc (pH 5.2) (Sigma Aldrich) and 750 µl of -20°C 96% ethanol were added. This solution was inverted until the DNA precipitated out. The precipitated DNA solutions were then centrifuged for 5 min at 14,000 rpm. The pellets were washed with 200 µl 70% ethanol and centrifuged for a final time (2 min at 14,000 rpm). The pelleted DNA was dried at room temperature and re-suspended in 75 µl TE buffer.

3.4 Colony Counting

To measure colony forming units (CFU) samples were serially diluted in phosphate-buffered saline (PBS) (50 µl in 450 µl). 20 µl of each dilution was pipetted in duplicate onto a plate, with each plate split between two dilutions. The plates were tilted to spread the drops for easier counting and incubated for 24 - 48 hours. Incubation time was strain dependent, with some strains requiring longer for accurate counting (i.e. better visibility of smaller colonies).

3.5 Real time quantitative PCR (qPCR)

3.5.1 Species-specific primer design

Primers were designed to target either the topoisomerase I (*topI*) or DNA gyrase subunit A (*gyrA*) region of each strain. These two genes were chosen for their single copy number within the genome. The designing of the primers was carried out using Primer-BLAST, this enables a high level of species specificity to be engineered in at the *in situ* level (Ye *et al.*, 2012; Huang *et al.*, 2015). Primers were designed to create an amplicon of 100-150 bases, with an annealing temperature of 59-60°C, all primers were screened against the 'nt' database for specificity. Suitable primers were then checked using 'Thermo Fisher's Multiple Primer Analyzer', a web-based script which looks for any possible primer-dimer structures. Any primers found to form dimers were ruled out. The qPCR was conducted with the Agilent Mx3005P qPCR System

and the 'Luna® Universal qPCR Master Mix'. The temperature profile used throughout was the recommended standard for the master mix.

3.5.2 Conversion to bacterial number

To convert from a qPCR output cycle threshold (Ct) to a predicted bacterial number we utilized methods described in (Ammann *et al.*, 2013; Huang *et al.*, 2015). This required creating a standard curve for each species, the gradient of which is related to the primer amplification efficiency. The standard curve is a serially diluted sample where the Ct value and the DNA mass for each dilution is known, and the curve maps the relationship between the two. DNA concentration was measured using the Qubit fluorometer 2.0 (Thermo Fisher) and the dsDNA Qubit kit (Thermo Fisher), depending on the mass this would vary between high sensitivity and broad spectrum.

Once the standard curve was established, we used it to convert CT values into the starting mass of DNA (M_{DNA}) (Equation 1). Using the assumption that one genome weight worth of DNA is equal to one bacterium, we were able to predict the total number of bacteria by dividing the starting amount of DNA by the calculated genome mass (M_{Genome}) (Equation 2). The mass of each bacterial genome was calculated; by multiplying the length of the genome (G_{Length}) by the average weight of one base pair (bp). Commonly the average weight of a nucleotide is expressed as the weight of one mole (W_{Base}) not a singular base, this is equal to 650 da. To convert from one mole to 1 bp we divided through by Avogadro's number (N_A).

Equation 1: Using the gradient (m) and intercept (c) from the standard curve, we can use the cycle threshold (CT) value of the current qPCR run to predict the starting DNA amount (M_{DNA}).

$$M_{DNA} = 10^{\frac{CT-c}{m}}$$

Equation 2: Assuming one bacterial weights worth of DNA is equal to one bacterium we can divide the predicted starting genome mass (M_{DNA}) by the mass of one bacteria genome (M_{Genome}) to get an estimate on the bacterial number. The mass of one genome is calculated from the genome length (G_{Length}) and the average weight of one mole of nucleotide bases (W_{Base}). Avagadro's number (N_A) is used to convert average weight of one mole to the average weight of a base pair.

$$Predicted\ Bacterial\ Number \approx Number\ of\ Genomes$$
$$= M_{DNA}\left(\frac{1}{M_{Genome}}\right) = M_{DNA}\left(\frac{N_A}{G_{Length}W_{Base}}\right)$$

3.6 Biofilm assays

3.6.1 *B. dorei* & *C. difficile*

B. dorei and *C. difficile* were cultured overnight in brain heart infusion (BHI) media (Sigma Aldrich) supplemented with 0.5 mg/ml yeast extract (Fisher Scientific) and 0.001 mg/ml L-cysteine (BHIS). After which, cultures were diluted down to 0.1 OD and added to a 24-well polystyrene tissue culture treated plate. Each well was made up to a total of 1 ml with monocultures having a mix of 0.5 ml culture and 0.5 ml BHIS media, and cocultures containing 0.5 ml of each species. The resulting end concentration was 0.05 OD_{600}. At set timepoints the biofilms were washed twice with 1 ml PBS, then manually resuspended in 1 ml PBS. When plated on BHIS with *C. difficile* supplement (Oxoid), *C. difficile* and *B. dorei* have two distinct colony morphologies. This enabled us to conduct standard CFU assays on the mixed biofilms.

3.6.2 Microbiota

For mixed biofilms with multiple microbiota species, individual overnight cultures were diluted the following day to achieve a final concentration of 0.1 OD_{600} per species within the mixed culture. After each timepoint the samples were washed twice and resuspended in PBS then treated with PMA. Following PMA treatment, a DNA extraction was conducted.

3.7 Proteomics

3.7.1 Cell lysis, Protein Extraction and Mass Spectrometry

Biofilms were washed twice with PBS and resuspended in 8M Urea lysis buffer; 8M Urea, 1% Glycerol, 1% SDS, 10 mM Tris (pH 6.8) and 1 cOmplete ™ protease inhibition cocktail (Sigma Roche) tablet per 10 ml. Three wells were combined for each sample to ensure high enough protein concentrations. Cells were lysed using a FastPrep-24 5G homogenizer and Lysing matrix B beads (MP biomedicals). The bead beating was repeated six times at 6 M/sec for 20 sec, with a 180 sec pause on ice.

Lysed cells were digested using a filter aided soluble protein (FASP) protocol, 400 µl of the lysate was added to the filter unit then spun 20 min at 8000 g. This was then washed twice with 8M Urea (20 min at 8000 g) to remove any lingering SDS. The buffer was then exchanged using 400 µl of 50 mM ammonium bicarbonate (ABC) (20 min at 8000g). This exchange was repeated twice. The solution was reduced and alkylated using 10 mM tris(2-carboxyethyl)phosphine (TCEP) and 40 mM 2-chloroacetamide (CAA) in ABC for 30 min at room temperature. TCEP and CAA was then removed, 20 min spin at 8000 g. The filter was then washed twice using ABC, 5 min spin at 8000 g. The protein was then digested using Trypsin (2 µg per 100 µg protein), incubated overnight at 37°C. After digestion the solution was spun out the filter unit - 20 min at 8000 g. We then eluted the protein using 400 µl water at 8000 g for 20 min.

Once the sample was digested, we did a C18-StageTip clean-up to remove any impurities. Two layers of C18 membrane were pushed into a 200 µl pipette tip, using an adapter this was placed inside an Eppendorf. The membrane was prepared using 50 µl of 100% methanol spun at 2000 rpm for 2 min. Next, we equilibrated the membrane with 50 µl of 100% acetonitrile (spun at 2000 rpm for 2 min). The final equilibration was carried out using 2% acetonitrile 0.1% TFA (Trifluoroacetic acid), spun this time for 4 min at 2000 rpm. Samples can now be loaded onto the membrane. 10-20 µg of sample peptides was diluted in 2% acetonitrile/0.1% TFA (final volume 100-150 µl), and added to the C18

membrane. Two washes were performed; first using 50 µl Ethyl acetate in 1% TFA then 50 µl 2% acetonitrile in 0.1% TFA. After each addition a spin of 2000 rpm for 4 min was performed. Peptides were finally eluted in 20 µl of 80% acetonitrile (Centrifuged at 2000 rpm for 2 min). Prior to mass-spec the 80% acetonitrile was removed from the samples using a Speedvac for 15 min. The samples were then resuspended in 2% acetonitrile 0.1% TFA solutions. Each sample was run on the Orbitrap Fusion with UltiMate 3000 RSLCnano System (Thermo Scientific) for 1 hour by the University of Warwick proteomics research technology platform.

3.7.2 Protein analyses

Protein identification from the raw mass-spec data was carried out using Maxquant (Version 1.6.7) (Cox and Mann, 2008). The two databases used to compare to were: *C. difficile* - UP000002070 and *B. dorei* - UP000005974. We used the default values other than label-free quantification was enabled. Once identified we passed the Maxquant output into the protein statistical analyses software Perceus (Version 1.6.7) (Tyanova *et al.*, 2016). We initially used Perseus to remove any reverse and potential contaminants database hits. We then proceed log2 transform the label free quantification intensity result. At this point we exported our database files, and imported them into the programming language R for the removal of “NaN” data (Appendix 1 for code). If a protein was not present in two or more samples within either condition (single or coculture) it was removed. After this, if two out of the three sample biological triplicate contained data, we replaced the missing data with the average of the other two. If the opposite was true, meaning two out of the three contained “NaN”, we replaced the missing data with the global minimum. Once the “NaN” data was removed, we re-input the data back into Perseus for principal component analysis and volcano plots, where we used the default values of the program.

3.8 Mammalian cell culture

A mix of Caco-2 (ATCC) and HT29-MTX (Natalie Juge, IFR) were used to represent the gut epithelium in the E-VDC. Before seeding the VDC Snapwells each cell line was grown separately. Caco-2 cells were cultured in Dulbecco's Modified Eagle's Medium (VWR) supplemented with 10% heat inactivated fetal bovine serum (FBS, Sigma Aldrich) (DMEM-10), 1% penicillin and 1% streptomycin. HT29-MTX were cultured in DMEM-10 supplemented with 1% penicillin, 1% streptomycin, 1% Non-essential amino acids (Fisher Scientific) and 2 mM Glutamine (VWR). Once a confluency of 80-90% was reached cells were trypsinized and pelleted down (1100 rpm at 4°C for 5 min), then re-suspended in HT29 medium ($4x10^9$ cells/ml). These two cultures were mixed in a 1:9 ratio favouring the Caco-2 cells, and used to seed the Snapwells (Corning). The Snapwells were incubated for fourteen days before been introduced into the VDC, this was to allow the cells to mature and become polarized - forming a complete monolayer. Media was refreshed every other day, HT29 medium in the insert and DMEM-10 in the main well.

3.9 Epithelial Vertical Diffusion Chamber (E-VDC): Gut model

3.9.1 Infection assays

The VDC was assembled around the 14-day old Snapwells, 3 ml of DMEM-10 was added to each chamber. Before the bacterial culture was added an initial TEER measurement was taken using an epithelial voltage clamp (Warner Instruments, model EC-800). Bacterial cells were grown overnight then pelleted at 5000 rpm for 5 min. The pellet was re-suspended in DMEM-10;

- For *C. difficile/B. dorei* OD_{600} was measured, but not used for normalisation as OD_{600} values for *B. dorei* do not correlate well with CFU/ml. Cultures were instead resuspended in double their initial volume using DMEM-10. Prior to loading in the VDC the CFU/ml of the diluted cultures were taken to ensure that equal numbers of *C. difficile* to *B. dorei* were present. Equal volumes of the two species' cultures were mixed prior to loading into the VDC. For the single species controls DMEM-10 was used instead of the second species. This

approach gave an MOI of 500-1000:1. The cell culture medium on the apical side was removed and replaced with 3 ml of the bacterial culture. After 3 hours, the apical media/culture was removed, and the VDC was gently washed with PBS. Once washed the media was replaced with reduced DMEM-10.

- For the mixed representative microbiota, we used a final concentration of 0.1 OD_{600} for each species. Conditions not containing *C. difficile* were supplemented with media. Normalizing to a set CFU concentration for every species we believed would be too laborious to be a realistic aim.

3.9.2 Decontamination

Decontamination of the VDC was carried out using 10% Chemgene. Emptied VDCs were placed into a Chemgene bath for 30 min. After the initial wash the chambers were rinsed with sterilized water, and soaked in water overnight, this was done to remove any remaining Chemgene residue.

4 The interactions between *C. difficile* and *B. dorei*

4.1 Introduction

C. difficile is an anaerobic, opportunistic gut pathogen, causing *C. difficile* infection (CDI). CDI is a healthcare-associated disease, with symptoms ranging from diarrhoea to pseudomembranous colitis. The best defence against *C. difficile* colonisation is our gut microbiota, providing a natural immunity to the disease when in a healthy state. Antibiotics negatively affect our microbiota alongside the pathogens they are aimed at (Haak *et al.*, 2018). This dysbiosis of the gut microbiota increases the likelihood of CDI (Jernberg *et al.*, 2007; Deshpande *et al.*, 2013). The use of broad-spectrum antibiotics in healthcare makes patients more susceptible to CDI (Deshpande *et al.*, 2013). Current treatments for CDI are metronidazole, vancomycin and fidaxomicin, however, the frequency of resistance to these treatments is growing alarmingly (Peng *et al.*, 2017; Asempa and Nicolau, 2017). Unfortunately, these antibiotic treatments do not always work long term. CDI has very high rates of recurrence (Lessa *et al.*, 2015). *C. difficile* has the ability to form resilient biofilms and spores, allowing it to survive to some degree antibiotic treatment (Đapa *et al.*, 2013; Edwards *et al.*, 2016). The antibiotics used against CDI causes the same gut microbiota dysbiosis that makes patients more susceptible to infection, so any surviving *C. difficile* is also in an ideal situation to recolonise (Weingarden *et al.*, 2013; Khan *et al.*, 2019).

The well recognised idea that the gut microbiota has an involvement in preventing *C. difficile* colonisation has been around since the 1970s, with early hamster models requiring a pre-treatment with vancomycin in order to be infected. Larson *et al.*, 1978 wrote: “Presumably this susceptibility is a result of a change in the bacterial flora, and this may be brought about by a wide range of antibiotics”. The exact mechanism and species involved in colonisation resistance are still to this day unclear as the identification of key species involved in resistance is difficult. Comparing the gut microbiota of CDI and non-CDI, does not guarantee that any microbes found to be different between the two are linked to prevention (Seekatz and Young, 2014; hubert *et al.*, 2014). Furthermore, there is inherent microbiota variability across

individuals that only worsens this problem (Proctor, 2011; Rinninella *et al.*, 2019). From a mechanistic point of view, it has been established that the microbiota mediated conversion of primary bile acid into secondary inhibits *C. difficile* ability to germinate (Wilson, 1983; Sorg and Sonenshein, 2008; Weingarden *et al.*, 2013). Faecal transplants have been however shown to cure CDI patients who are already colonised (post-germination) with *C. difficile,* implying that the resistance to *C. difficile* is potentially not solely achieved through bile acid conversion. Generally, the gut microbiota has a positive effect on the immune system, this boost from a healthy microbiota could account for *C. difficile* resistance, although a recent publication showed that clearance of *C. difficile* by the gut microbiota is independent of the adaptive immunity (Leslie *et al.*, 2019). If the gut microbiota is protecting against *C. difficile,* possibly without any input from the immune system, how is it doing it? Investigating the interactions between individuals from the gut microbiota and *C. difficile* may lead to the discovery of a novel inhibitory interaction, and possibly lead to new treatments.

Bacteroidetes are one of the major phyla found in a healthy gut microbiota and are significantly reduced in number and diversity in successful *C. difficile* infections (Shahinas *et al.*, 2012). Bacteroidetes are Gram-negative, non-spore-forming, mainly anaerobic, rod and coccobacilli shaped bacteria. They are vital to the fermentation of carbohydrates, providing a source of volatile fatty acids for the body (Wexler, 2007; Flint *et al.*, 2012). The phylum possesses a large number of carbohydrate-active enzymes able to degrade a range of plant polysaccharides. Individual species such as *Bacteroides cellulosilyticus*, *B. dorei, B. fragilis, B. ovatus, B. intestinalis, B. thetaiotaomicron, B. uniformis* and *B. xylanisolvens* have been shown to have an extensive range of carbohydrate degrading activities (Flint *et al.*, 2012). This broad range allows them to utilize multiple carbohydrates sources and may explain their prevalence as dominant species in the gut (Xu *et al.*, 2003). Multiple Bacteroidetes have been found to have inhibitory properties against *C. difficile* (Rea *et al.*, 2010; Yoon *et al.*, 2017; Mathur *et al.*, 2017; Deng *et al.*, 2018; Slater *et al.*, 2019).

Generally, *Bacteroidetes* produce bile salt hydrolase (BSH), this hydrolase converts primary bile acid into its secondary form, i.e. they aid in the bile acid-mediated inhibition of *C. difficile*. *B. ovatus* is a good example of this and has been shown to significantly inhibit *C. difficile* through cell-free supernatant alone (Yoon *et al.*, 2017). In the case of *B. thuringiensis,* however, its inhibition is direct. It inhibits *C. difficile* through the secretion of thuricin CD, a narrow-spectrum post-translationally modified bacteriocin which actively targets *C. difficile* spores (Rea *et al.*, 2010). The bacteriocin is made of two membrane-acting peptides Trnα and Trnβ, which together cause a membrane potential collapse in *C. difficile* (Mathur *et al.*, 2017). The third mode of inhibition was found in *B. fragilis* when tested in mice infected with *C. difficile* it restores epithelial barrier function namely Zonula occludens-1 (ZO-1) and MUC2 expression. This restoration of mucin not only impacts *C. difficile* infection capabilities but increases the microbial diversity as a whole helping to restore colonisation resistance (Deng *et al.*, 2018). Recently it was shown that *B. fragilis* inhibits *C. difficile* within an *in vitro* dual-species biofilm model (Slater *et al.*, 2019). It suggested that the reduction in *C. difficile* growth was through an AI-2 mediated metabolic change in *B. fragilis*. The effects of other individual Bacteroides species on *C. difficile* have not been well studied.

Dual species modelling of *C. difficile* has thus far largely ignored the human component of the infection, with the sole focus being on bacterial interactions. Given the large gaps in our understanding of how colonisation resistance is established, and the potential role epithelial and immune cells could have, we believe it is essential to study interactions in more physiologically relevant settings. Animal models have been the primary approach used to understand *C. difficile* pathogenesis (Chen *et al.*, 2008; Kuehne *et al.*, 2010; Leslie *et al.*, 2019). However, using them to understand host, pathogen and microbiota interactions would be challenging, especially to study interactions occurring at the gut mucosal interface. *In vitro* gut epithelial models reduce the complexity of the system and provide easier testing of multiple conditions (Anonye *et al.*, 2019).

To model the gut epithelium, we elected to use a vertical diffusion chamber model (E-VDC). The E-VDC consists of two chambers separated by a semi-permeable membrane, each chamber is fed with a different gas mixture, creating aerobic (5% O_2 and 95% N_2) and anaerobic (10% H_2, 10% CO_2 and 80% N_2) conditions. Gut epithelial cells are grown at the interface of these two environments to simulate the gut membrane-lumen interaction (Schüller and Phillips, 2010; Naz *et al.*, 2013).

Bacteroides dorei is an abundant gut commensal discovered in 2006 and found to be a member of a healthy microbiota (Bakir *et al.*, 2006; Martínez, Muller and Walter, 2013). To date, no study has been done on the interaction between *B. dorei* and *C. difficile*. In this chapter, we will investigate the effects of *B. dorei* on *C. difficile* within biofilms as well as within an E-VDC, an *in vitro* gut epithelial model established within the group (Anonye *et al.*, 2019).

4.2 Results

4.2.1 Quantifying individual species from *C. difficile* and *B. dorei* cocultures

Slater *et al.*, 2019 showed *C. difficile* and *B. fragilis* could be grown on BHIS media and plates; distinct morphologies were observed when *C. difficile* supplement is added to BHIS. *C. difficile* supplement was designed to help isolate *C. difficile* from samples by enhancing its growth and limiting the growth of other species. The supplement is commercially available and contains two antibiotics; D-cycloserine and cefoxitin. We tested the viability of this approach with *B. dorei* and *C. difficile* (Figure 4). We found that *C. difficile* colonies grew larger and were white/yellow in appearance, whereas *B. dorei* was smaller in size and are moderately translucent. Thus, we were able to use the standard colony-forming unit (CFU) assay in BHIS+*C. difficile* supplement agar to quantify *C. difficile* and *B. dorei* from mixed cocultures.

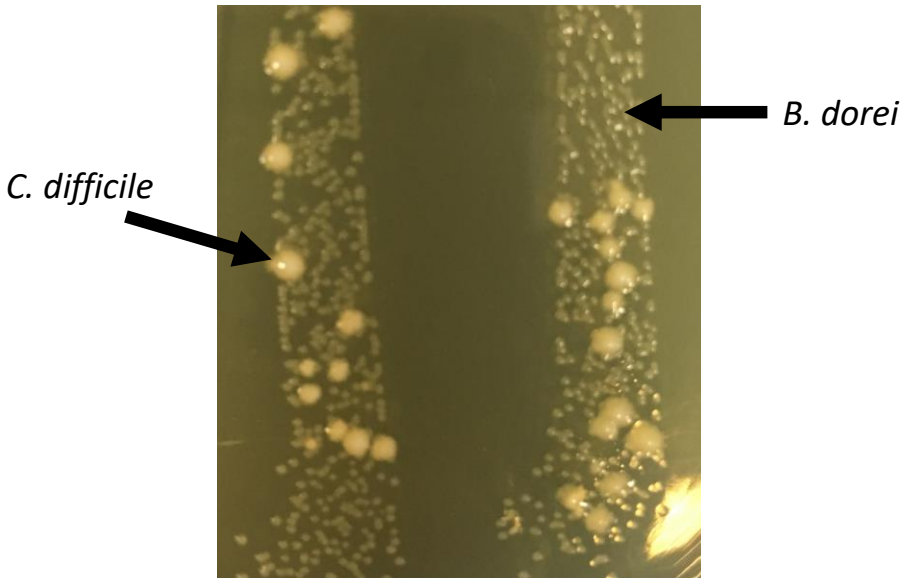

Figure 4: **Morphology differences between *C. difficile* and *B. dorei* when cultured on BHIS with *C. difficile* supplement.** *C. difficile* colonies are larger in size and were more yellow in appearance than *B. dorei*.

4.2.2 Reduced *C. difficile* numbers in mixed biofilms with *B. dorei*

Several *Bacteroidetes* have been shown to inhibit *C. difficile*. As bacteria in the gut are attached to the gut surfaces, and in close proximity with each other, we evaluated *C. difficile* (R20291, Trevor Lawley) interaction with *B. dorei* (CL02T00C15, BEI resources) within adherent communities. The two species were cultured overnight as described in Methods 3.6 and diluted to 0.1 OD_{600} before addition to a 24-well polystyrene plate. Three conditions were tested: *C. difficile* and *B. dorei* as monocultures and a coculture of both species. At 24 hours, the biofilms were washed, and CFUs were counted. In the cocultures, we found that the presence of *B. dorei* significantly reduced (by over 10-fold) the number of *C. difficile* when compared to its monoculture control (unpaired Student T-test, *P*-value = 0.0004) (Figure 5). In contrast, *B. dorei,* when cultured with *C. difficile* grew far better than when cultured alone (unpaired Student T-test, *P*-value = 0.0006). This reduction in *C. difficile* numbers indicated an inhibition mediated by *B. dorei*. To ensure there was no bias in the initial biofilm inoculums, we measured the CFU values of each species, no significant differences were observed between *C. difficile* and *B. dorei* (Appendix 2, Supp Figure 1). We attempted to study this interaction further using immunofluorescent microscopy but found *B. dorei* biofilms extremely fragile on glass slides resulting in their loss during the staining process.

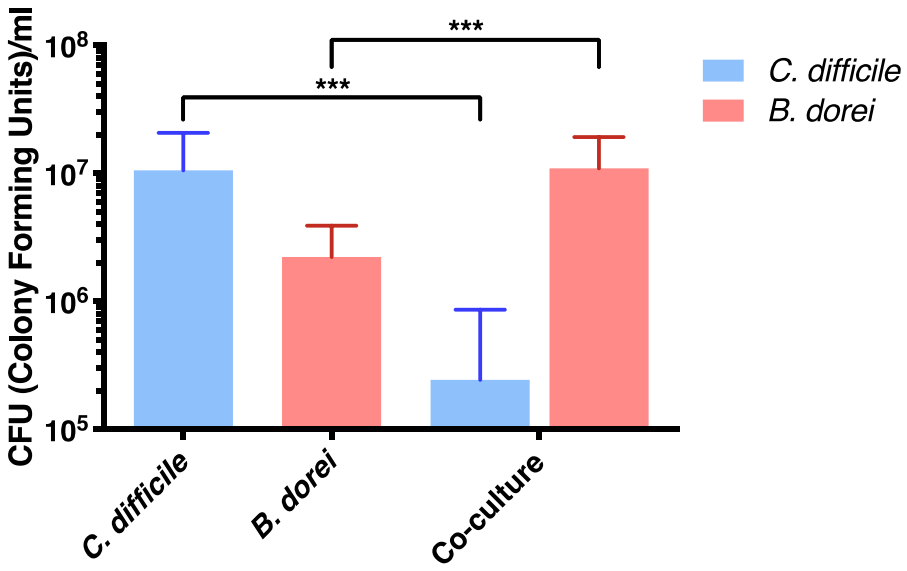

Figure 5: ***B. dorei* interactions with *C. difficile* within biofilms.** Single or mixed cultures of *B. dorei* and *C. difficile* were incubated on polystyrene plates for 24 hours. Biofilms

were washed prior to CFU values been taken. Data shown is the mean of three independent tests, with error bars indicating the standard deviation. Significant difference was determined by an unpaired Student T-test, *** indicating a *P*-value < 0.001.

4.2.3 Testing proximity and secretion of interaction

Having observed a potential inhibitory interaction between *C. difficile* and *B. dorei*, we investigated the mode of action. Firstly, we determined the proximity at which *B. dorei* was able to inhibit *C. difficile*. Planktonic cultures allow for more spatial separation than their biofilm counterparts. Overnight inoculums of each species were diluted to 0.1 OD_{600} were added to 15 ml Falcon tubes and incubated anaerobically at 37°C for 24 hours. The same three conditions were used as before; two monocultures and a coculture of the two species. In planktonic cultures, we saw that there was no reduction in *C. difficile* numbers as seen in the biofilm (Figure 6). However, when tested with an unpaired student's T-test, we still see significantly more *B. dorei* in coculture conditions than in the monoculture (*P*-value = 0.0001). The lack of inhibition implies that *B. dorei* needs to be in close proximity to *C. difficile* to have an impact.

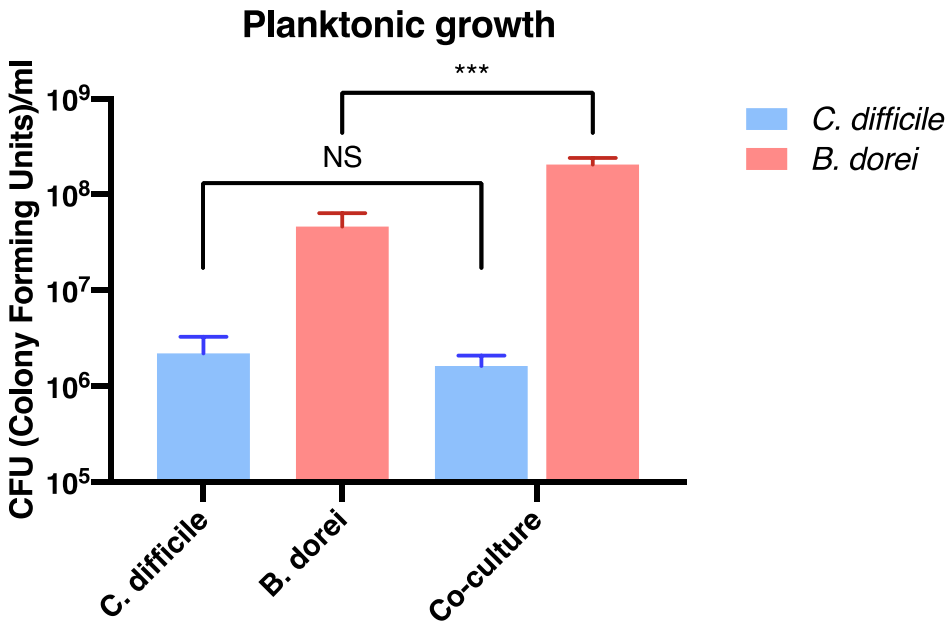

Figure 6: **The effect of planktonic conditions on the interaction between *B. dorei* and *C. difficile*.** Planktonic cultures of *B. dorei*, *C. difficile* and a mixed culture of the two were grown for 24 hours. Data shown is the mean of three biological triplicates, with error bars

indicating the standard deviation, significant difference was determined by an unpaired Student's T-test, *** indicating a *P*-value < 0.001.

To determine if the inhibition is due to a secreted molecule, we tested if *C. difficile* biofilm formation was affected when cultured with cell-free supernatant (spent medium) from a *B. dorei* culture. Cells were removed from *B. dorei* overnight cultures by centrifugation and 0.05 μm filtration leaving just spent media. Solutions were made up to contain either 100% fresh medium (0% spent), 10% spent – 90% fresh mix, or 100% spent medium. Each solution was then added to *C. difficile* cells collected from overnight cultures to achieve 0.1 OD_{600}. Fresh medium and the 10% spent mix performed similarly, with no inhibition seen (Figure 7). However, when using 100% spent medium we saw no signs of *C. difficile* growth. We suspect the nutritional loss at 100% likely becomes the major factor preventing *C. difficile* growth.

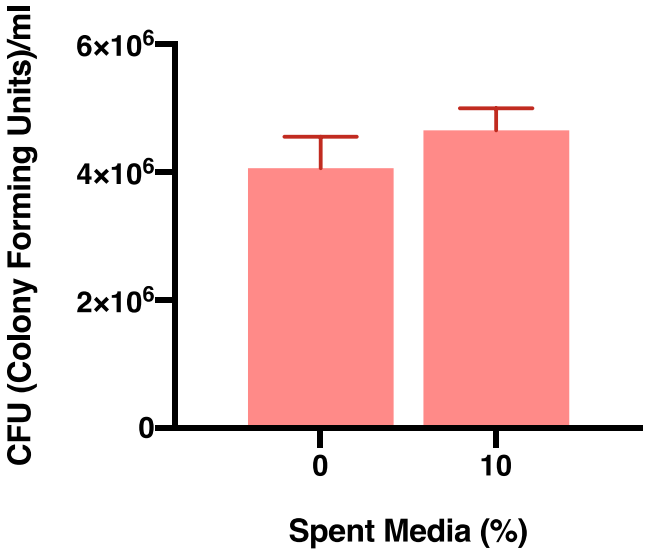

Figure 7: ***C. difficile* is uneffected by low concentration of cell-free spent *B. dorei* medium.** Overnight cultures of *B. dorei* were centrifuged and the supernatant filtered to remove cells. This medium was used to culture *C. difficile* at three concentrations 0, 10 and 100%, diluted using fresh medium (BHIS). Using 100% spent medium resulted in no growth. Data shown is result of three biological repeats.

4.2.4 Proteomics

In order to identify what causes an inhibition interaction to occur between *C. difficile* and *B. dorei* during coinfection, we studied the whole-cell proteins in single species cultures and coculture conditions at 24 hours in *in vitro* biofilms using mass spectrometry. Proteomics has successfully been used to study the interaction between *Staphylococcus aureus–Candida albicans* in a similar biofilm setup as described here (Peters *et al.*, 2010). Slater *et al.*, 2019 investigated the interaction between *C. difficile* and *B. fragilis* a phylogenetically close relative of *B. dorei* (Lange *et al.*, 2016). Similarly, to our work they used BHIS and studied the interaction in both biofilm and planktonic conditions. Slater *et al* found *B. fragilis* much like *B. dorei* is only able to inhibit *C. difficile* when in close proximity. Using RNAseq they compared RNA expression between single and duel culture of *B. fragilis* and *C. difficile*, finding that *B. fragilis* inhibition on *C. difficile* was a metabolically based one. We hypothesize *B. dorei* is using a similar method and we expected to see changes in protein levels reflecting this (Slater *et al.*, 2019).

Biofilms were prepared as before in three conditions; two monocultures of each species and a coculture of the two. At 24 hours biofilms were washed and then resuspended in 8M Urea Buffer, technical replicates were combined to increase the protein concentration. The cells were lysed through bead beating, and the proteins were purified (See Methods 3.7). We used the following two uniport databases to match our Mass-spec peptides; UP000002070 for *C. difficile* (Stabler *et al.*, 2009) and UP000005974 for *B. dorei* (Gevers *et al.*, 2012).

Only proteins found to be present in two or more biological repeats were carried forward from the initial identification, leading to a total of 844 proteins; 486 for *C. difficile* and 358 for *B. dorei* (Appendix 2, Supp Table 1 & 2). We found a number of proteins either detected in monoculture or coculture but not present in the other condition. These proteins were excluded from our statistical analyses (Table 2 & Table 3). When values were not present in both conditions, there was no way to accurately calculate fold change between the two, however, given they were not detected in the other condition they were

likely to be significant. The remaining proteins were statistically analysed. From principal component analyses (PCA) of the two species, we saw weak clustering of the coculture data (Figure 8). The only tight clustering present was that of *B. dorei* monocultures, this means the data contained a large amount of variance. To establish which proteins had significantly changed between the two culture conditions, we used a *P*-value cut-off of 0.05 and a log2 Fold Change > |0.1| (Figure 9). A total of 15 *C. difficile* and 7 *B. dorei* proteins were found to be significantly altered (Table 4 & Table 5).

Table 2: ***C. difficile* proteins found in coculture with *B. dorei*.** The following *C. difficile* proteins were only detected by mass-spec when cultured with *B. dorei*. These were removed from future statistical testing as fold change cannot be calculated.

Protein ID	Protein Description/Name	Associated Gene
C9YHH6	**DNA integrity scanning protein DisA**	**disA** CDR20291_0017
C9YHW1	**4-hydroxyphenylacetate decarboxylase large subunit, EC 4.1.1.83, HpdB**	**hpdB** CDR20291_0152
C9YHZ6	**Orotate phosphoribosyltransferase, OPRT**, OPRTase, EC 2.4.2.10	**pyrE** CDR20291_0188
C9YIW7	Uncharacterized protein	CDR20291_0512
C9YJX9	Putative transcriptional regulator	CDR20291_0879
C9YKC1	**3-oxoacyl-[acyl-carrier-protein] synthase 2, KAS-II, EC 2.3.1.179**	**fabF** CDR20291_1022
C9YKX7	GntR-family transcriptional regulator	CDR20291_1229
C9YL03	**D-alanine--D-alanine ligase, EC 6.3.2.4**	**ddl** CDR20291_1255
C9YLT0	Tellurium resistance protein	CDR20291_1533
C9YM07	**UPF0145 protein CDR20291_1610**	CDR20291_1610
C9YMQ2	**Biotin carboxylase, EC 6.3.4.14, EC 6.4.1.2**	**accC** CDR20291_1861
C9YMQ7	Uncharacterized protein	CDR20291_1866
C9YNT2	**Thioredoxin reductase, EC 1.8.1.9**	**trxB3** CDR20291_2243
C9YPE7	**Ribulose-phosphate 3-epimerase, EC 5.1.3.1**	CDR20291_2461
C9YPQ8	Putative regulatory protein	CDR20291_2573

Table 3: ***B. dorei* proteins only present in coculture with *C. difficile*.** The following *B. dorei* proteins were only detected by mass-spec when in cocultured with *C. difficile*. These were removed from future statistical testing, as fold change cannot be calculated accurately.

Protein ID	Protein Description/Name	Associated Gene
I9FQD9	Uncharacterized protein	HMPREF1064_01799
I9R2T7	**Ribokinase, RK, EC 2.7.1.15**	**rbsK** HMPREF1064_01567

From the two list sets generated for *C. difficile* (Table 2 & Table 4), we found there are a number of proteins linked with iron associated stress; thioredoxin reductase (*trxB3*), CooS (*cooS*), RnfE (*rnfE*), transketolase (*tkt*), OPRT (*pyrE*) and KAS-II (*fabF*) (Berges *et al.*, 2018). *B. dorei* could be competing with *C. difficile* for iron, when compared to the protein changes found in low iron conditions by Berges *et al.*, 2018; we found matches in the increased abundance of transketolase, OPRT and KAS-II. However, thioredoxin reductase, CooS and RnfE all contradicted their low iron expected result. These proteins may be associated with the general stress response in *C. difficile*, as we also saw the DNA repair protein DisA in higher abundance in coculture. Changes in fatty acid synthesis were also observed with Biotin carboxylase (*accC*) and KAS-II was found to be more abundant in coculture, changes in fatty acid synthesis were also observed in *C. difficile* when coculture with *B. fragilis* (Slater *et al.*, 2019). Interestingly, we also saw proteins associated with *D-alanine* and *L-alanine* production in differing states; alanine:alanine ligase (*ddl)* was in higher abundance in coculture whereas alanine racemase (*alr)* was more abundant in the monoculture control. The final protein of interest found more abundant when *C. difficile* is in coculture was HpdB (*hpdB*). HpdB is required for the formation of pare-cresol (p-cresol), a bacteriostatic compound that has been shown to adversely affect the gut microbiota (van Leeuwen *et al.*, 2016; Passmore *et al.*, 2018). *C. difficile* may therefore attempt to inhibit *B. dorei* using p-cresol.

When examining proteins associated with *B. dorei* we found an increased production of SecA (*secA*) in the coculture condition, this protein is part of the Sec translocase complex used to actively transfer proteins across the cell membrane. This could indicate *B. dorei* was actively secreting a compound to

inhibit *C. difficile*. Metabolic stress could have also caused *B. dorei* to increase SecA production alongside DnaK (*dnak*) (van Wely *et al.*, 2000; Anglès *et al.*, 2017).

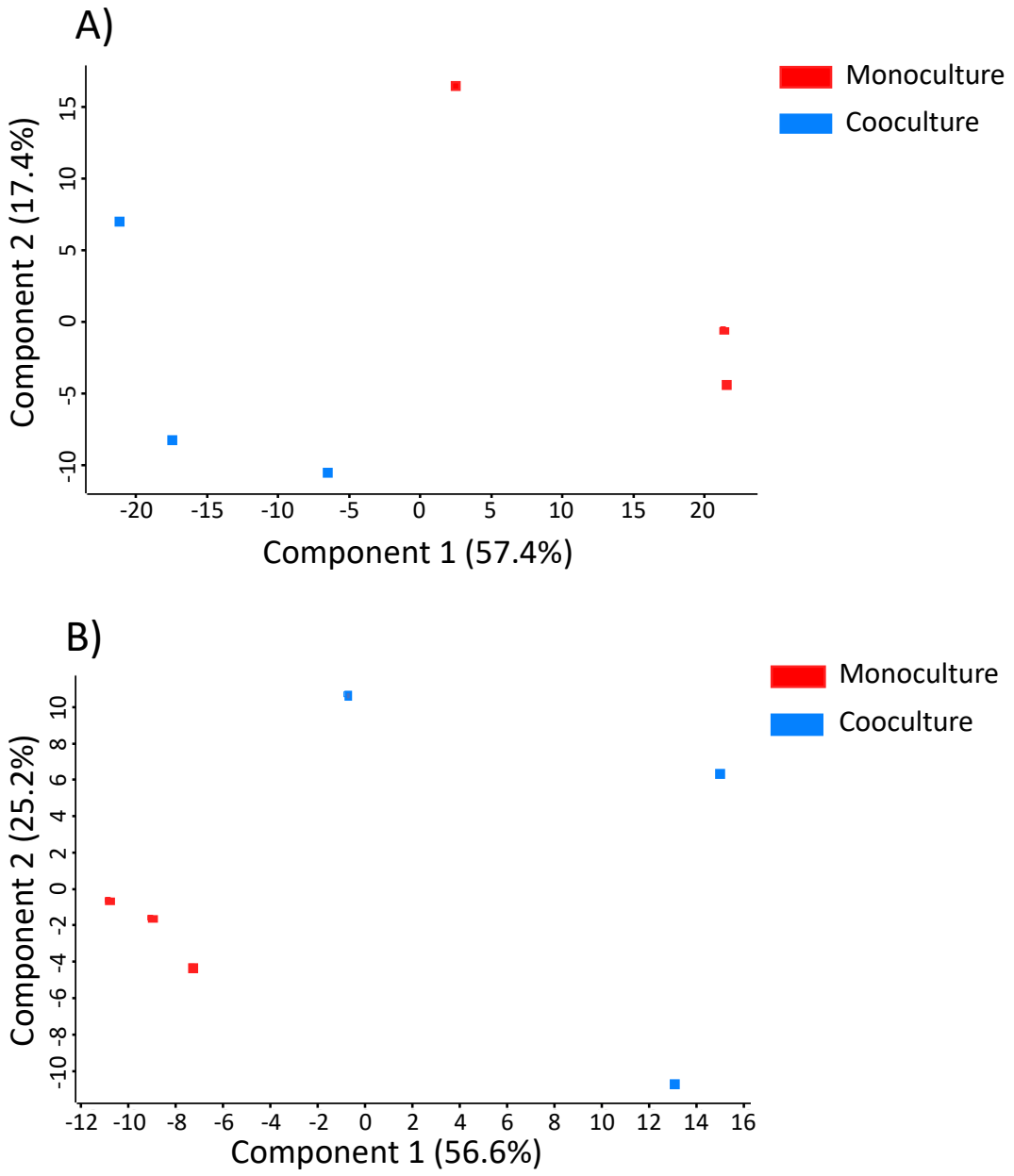

Figure 8: **Principal component analysis (PCA) plot of *C. difficile* and *B. dorei*.** A comparison between the proteomics of monocultures and cocultures of the two bacteria was done for **A)** *C. difficile* and **B)** *B. dorei*.

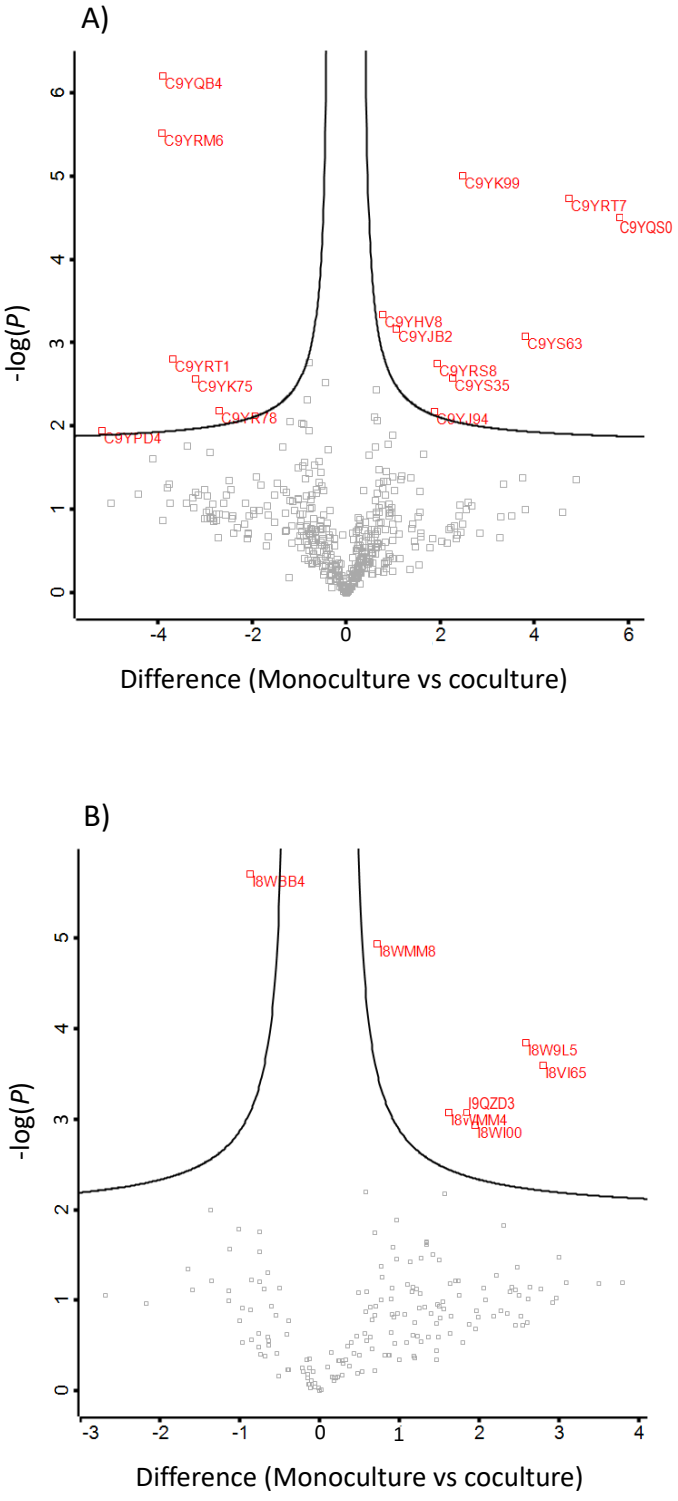

Figure 9: **Volcano plots of statistical significance against foldchange between single species cultures of *B. dorei* and *C. difficile* and a mixed cocultured A)** *C. difficile* and **B)** *B. dorei*. A protein was marked as significantly changed when its *P*-value < 0.05 (-log(*P*) < 1.3) and a log2 Fold Change > |0.1|.

Table 4: ***C. difficile* proteins significantly altered between mono- and coculture conditions with *B. dorei*.** A protein was marked as significantly changed when its P-value < 0.05 (-log(P) < 1.3) and a log2 Fold Change > |0.1|. A negative fold change indicates that the protein was more abundant in the monoculture, with a positive change indicating more of a presence in the coculture.

Protein ID	Protein Description/Name	Associated Gene	-log(*P*-value)	Fold Change
C9YHV8	Putative glycoprotease	CDR20291_0149	3.344383521	0.764368693
C9YJ94	**Carbon monoxide dehydrogenase, CooS, EC 1.2.7.4**	**cooS** CDR20291_0643	2.180489187	1.876255671
C9YJB2	Uncharacterized protein	CDR20291_0661	3.168741422	1.053012212
C9YK75	**Ion-translocating oxidoreductase complex subunit E, RnfE**	**rnfE** CDR20291_0976	2.565084525	-3.208879471
C9YK99	**50S ribosomal protein L27**	**rpmA** CDR20291_1000	5.007203511	2.472389857
C9YPD4	**50S ribosomal protein L28**	**rpmB** CDR20291_2448	1.944797508	-5.190443675
C9YQB4	**Permease IIC component**	**celB** CDR20291_2779	6.203635112	-3.908596675
C9YQS0	**Peptidase M20 domain-containing protein 2**	CDR20291_2937	4.513044644	5.802981059
C9YR78	**Probable membrane transporter protein**	CDR20291_3096	2.183480443	-2.700681686
C9YRM6	Sirohydrochlorin cobaltochelatase	**cbiK** CDR20291_3244	5.519976528	-3.932998657
C9YRS8	Transketolase, thiamine disphosphate-binding subunit	**tkt** CDR20291_3296	2.749546573	1.920532227
C9YRT1	**Alanine racemase, EC 5.1.1.1**	**alr** CDR20291_3299	2.811694701	-3.700857162
C9YRT7	**ATP synthase gamma chain** (ATP synthase F1 sector gamma subunit)	**atpG** CDR20291_3305	4.737640491	4.736573537
C9YS35	**4-diphosphocytidyl-2-C-methyl-D-erythritol kinase, CMK, EC 2.7.1.148**	**ipk** ispE, CDR20291_3403	2.575605343	2.255695343
C9YS63	Uncharacterized protein	CDR20291_3431	3.076369059	3.799568176

Table 5: ***B.dorei* proteins significantly altered between mono and coculture conditions with *C. difficile*.** A protein was marked as significantly changed when its P-value < 0.05 (-log(P) < 1.3) and a log2 Fold Change > |0.1|. A negative fold change indicates that the protein was more abundant in the monoculture, with a positive change indicating more of a presence in the coculture.

Protein ID	Protein Description/Name	Associated Gene	-log(*P*-value)	Fold Change
I8VI65	**Elongation factor Ts, EF-Ts**	**tsf** HMPREF1064_05075	3.597038221	2.793612162
I8W9L5	**DNA-directed RNA polymerase subunit beta, RNAP subunit beta, EC 2.7.7.6**	**rpoB** HMPREF1064_01951	3.846463583	2.579786301
I8WBB4	**Pyruvate kinase, EC 2.7.1.40**	HMPREF1064_01850	5.711204549	-0.882769903
I8WI00	**Chaperone protein DnaK** (HSP70)	**dnaK** HMPREF1064_00889	2.941571434	1.938463211
I8WMM4	**Protein translocase subunit, SecA**	**secA** HMPREF1064_00664	3.079606063	1.604860942
I8WMM8	Uncharacterized protein	HMPREF1064_00669	4.945887767	0.709132512
I9QZD3	**30S ribosomal protein S10**	**rpsJ** HMPREF1064_01957	3.079308419	1.836484909

4.2.5 Reduction in adherent *C. difficile* when cultured alongside *B. dorei* in a gut model

To better study the interaction between the two bacteria, we incorporated them into a more physiologically accurate model. We used an *in vitro* dual-chamber gut model (E-VDC) to culture *B. dorei* and *C. difficile* alongside gut epithelial cells (Caco-2 and HT29-MTX). Before culturing *B. dorei* and *C. difficile* in the system we had three main questions;

- Does this system allow the culturing of non-spore forming, strictly anaerobic bacteria?
- Does the system allow the maintenance of two species?
- What is the impact of the epithelial representative on their interaction?

Prior to our publication (Anonye *et al.*, 2019), of which this work is part of, to our knowledge the E-VDC system had only been used only for single-species experiments with facultative anaerobes or microaerophilic bacteria (Grass and Sweetana, 1988; Schüller and Phillips, 2010; Mills *et al.*, 2012; Tran *et al.*, 2014). *B. dorei* is a strictly anaerobic bacterium, with no spore-forming capabilities making it the first to be tested in the system.

The epithelial cells were cultured for two weeks prior to any infection to allow a monolayer to form. Overnight cultures of *C. difficile* and *B. dorei* were grown to stationary phase in BHIS. The cultures were then centrifuged and resuspended in DMEM-10 (antibiotic-free). No OD_{600} adjustment was carried out, as at high OD_{600} values *B. dorei* has a poor OD to CFU/ml correlation. We found that diluting the resuspended cultures 1:1 in DMEM-10 gave us reliable and useable CFU/ml values; 5×10^7–2.9×10^8 CFU/ml. This result gave a MOI of 500–1000:1. As we were interested in the adherent bacterial populations, or those interacting with the epithelial cells, we removed the basolateral media and washed once with PBS 3 hours post-infection, replacing with fresh reduced DMEM-10. The infected cells were further incubated for 24 hours.

When cultured within the E-VDC, we observed that both monocultures of each species grew over the 24 hour period (Figure 10A and B), meaning non-spore forming strictly anaerobic bacteria can be used in the E-VDC. When tested with an unpaired Student's T-test we saw at 24 hours significantly less *C. difficile* in coculture with *B. dorei* than when cultured alone. This matches the result seen in the biofilm conditions. However, unlike the biofilm result, there was no significant difference between *B. dorei* alone and in coculture at 24 hours. We investigated an earlier time point of 3 hours to see if initial adherence impacts the interaction between the two species. We found that *B. dorei* had no inhibitory effect on *C. difficile* at this earlier time point. However, *B. dorei* did have significantly more colonies in coculture than compared to its monoculture counterpart (Unpaired Student's T-test, *P*-value = 0.0007).

To assess the health of the epithelial cells, the E-VDC allows for measurements of transepithelial electrical resistance (TEER). TEER values indicate the integrity of cellular barriers. It is a quantitative measurement of the integrity of the tight junction dynamics of the epithelial monolayers (Srinivasan *et al.*, 2015). TEER is a measurement of electrical resistance, the higher the value, the tighter junction gaps are between cells, the higher the TEER value, the healthier the system. We found that *C. difficile* monocultures rapidly decayed the cell layer, lowering the TEER value (Figure 10C). After 24 hours, *C. difficile* lowered the TEER value on average to 273 Ω, with ~600 Ω been that of an uninfected Snapwell insert. *B. dorei,* which is a commensal, showed signs of TEER decay too, but at a much slower rate similar to that seen in the uninfected control (Figure 10D). We believe the initial decline from 0 to 3 hours in our uninfected control was likely the result of some form of cell shock/stress due to the cells being moved into the new system. Although we saw a reduction in *C. difficile* numbers when cocultured with *B. dorei,* there was no reduction seen in TEER decay when compared to the monoculture. This could have been because the reduction in *C. difficile* numbers was small, so any toxins released will probably have remained at similar levels, causing similar levels of decay.

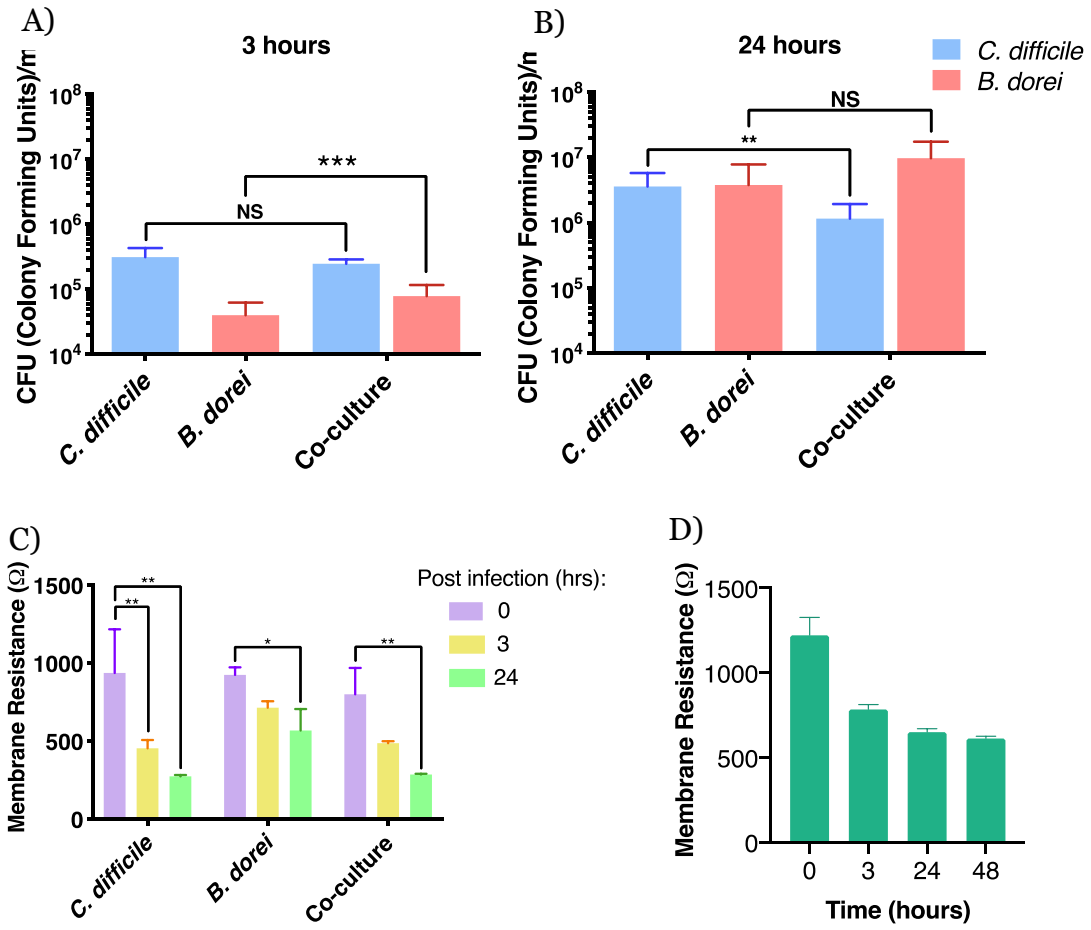

Figure 10: **Studying the *C. difficile* – gut commensal *B. dorei* interactions within the dual environment gut model.** *B. dorei* and *C. difficile* mono- and mixed cultures were incubated with an epithelial monolayer (Caco-2 and HT29-MTX) in the E-VDC for **A)** 3 hours and **B)** 24 hours. The epithelial layer was washed and resuspended prior to CFU values been taken. Data shown is the mean of three independent repeats with error bars indicating standard deviation. Significant difference was determined by unpaired Student's T-test, *P*-values - *** < 0.001, ** < 0.01 and NS – not significant. **C)** Reduction of the epithelial monolayers was measured by TEER. A two-way ANOVA determined a significant difference between time points (*P*-value = 0.0002). The Post-hoc Sidak's test was used to determine specific difference – *P*-values - ** < 0.01, * < 0.05. **D)** An uninfected gut epithelial layer integrity was tracked over 48 hours with the E-VDC, this work was conducted in collaboration with Dr Blessing Anonye. Data shown for A, B and C is the mean of three biological triplicates, for D data is the mean of three biological repeats (no technical).

4.3 Discussion

We believe *B. dorei* has an inhibitory effect on *C. difficile*, as its presence negatively impacts *C. difficile* both in the gut model (E-VDC) (Figure 10) and in biofilm conditions (Figure 5). Compared to previous work with *B. fragilis* carried out in biofilm conditions (Slater *et al.*, 2019), we found that *B. fragilis* impacts *C. difficile* 10-fold more than *B. dorei*. Interestingly *B. fragilis* much like *B. dorei* had higher numbers in mixed culture with *C. difficile* than it did on its own. This result was unexpected as individuals infected with *C. difficile* generally have a reduction in the abundance and diversity of *Bacteroidetes* (Shahinas *et al.*, 2012). The initial reduction in Bacteroidetes was likely the result of the dysbiosis causing factor which leads to a *C. difficile* infection, such as antibiotic treatment. However, given the improved growth seen by *B. dorei* and *B. fragilis* it would imply that they would be able to recover during the infection. It would be interesting to investigate the effects of Bacteroides on a pre-established *C. difficile* biofilm, to determine if it causes the same improved growth, or once established begins to prevent initial binding or early growth leading to the inhibition we see *in vivo*.

Research has shown that *C. difficile* is able to influence the gut microbiota through the production of indole (Darkoh *et al.*, 2019), a heterocyclic organic compound produced from tryptophan by species within the gut microbiota. Darkoh *et al.*, 2019 screened stool from CDI patients and found it more abundant in indole when compared to non-CDI patients. This was an unusual result as none of the sequenced genomes of *C. difficile* contained the tryptophanase (tnaA) gene homolog required to make indole. Further investigation found that *C. difficile* is able to manipulate species in the gut microbiota to produce indole, *E. coli* when cultured with *C. difficile* showed a significant upregulation of tnaA, leading to an increase in indole. Indole has an inhibitory effect on bacterial growth, concentrations observed in CDI patients were higher than the MICs of numerous bacteria, including *B. fragilis* (Darkoh *et al.*, 2019). If *C. difficile* is controlling Bacteroidetes levels in this way it may explain the lack of *B. dorei* and *B. fragilis* inhibition seen in dual species interaction.

B. dorei, when cultured in planktonic conditions with *C. difficile,* had no inhibitory properties, this result again matches with data obtained with *B. fragilis*. Given the similarities between the two, it could be possible that the inhibition is through the same mechanism. *C. difficile* uses the AI-2 a quorum-sensing molecule, and upon sensing this molecule, *B. fragilis* appears to trigger a change in metabolism that leads to an inhibition of *C. difficile* (Slater *et al.*, 2019). To establish the mode of action for *B. dorei* inhibition of *C. difficile* we investigated whether a secreted molecule is produced in the spent media of *B. dorei*. We tested *C. difficile* biofilm growth in two concentrations of spent media; 10 and 100%. We found polarising results with 10% showing no inhibition and at 100% showing complete inhibition (Figure 7). The problem with using a spent medium approach is that the medium will be highly nutritionally depleted, although it could potentially contain inhibitory molecules. A lack of nutrients could lead to false positives (signs of inhibition) with essential components missing for *C. difficile* growth. Separating the nutrition impact from the potential inhibitory molecules is quite difficult. For this experiment, we used cell-free spent media from overnight planktonic cultures of *B. dorei*. Given the result that planktonic *B. dorei* is unable to inhibit *C. difficile* when we repeat this work to increase the range of spent media concentration, we plan to use medium taken from *B. dorei* in biofilm conditions. An alternative approach to using spent medium would be the use of a Transwell assay. A Transwell spatially separates the two bacteria spatially but allows them to share the same media through a porous membrane (Fang, Jin and Hong, 2018).

To establish how the two bacteria were interacting and the possible mechanism by which *B. dorei* was inhibiting *C. difficile,* we used a proteomic approach. We found that compared to a monoculture *C. difficile* was exhibiting differences in proteins associated with iron stress. This led us to suspect that *B. dorei* was competing with *C. difficile* for iron, causing *C. difficile* to have an iron-deficiency. Comparing our result to that of Berges *et al.*, 2018, we found inconsistencies with transketolase, OPRT and KAS-II. All three having the opposite response to the published iron deficient result (Berges *et al.*, 2018).

It may be more likely that these 7 proteins are associated with a general stress response. Interestingly we found two fatty acid biosynthesis proteins, biotin carboxylase and KAS-II in higher abundance when *C. difficile* is in coculture. Fatty acid biosynthesis was upregulated in gene expression data from *C. difficile* when cultured with *B. fragilis,* also biotin carboxylase was similarly found to be upregulated (Slater *et al.*, 2019). The upregulation in fatty acid production by *E. coli* and *S. aureus* is associated with a stress response, the bacteria adjust membrane fluidity and diffusion rates likely to cope with environmental stress (R. Wang *et al.*, 2018). In coculture, we saw an abundance of HpdB, but no levels were detected in the monoculture control. HpdB is involved in the synthesis of p-cresol a phenolic bacteriostatic compound that targets Gram-negatives it has been shown to negatively affect the gut microbiota (Passmore *et al.*, 2018). We hypothesize that *C. difficile* can detect *B. dorei* and tries to emit a p-cresol response in defence. However, p-cresol is made through the conversion of 4-hydroxyphenylacetic acid obtained by the fermentation of tyrosine (van Leeuwen *et al.*, 2016). The BHIS medium we used contained only low levels of tyrosine meaning *C. difficile* would have been unable to produce sufficient levels of p-cresol to cause an inhibitory effect. This could account for why *B. dorei* was able to survive in coculture. When focusing on *B. dorei*, there was nothing evident in the proteomics data that could explain the inhibition of *C. difficile*. We can only surmise that there was a resource competition occurring between the two species, and *B. dorei* was winning.

There are two published gut models that can be used to culture *B. dorei* and *C. difficile* alongside gut epithelial cells; the HuMiX (Shah *et al.*, 2016) and the Gut-on-a-chip (Shim *et al.*, 2017). Both these systems are fluidic, and hence they can be cultured for a longer duration than the E-VDC. The static nature of the E-VDC system limits the time frame of our experiments but greatly reduces setup complexity and cost. The VDC system benefits from a robust seeding mechanism as it uses the well-established Snapwell/Transwell culturing apparatus. Microfluidic systems like the gut-on-a-chip are plagued by unreliability at early stages, with gas bubbles causing irreversible damage to the cell layer. The HuMiX system avoids this seeding difficulty by being

much larger (millifluidics), however, its design means that gut epithelial cells are spatially separated from bacteria by a microporous membrane. This prevention of direct contact limits experiments to non-adhesion investigations. As a result, we would be unable to study bacteria adhered to the cell surface/mucus layer where they would normally reside. This led us to choose the E-VDC for our experiments.

We successfully showed that strict anaerobic bacteria could be cultured in the E-VDC model, with both species able to adhere and grow on the epithelial/mucus layer. When testing the coculture, we found that the inhibition of *C. difficile* was noticeably reduced when performed in the gut model (Figure 10). The main difference between the gut model and the biofilm assay, aside from the addition of epithelial cells was the change from BHIS to DMEM-10. One could hypothesize that the media change may affect inhibition, especially if the inhibition was through the competition of a resource. Given that *C. difficile* and *B. dorei* need to be in close proximity for inhibition of *C. difficile* growth to occur (shown by our planktonic assay), we predict that there is a spatial aspect to the inhibitory properties of *B. dorei*. We hypothesize that the uneven epithelial layer may create pockets where *C. difficile* can escape from *B. dorei* and avoid the inhibitory effects to some degree. The density of *B. dorei* and *C. difficile* was also far lower on epithelial cells than the polystyrene membrane used for the biofilm assays. This spatial hypothesis can be further explored with the use of microscopy, labelling both the bacteria will allow one to see where they establish themselves on the epithelial layer.

Experiments carried out in the gut model revealed that *C. difficile* could damage the epithelial cells which agreed with work carried out in *in vivo* models (Chen *et al.*, 2008; Hutton *et al.*, 2014). *C. difficile* produces two toxins that are known to disrupt epithelial cell layer (Mahida *et al.*, 1996; Kuehne *et al.*, 2010; Kasendra *et al.*, 2014). We have tracked both toxin A and B levels in the E-VDC using an ELISA assay (Conducted by Dr Blessing Anonye, Anonye *et al.*, 2019). We found that toxin A and B were both present, with toxin A significantly increasing over 24 hours. However, both toxins were detected at

low levels, below what had been previously shown to impact Caco-2 cells (Mahida *et al.*, 1996; Kasendra *et al.*, 2014; Anonye *et al.*, 2019). Low levels of the two toxins may be able to cause the loss of membrane integrity we observed as *C. difficile* may also produce other secreted enzymes that augment toxin activity.

When testing the TEER of epithelial cells in the presence of *B. dorei* we saw a trend over time similar to our uninfected controls (Figure 10C & D). Both had a decay in TEER, however at a much slower rate than epithelial cells with *C. difficile*. We predict that the decline seen was a result of stressed epithelial cells during their transition into the E-VDC. Mills *et al.*, 2012 also observed in the E-VDC model a similar decrease in TEER at 3 hours followed stabilisation at later time points. In coculture condition, although a decrease in *C. difficile* numbers occurred, a TEER decay trend similar to that observed in the *C. difficile* monoculture was apparent. Although untested, we predict that similar levels of the two toxins would be present as the reduction in *C. difficile* numbers is only small.

To identify why the inhibitory effect of *B. dorei* on *C. difficile* appeared to be less in the E-VDC, we need to further study whether this effect is observed from changing medium to DMEM-10 or due to the presence of gut epithelial cells. To do this, we plan to repeat the biofilm assay in DMEM-10, any result from this will be independent of the epithelial cells. The static nature of the E-VDC has been a major drawback which needs to be addressed in the future. Although we argued the benefit of the simplistic setup, it is a limiting factor as epithelial cells cannot be cultured for long periods. To improve this, we plan to use lower densities of epithelial cells to allow for longer 48-hour cultures. Epithelial cells have been shown to be stable in the VDC for up to 72 hours. However, ultimately, we need to introduce flow into the systems it would allow us to study *C. difficile* behaviours over much longer periods. We believe this is necessary because, for example, during the observed 24-hour period the inhibition from *B. dorei* did not completely remove *C. difficile,* therefore, we do not know whether *C. difficile* is on a downward trajectory or whether it has the possibility to recover.

To conclude, we have established that *B. dorei* has a possible inhibitory effect on *C. difficile* when co-cultured in biofilms and in a gut model, but this effect is not present in planktonic conditions. To understand how *B. dorei* and *C. difficile* interact, a more in-depth analysis of the proteomics data generated here must be carried out. Unfortunately, this has not yet been possible due to time constraints. I believe that by utilising KEGG pathway analysis it may be possible to decipher the specific contributing factor(s) to the inhibitory effect *B. dorei* has on *C. difficile*, potentially establishing a mechanism of inhibition. Given that multiple other Bacteroidetes species have been reported to inhibit *C. difficile,* we plan to screen the phylum for more inhibitory species, with the aim of finding common mechanisms of inhibition.

5 Development of tools for tracking individual species in a mixed culture

5.1 Introduction

In the previous chapter, we studied the effect of what one commensal bacterium had on *C. difficile*. Representing the gut microbiota as a single species is useful for finding direct interactions, but any community-based effects would be overlooked. To truly model the gut, the microbiota needs to be represented by more than one species.

Identifying and quantifying species in a mixed community is challenging, simple microscopy cannot be used as cells are often morphologically too similar (Manz *et al.*, 1994). One option is to use selective media these have proven to be successful with small communities (Vandeplassche, Coenye and Crabbé, 2017). However, the difficulty of finding species-specific media increases as the community gets larger, such specific media also often detrimentally effects the growth of the species. In a mixed anaerobic population, propidium monoazide - qPCR (PMA-qPCR) has been shown to be successful at predicting cell concentration and biomass formation of individual species (Klein *et al.*, 2012; Yasunaga *et al.*, 2013; Ammann *et al.*, 2013).

The raw output curve from a qPCR run can be represented as a single value called the cycle threshold (Ct), this value is the point at which the fluorescent signal from the amplification of DNA is detected above the background. The more DNA present at the start of a qPCR run means the time required to reach Ct value is lower, as the number of amplification rounds (doublings of the initial DNA amplicon) will be less. The opposite is true for when there is less DNA, more cycles will be needed to reach the same Ct value. Thus, if there are more cells (in turn more DNA), there will be a lower Ct value. However, a Ct value is arbitrary on its own, as a small change can equal a substantial shift in bacterial number. The relationship between a species' bacterial number and Ct value is calculated through the use of a standard curve (Huang *et al.*, 2015). To improve the accuracy of the quantification, it is essential to quantify only active/live cells. Standard qPCR will quantify all cells, 'dead' and 'active' alike,

which gives an inaccurate abundance of individual species within a population. Treating with propidium monoazide (PMA) can rectify this (Figure 11). PMA is a photo-activated DNA binding dye that can only target cells with ruptured membranes or 'dead' cells (Nocker, Cheung and Camper, 2006; Nocker *et al.*, 2007; Yang, Badoni and Gill, 2011; Bellehumeur *et al.*, 2015; Lee, Lee and Kim, 2015; Tavernier and Coenye, 2015; Tantikachornkiat *et al.*, 2016). When PMA is photo-activated, it covalently binds to dsDNA, crosslinking the two strands, and this binding prevents DNA amplification during PCR (Yasunaga *et al.*, 2013). PMA also has a secondary effect, once bound it renders the DNA insoluble, causing a proportion to be lost during DNA extraction (Nocker, Cheung and Camper, 2006).

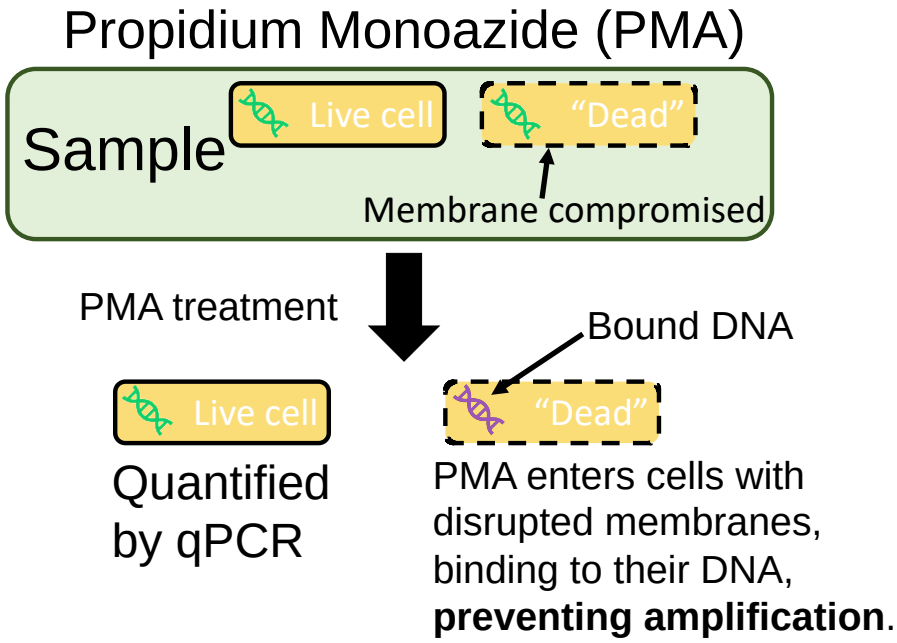

Figure 11: **Mechanism of action for propidium monoazide (PMA).** PMA is a DNA binding dye that can only enter cells with compromised cell membranes. When photoactivated, PMA forms a covalent bond with DNA that prevents PCR.

PMA-qPCR has been routinely used in the quantification of species from dental biofilms (Loozen *et al.*, 2011). *Streptococcus mutans* and *Streptococcus sobrinus* are key pathogens in the role of tooth decay. Assessing their numbers accurately is vital for understanding how well a treatment is working. Conventional DNA detection systems overestimated the cell population but PMA-qPCR was shown to better reflect an accurate total (Yasunaga *et al.*, 2013). *Candida albicans* is an opportunistic pathogenic yeast that is a common member of the gut microbiota and is responsible for oral candidiasis. The testing of treatments against *C. albicans* are carried out in mixed cultures as when tested alone there is a tendency to overestimate treatment effectiveness (Falsetta *et al.*, 2014). Luo *et al.*, 2017 successfully used PMA-qPCR to study the use of Peptoid (an antimicrobial peptide mimic) against mixed dental biofilms. In terms of the gut microbiota, the technique has been used to quantify *Bifidobacterium breve* (Yakult) from faecal samples (Fujimoto *et al.*, 2011), but its primary use has been in the detection of foodborne pathogens; *Escherichia coli*, *Campylobacter*, *Salmonella, Vibrio parahaemolyticus, Staphylococcus aureus and Listeria monocytogenes* (Banihashemi, Dyke and Huck, 2012; Zeng *et al.*, 2016). We believe PMA-qPCR enables the quantification of individual species within a representative microbiota.

The gut microbiota is made up of two general populations; planktonic bacteria and adhered biofilms. Few studies have been carried out on the adherent microbiota population of a healthy human gut as they require invasive biopsies (Crowther *et al.*, 2014a). As a consequence, little is known about the makeup and dynamics of the gut microbiota biofilms (de Vos, 2015). Biofilms are an essential mode of growth for many bacteria offering a heightened resistance to antimicrobial agents (Mah and O'Toole, 2001). Within the gut, the biofilm state of growth provides a spatial and metabolic niche (Macfarlane and Macfarlane, 2006). Planktonic bacteria are subject to 'wash out' from the continuous flow of the intestinal passage and may resort to biofilm reservoirs to avoid depletion. We aimed to create a trackable representative microbiota community, that can be used to investigate microbiota interaction in biofilm conditions.

5.2 Results

5.2.1 Tracking a nine species mixed biofilm

To expand from a single species representative, we elected to engineer a trackable synthetic microbiota. In the Methods section 3.5, we outline how we created a PMA-qPCR tracking system based on Ammann *et al.*, 2013 & Huang *et al.*, 2015 (Figure 12). The basic concept consists of sample DNA extraction followed by a qPCR run, which generates cycle threshold Ct values, a standard curve is then used to convert the Ct values to a DNA mass. Ct values are inversely related to the starting mass of DNA, the more DNA present the less cycles required for detection. Once the DNA mass is obtained, we calculated a bacterial number using the assumption that one genomic weights worth of DNA is equal to one bacterium.

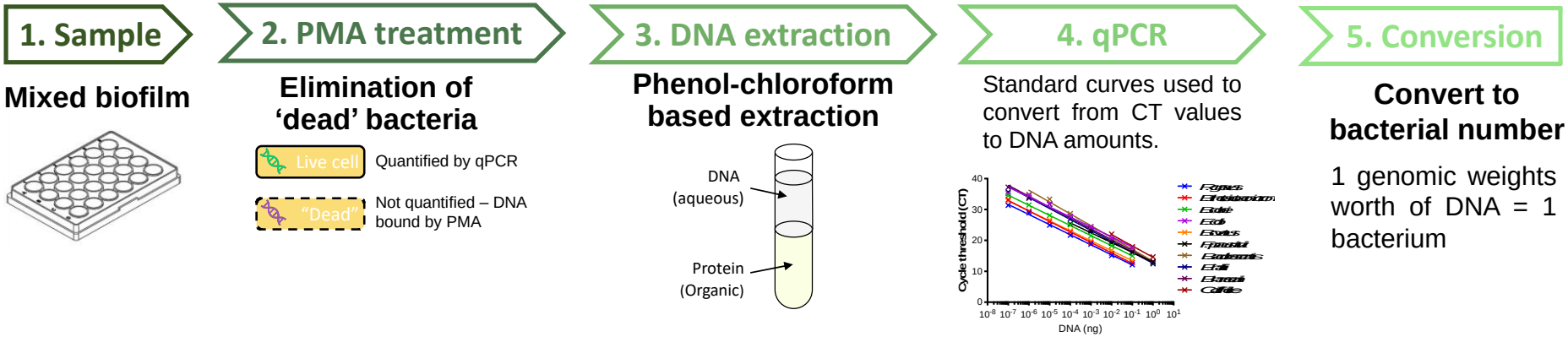

Figure 12: **Pipeline used to quantify individual species in a mixed biofilm.** Samples are PMA (Propidium monoazide) treated to ensure we quantify only 'live' DNA. Once treated cells are lysed and DNA extracted. In this state cells can be quantified using qPCR and our conversion too

5.2.2 Species selection and primer specificity

A total of nine gut commensal species were selected and obtained (Table 6); these species were shortlisted from the following microbiota papers (Qin *et al.*, 2010; 2012; Schloissnig *et al.*, 2013; Li *et al.*, 2014). The selection criteria consisted of: high relative abundance, present across multiple regions (Europe, America and Asia), and has a sequenced genome. *Firmicutes* and *Bacteroidetes* were overrepresented as these genera are the dominant phylum in the gut (Eckburg *et al.*, 2005).

Primers were designed to target either the topoisomerase I (*topI*) or DNA gyrase subunit A (*gyrA*) region of each strain (Table 7). These genes were chosen as unlike the conventional 16S gene, they have a single copy number within the genome which improves the accuracy of assumptions made in converting DNA mass to bacteria number. For qPCR-based quantification to be successful primers have to be highly specific, with little to preferably no off-target amplification. To test specificity, we created a primer vs DNA matrix, genomic DNA obtained from each species was tested against all other primers. We found high levels of specificity with no cross-reacting bands outside of the correct lane (Figure 13).

Table 6: **List of representative species used to construct a gut microbial community.** Deutsche Sammlung von Mikroorganismen und Zellkulturen (DSMZ) and Biodefense and Emerging Infections Research Resources Repository (BEI).

Species	Phylum	Source
Bacteroides dorei (CL02T00C15)	*Bacteroidetes*	BEI resources
Bacteroides ovatus (3_8_47FAA)	*Bacteroidetes*	BEI resources
Bacteroides thetaiotaomicron (VPI-5482)	*Bacteroidetes*	Dr Anne Marie Krachler
Bifidobacterium adolescentis (L2-32)	*Actinobacteria*	BEI resources
Blautia hansenii (20583)	*Firmicutes*	DSMZ
Clostridioides difficile (R20291)	*Firmicutes*	Trevor Lawley
Escherichia coli (83972)	*Proteobacteria*	BEI resources
Eubacterium hallii (3353)	*Firmicutes*	DSMZ
Faecalibacterium prausnitzii (17677 A2-165)	*Firmicutes*	DSMZ
Ruminococcus gnavus (CC55_001C)	*Firmicutes*	BEI resources

Table 7: **Primers sequences used in PMA-qPCR quantification.**

Species	Gene of interest	Sequences
B. dorei	*topI*	Forward: AAGCGGCTTCAAGAAACAGG Reverse: GTGCCCTTTACCTTGGGAAC
B. ovatus	*topI*	Forward: GGGCCTATTATCGCAACCGA Reverse: AGGTGCATACGTAGACGGAC
B. thetaiotaomicron	*topI*	Forward: GTCTGTAATCAAGTCCGCCG Reverse: AATGCCGGAAAGCGGTAAAC
B. adolescentis	*topI*	Forward: CTCCGGATACACGGTCATGG Reverse: GTCTTCGATATCCACGCCGA
B. hansenii	*gyrA*	Forward: GACGTAAGAAGCACCGGTAGA Reverse: ATAATCGCCCTGACAGGTAAGC
C. difficile	*gyrA*	Forward: GGTTGAAAGAATAGCAGAGTTAGTT Reverse: GCATTAGCATCCCTCTTTAATTCTA
E. coli	*gyrA*	Forward: GAACTCGGTGAGGACGGTTT Reverse: GCTGGAACAGGACGAACGTA
E. hallii	*gyrA*	Forward: TACCGCCTCATCGGACTTGA Reverse: TCATGGAGGCTGGATGCTCT
F. prausnitzii	*gyrA*	Forward: CCGGTGTCCGTGTCATGC Reverse: CTCAGCCTCTACTGTCTCGG
R. gnavus	*gyrA*	Forward: GCTGAACAGAGCAGAAGAGC Reverse: TCCTTCGCAGTCTGAACATTCT

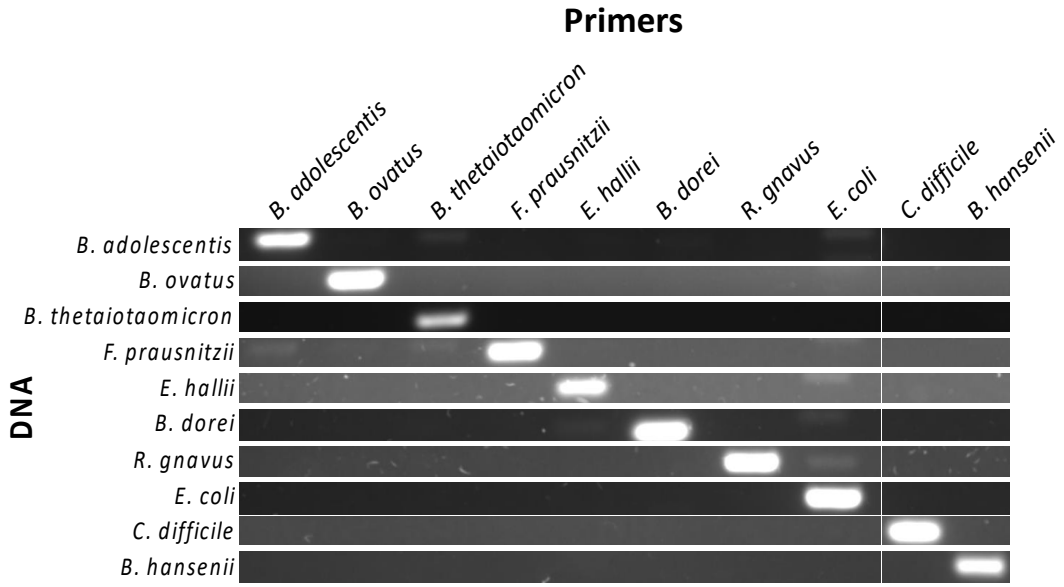

Figure 13: **Primer specificity matrix.** PCR reactions were conducted against DNA from each individual species to confirm primer specificity. These products were analysed on a 2% agarose gel, with a product size between 100-150 bp depending on the species.

5.2.3 Optimisation of PCR quantitation

To convert Ct values to a DNA mass, a standard curve for each species was generated (Figure 14). The standard curve consists of the Ct value plotted against the known DNA mass (measured by Qubit) of serially diluted DNA samples. A semilog line was fitted to each curve, with a regression above 0.990 for all (Table 8). The primer efficiency for each species was calculated from the regression. An efficiency between 90 and 110% is generally accepted as good enough for accurate qPCR (Svec *et al.*, 2015), our chosen species all fall in this range except for *B. adolescentis* and *C. difficile*. Given that both are above 80% efficient and linear (semilog) over the range of DNA values we tested we believe they are acceptable for the demands of the experiments.

Once we have converted our Ct values into a DNA mass using the standard curve, we then converted it finally into a bacterial number. To achieve this, we used the assumption that one genomic weight worth of DNA is equal to one bacterium. We established genome weight using genome sequence length and the average weight of a single base pair (Table 9).

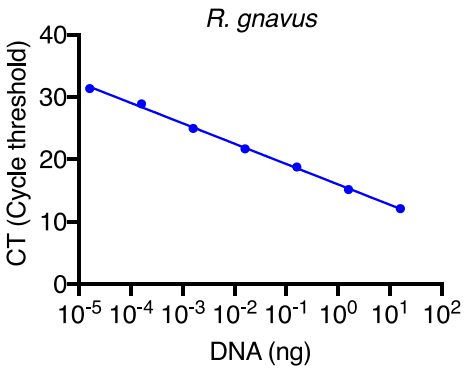
R. gnavus
CT (Cycle threshold)
40
30
20
10
0
10-5 10-4 10-3 10-2 10-1 100 101 102
DNA (ng)

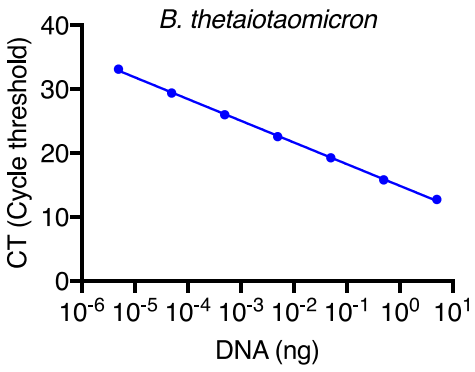
B. thetaiotaomicron
CT (Cycle threshold)
40
30
20
10
0
10-6 10-5 10-4 10-3 10-2 10-1 100 101
DNA (ng)

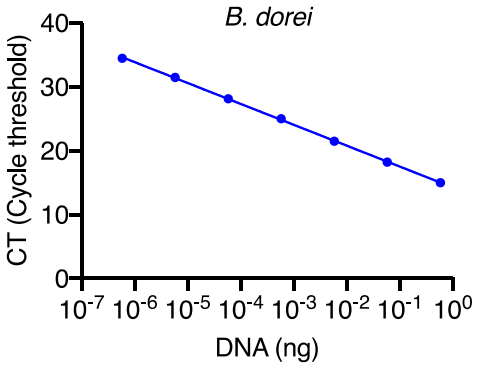
B. dorei
CT (Cycle threshold)
40
30
20
10
0
10-7 10-6 10-5 10-4 10-3 10-2 10-1 100
DNA (ng)

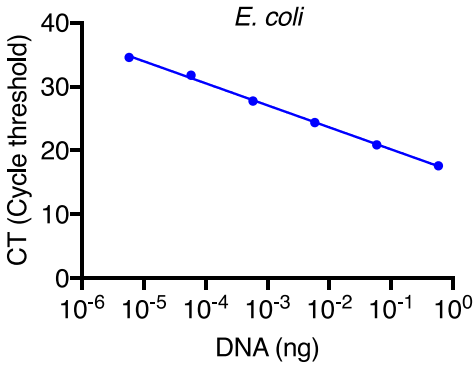
E. coli
CT (Cycle threshold)
40
30
20
10
0
10-6 10-5 10-4 10-3 10-2 10-1 100
DNA (ng)

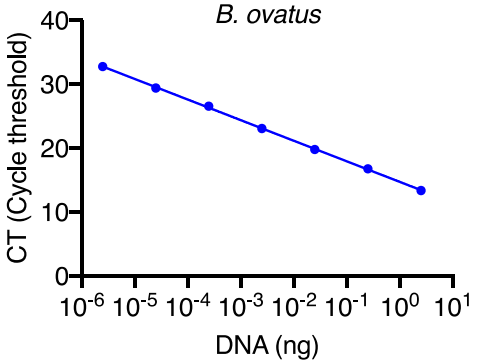
B. ovatus
CT (Cycle threshold)
40
30
20
10
0
10-6 10-5 10-4 10-3 10-2 10-1 100 101
DNA (ng)

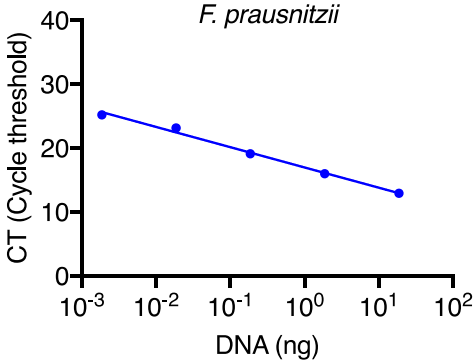
F. prausnitzii
CT (Cycle threshold)
40
30
20
10
0
10-3 10-2 10-1 100 101 102
DNA (ng)

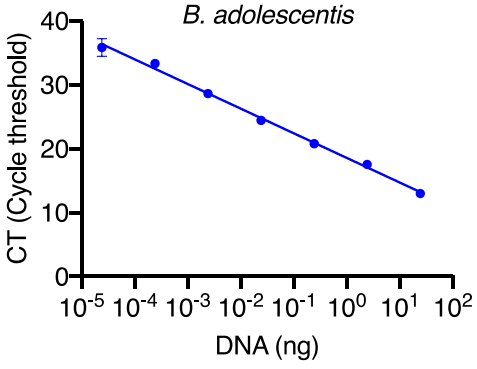
B. adolescentis
CT (Cycle threshold)
40
30
20
10
0
10-5 10-4 10-3 10-2 10-1 100 101 102
DNA (ng)

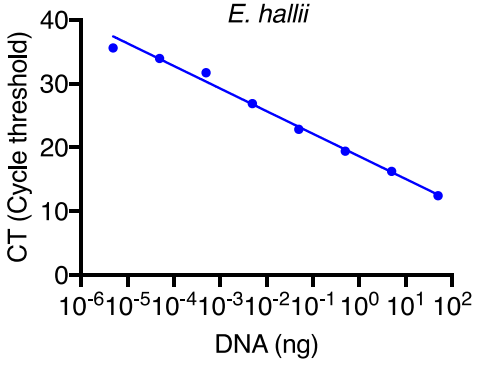
E. hallii
CT (Cycle threshold)
40
30
20
10
0
10-6 10-5 10-4 10-3 10-2 10-1 100 101 102
DNA (ng)

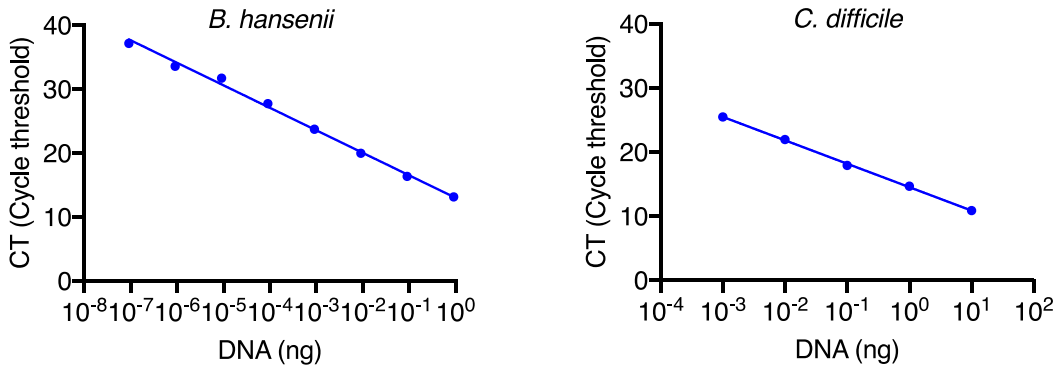

Figure 14: **Standard curves of the nine commensal bacteria and *C. difficile*.** Exponentially grown samples of each species were serially diluted to give a range of optical densities. DNA was then extracted from the different dilutions and measured using Qubit then measured again using qPCR. A semilog regression was fitted to the data. Data shown represent the mean of three technical triplicates.

Table 8: **Linearity and primer efficiency of standard curves.** Semilog regression was fitted to each of the standard curves, from the slope of this line primer efficiency can be calculated.

Species	Slope	Y-intercept	R^2	Primer efficiency (%)
B. dorei	-3.269	14.26	0.9994	102.26
B. ovatus	-3.224	14.74	0.9994	104.26
B. thetaiotaomicron	-3.396	14.91	0.9992	97.00
B. adolescentis	-3.858	18.57	0.9944	81.64
B. hansenii	-3.522	13.03	0.9951	92.28
C. difficile	-3.651	14.56	0.9991	87.89
E. coli	-3.450	16.73	0.9986	94.92
E. hallii	-3.545	18.61	0.9903	91.46
F. prausnitzii	-3.171	17.01	0.9927	106.71
R. gnavus	-3.263	15.98	0.9979	102.52

Table 9: **Genome length, weight and accession numbers of the sequences used for PMA-qPCR quantification.**

Species	Length (b)	Weight (ng)	NCBI Reference
B. dorei	6079576	6.56×10^{-6}	GCF_000273035.1
B. ovatus	6549476	7.07×10^{-6}	GCF_000218325.1
B. thetaiotaomicron	6293399	6.79×10^{-6}	GCF_000011065.1
B. adolescentis	2389110	2.58×10^{-6}	GCF_000154085.1
B. hansenii	3065949	3.31×10^{-6}	GCF_002222595.2
C. difficile	4191339	4.52×10^{-6}	GCF_000027105.1
E. coli	5106156	5.51×10^{-6}	GCF_000159295.1
E. hallii	3290996	3.55×10^{-6}	GCF_000173975.1
F. prausnitzii	3090349	3.34×10^{-6}	GCF_000162015.1
R. gnavus	3181861	3.43×10^{-6}	GCF_000507805.1

5.2.4 Optimisation of culture medium for growth of all species

To conduct experiments in mixed culture we needed to identify a common medium that all ten species could be cultured in. To do this we cultured the different species on a range of common anaerobic growth media (BHI, Schaedler anaerobic broth (SAB) and Fastidious), incubating them at 37°C anaerobically for 2 days. We found all species except for *F. prausnitzii* were able to grow in SAB. However, when supplemented with L-cysteine and vitamin K, we found we were able to grow all ten species. Ulluwishewa *et al.*, 2015 used a similar addition of L-cysteine and vitamin K to grow *F. prausnitzii* in BHI.

5.2.5 PMA testing

To improve the accuracy of our quantification we used PMA (propidium monoazide) to prevent the counting of 'dead' bacteria, i.e. those with compromised membranes. We tested a range of PMA values against exponentially grown *E. coli*, which should be free from dead cells. Exponentially growing cells were heat-inactivated at 95°C for 5 min (Lee and Levin, 2009). The heat-inactivated *E. coli* showed no signs of growth when plated (undiluted) on SAB+. When quantified by qPCR we found that as the amount of PMA increased in the heat-treated samples, an increase was also observed in Ct values (Figure 15), which indicates a higher number of PCR amplifications. The highest concentration of PMA (5 µl per 1 ml of sample) showed the greatest PCR inhibition, increasing the Ct value by ~19 cycles. However, we opted for 2 µl per 1 ml of sample as our treatment concentration. At 2 µl we saw an increase of ~16 cycle to the Ct value, we believe the added financial cost of extra PMA is not justified by a mere 3 cycle increase. No difference was seen between treated and untreated 'live cell' DNA at the highest concentrations of PMA, meaning our 2 µl PMA concentration should not have impacted the quantification of active cells.

To confirm PMA will inhibit amplification of all our species we tested each species with and without PMA treatment in single species biofilm conditions. Biofilms are an important mode of growth on the gut epithelium. By adhering

to the epithelial layer and forming biofilms bacteria can protect themselves from environmental stresses. To create biofilms, bacteria can use DNA as a building component and hence there would be a large amount of 'dead' DNA. We expected that without PMA treatment Ct values would be higher, and in-turn the quantitation of bacteria less accurate. Our results at 48 hours agreed with this prediction; all ten species had a reduction in Ct values when treated with PMA (Figure 16A & B). For the 24-hour time point we saw a similar trend for all but *E. coli*. It is unlikely that after 24 hours there was no dead *E. coli*, we suspect PMA treatment did not work for this set of samples. However, given that PMA worked at 48 hours for *E. coli* it was likely just a technical error. PMA on average increases Ct values by ~3 cycles at 24 hours and ~5 cycles at 48 hours. When converted from Ct value to bacterial number we found that PMA has a significant impact on the number of bacteria quantified with over a 10x less bacteria seen in some species (Figure 16C & D).

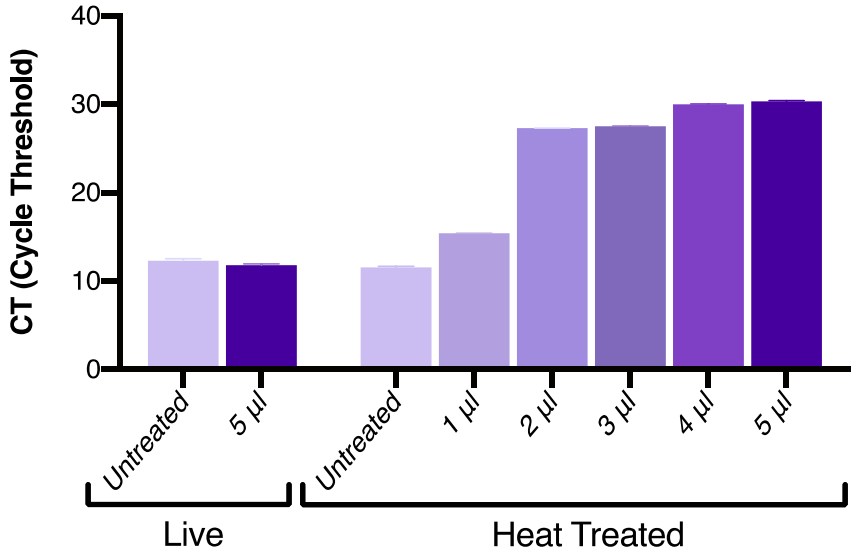

Figure 15: **Evaluating the effective concentration of PMA.** Exponentially grown *E. coli* cells were incubated at 95°C for 5 min. A live (exponential culture) control and the heat-treated samples were then treated with a range of PMA amounts (untreated – 5 µl). Data shown represent the mean of three technical replicates.

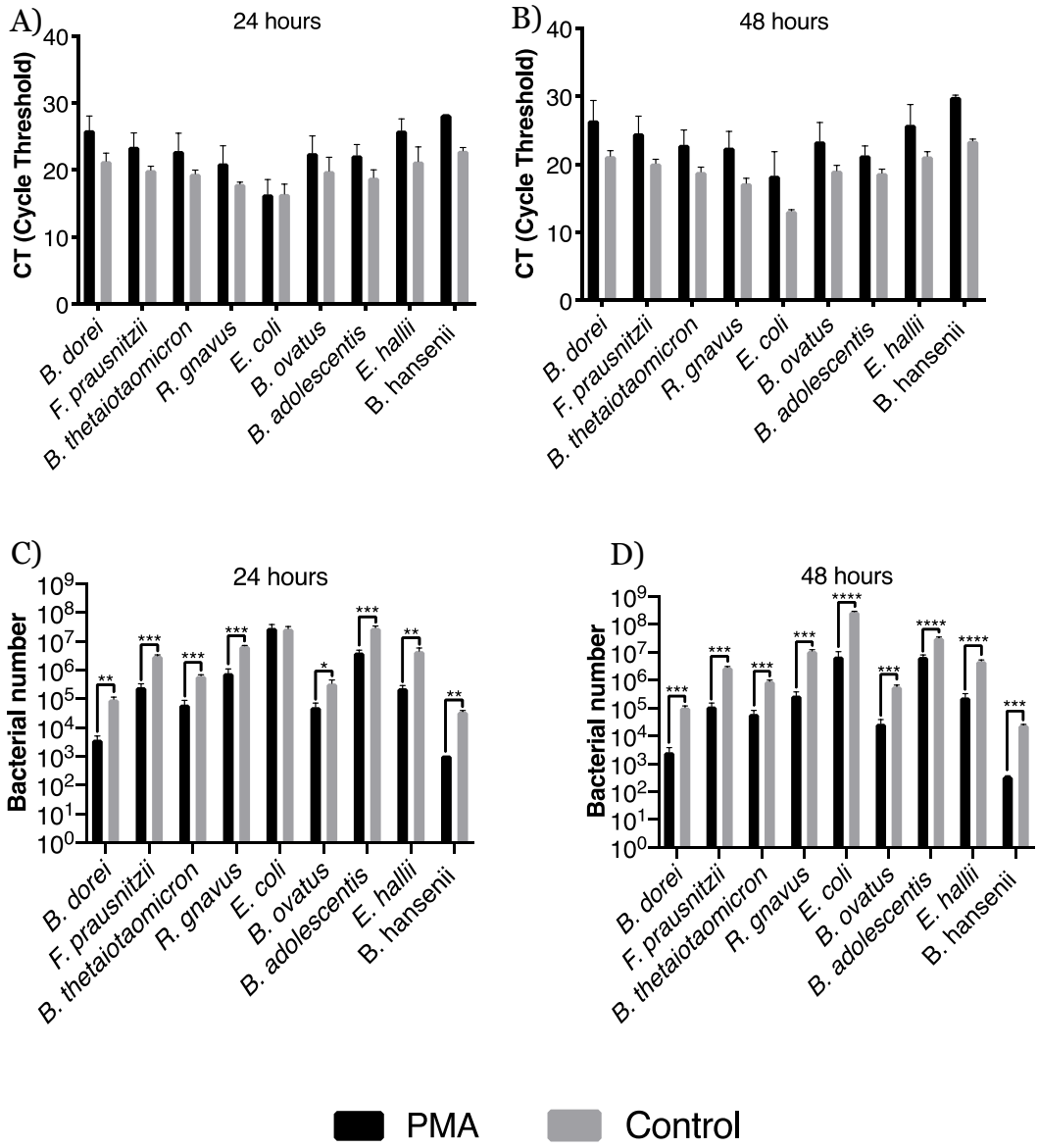

Figure 16: **Testing the effectiveness of PMA on single species biofilms.** Individual species biofilms were grown to 24 hours and 48 hours, at which point the biofilm was resuspended and split into two samples. One half was treated with 2 μl PMA and the other with water. **A & B)** show the cycle threshold (Ct) value of these biofilms. **C & D)** Ct values were converted to bacterial number to depict the impact of PMA treatment. Data shown is the mean of three independent biological triplicates. Significant difference tested by a student paired T-test, *P*-value - **** < 0.0001, *** < 0.001, ** < 0.01, * < 0.05.

5.2.6 CFU comparison with PMA-qPCR predicted values

To confirm the accuracy of our qPCR-based quantitation assay, we grew single species biofilms and tested the prediction from qPCR versus the actual CFU values obtained from plating (Figure 17). We chose a species from each phylum (Firmicutes, Bacteroidetes, Proteobacteria and Actinobacteria) to test in addition to *C. difficile*. We found that the predicted values are similar to that of the CFU assay, a two-way ANOVA predicts there is no significant difference between the two techniques. However, at the individual species level we see some discrepancies, especially in *C. difficile* where there was over 15-fold more estimated by CFU than the qPCR prediction.

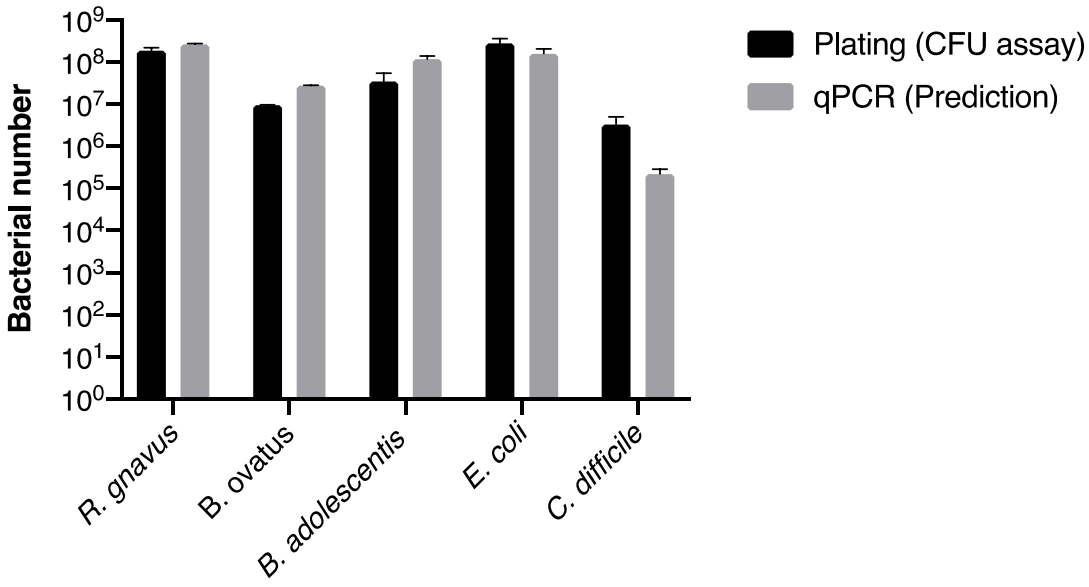

Figure 17: **A comparison between qPCR predicted bacterial numbers and bacterial numbers obtained from plating (CFU assay).** Biofilms of each species were grown for 24 hours, these were then washed and resuspended in 1 ml PBS. 50 µl of each sample was taken for serial dilution and plating, the rest was used in our PMA-qPCR pipeline. Data shown represents the mean of three independent experiments in triplicate. A two-way ANOVA showed no significant difference between plating and the qPCR technique.

5.2.7 Tracking individual species in a mixed biofilm

Having established the technique at the individual species level we tested our system with a mixed biofilm. The biofilm was created with the use of the nine species microbiota (refer back to Table 6) at a concentration of 0.1 OD_{600} per species and grown for 72 hours. All nine species were present after 72 hours, with *B. dorei* undergoing the most dramatic loss in numbers (Figure 18). *B. adolescentis* and *B. ovatus* both showed a positive trend at early timepoints (before 72 hours), while *B. thetaiotaumicron* remained neutral and all other species showed signs of decay. At 72 hours all species showed a decay in numbers, implying a general toxicity to the medium at this time point. This could be the result of a build-up of toxic secreted bi-products, or the nutritionally depleted spent medium. We can see from these results that not all species within a genus behaved in the same way, with *Bacteroides* having positive, neutral and negative trends over the first 48 hours. Blank (uninfected) wells were plated to test for contamination, with no signs of growth found.

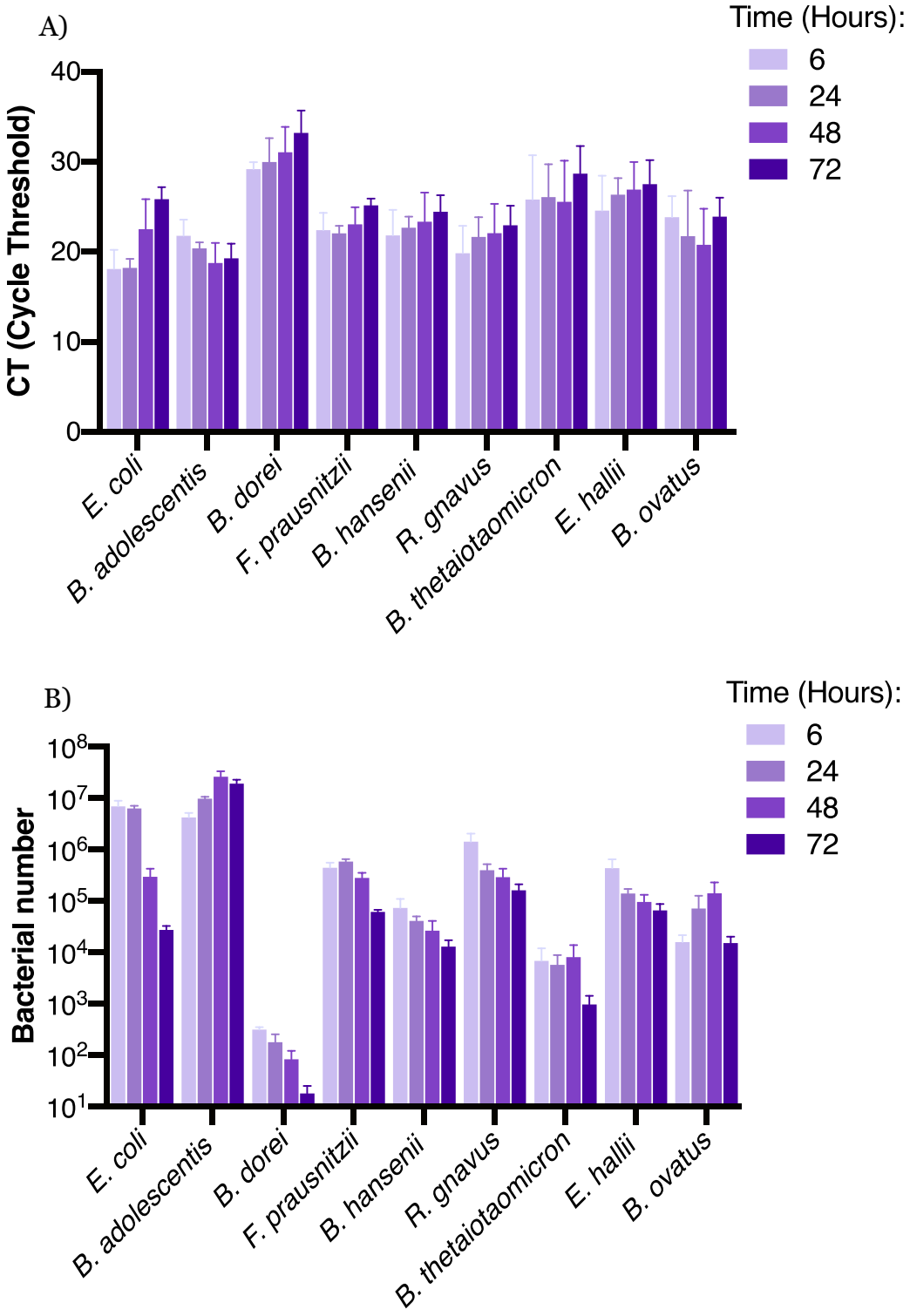

Figure 18: **A nine species mixed microbial gut community tracked over 72 hours.** Species specific changes in bacterial numbers within a mixed biofilm were tracked using PMA-qPCR. **A)** Raw cycle threshold (Ct) values and **B)** Ct values converted using our pipeline to represent total bacterial numbers. Data shown is the mean of three independent biological experiments in triplicate.

5.3 Discussion

The gut microbiota is a complex ecosystem with a wide array of benefits for the body. Understanding this community requires the development of new tools able to track complex samples containing multiple species. We designed a nine species synthetic microbiota community that is stable for 72 hours and we were able to track the growth dynamics of individual species using PMA-qPCR.

To build our microbiota, we chose to use a reductionist approach, whereby we selected a small number of species to act as our representative. By reducing the number of species, we made the output data more accessible and increased the resolution at which we could see interactions, from phylum/genus trends down to individual species. We acknowledge that some key species may get missed in this approach but given our chosen quantification technique, it would be possible to add it at a later date, so long as a species is sequenced.

Accurate quantification using PMA-qPCR relies on PMA stopping the amplification of DNA from dead cells. We tested a range of PMA amounts against heat-treated *E. coli* (Figure 15), this revealed as previously reported that PMA is not a perfect system and can be overwhelmed by high quantities of DNA from dead cells (Fittipaldi, Nocker and Codony, 2012; Taylor, Bentham and Ross, 2014). PMA impairs the detection of "dead" DNA, but unfortunately does not completely eliminate it. However, any treatment of PMA will improve the accuracy of our quantification whether it is 100% effective or not. After optimising the quantit y of PMA, we tested its effects across all our species (Figure 16A-D). All species showed a reduction in CT values as expected except for *E. coli* at 24 hours where it appeared unaffected by PMA treatment. This either means a 24-hour *E. coli* biofilm has little to no loss of cells, or that a technical error occurred in the PMA treatment of these cells. Given that at 48 hours *E. coli* resumed the expected trend we have more confidence that it was just an error.

We tested the qPCR assay from single species biofilms with known CFU values (Figure 17). A two-way ANOVA reported no significant difference between the qPCR predicted value and the measured CFU values. However, at an individual

level there appeared to be some differences, with *C. difficile* having the largest of 15-fold. *C. difficile* is the only species tested that is able to form spores. Our DNA extraction would likely be unable to lyse spores, so any that germinated during CFU plating would be unaccounted for by PMA-qPCR.

The conversion of the raw output data from the PMA-qPCR to a bacterial number required two assumptions. The first was that one genomic weights worth of DNA equalled one bacterium, for example this means a cell beginning the process of dividing with two copies of its chromosome would have been counted prematurely as two cells (Tavernier and Coenye, 2015). The more problematic scenario of this assumption is any bacteria which contained multiple copies of its chromosome naturally would have been over represented. We also assumed that the DNA extraction from single species cultures had the same level of efficiency as the extraction from a mixed culture. A number of papers have discussed the successful correlation between PMA-qPCR and the standard plating technique (CFU assay) (Tavernier and Coenye, 2015; Ditommaso *et al.*, 2015; Chang and Lin, 2018; Roussel *et al.*, 2018), but there are documented cases of discrepancies between the two approaches (Ammann *et al.*, 2013; Taylor, Bentham and Ross, 2014; Vondrakova *et al.*, 2018). Ammann *et al* reports greater discrepancies; however, the authors do not use PMA in their paper, which may explain the poor correlation observed.

The contradictions in the literature appear to be dependent on the type of quantification, the more successful studies examined trends overtime, not just using the prediction power of a single sample/timepoint. PMA-qPCR serves as a powerful tool to relatively quantify a species over time, highlighting the general trends but it does not lend itself well to absolute quantification. Of course, PMA-qPCR can be used for absolute quantification, but to do so requires carefully controlled conditions. Applying this to the discrepancies we see between the predicted and actually bacterial numbers, we conclude that PMA-qPCR is best used as an indication of changes within a species over time/conditions. Furthermore, we do not think it would be accurate to compare values between two differing species. To progress our PMA-qPCR system to include absolute quantification, we would need to determine the

relative difference between actual CFU and the predicted numbers of every species in the mix.

There are two main alternatives to PMA-qPCR; Q-FISH (Quantitative Fluorescent *in situ* hybridization) and genome sequencing. In a comparison carried out between qPCR and Q-FISH it was found that Q-FISH is less sensitive and more time-consuming (Huang *et al.*, 2015). FISH would best serve as a complementary assay to qPCR, adding spatial details rather than using it as a quantification tool (Poon and Lansdorp, 2001). The second option is genome sequencing, this approach would allow for much larger communities to be quantified. The main drawback of sequencing is its expense, it is therefore no surprise that it is often only used for analysis of complex samples which contain hundreds of species (Qin *et al.*, 2012; Li *et al.*, 2014; Tramontano *et al.*, 2018). Genome sequencing, like standard qPCR, does not eliminate the quantification of "dead" DNA. When examining a small community of known species, we believe it is more practical to use targeted PMA-qPCR approach.

We used PMA-qPCR to investigate our nine species microbiota community over 72 hours in biofilm conditions (Figure 18). We were able to successfully track all nine species over this time period. A noticeable result from this experiment was the decline in bacterial numbers across all species at 72 hours. Even species which showed positive signs of growth up until this point went into sudden decline. We think this is because by 72 hours the spent media may have become toxic and/or growth limiting. Surprisingly no single species dominated over others during the experiment, this led us to believe that direct competition was not occurring but rather a form of species cross-feeding, in which species obtain things of nutritional value form each other. Henson and Phalak, 2017 using an *in silico* biofilm metabolic model predicted that a stable cross-feeding relationship between *F. prausnitzii*, *B. thetaiotaumicron* and *E. coli* can be achieved. However, given the trajectory of several species before the 72-hour timepoint we believe the system as a whole is not stable.

Mixed microbiota communities have been mainly modelled using fermentation style systems, with the SHIME (Simulator of the human intestinal microbial ecosystem) model been the most well studied (Van de Wiele *et al.*, 2015). The SHIME model is seeded with human faecal material, which is likely a more realistic representation of a microbiota compared to the nine species microbiota we have used. However, the complexity of their faecal inoculum means tracking of their microbiota can often only be carried out at the genus to phylum level (McDonald *et al.*, 2013; Reygner *et al.*, 2016; Yin *et al.*, 2017; Wu *et al.*, 2019). The results from our 72-hour mixed biofilm showed that species even within the same genus can behave very differently, this is best seen in the three *Bacteroides* species who each have a different trend over the first 48 hours. Clustering at a higher order especially in large metagenomic data sets is necessary, but it could however be misleading given the species level differences we saw.

We have generated a method that reliably tracks the changes of a mixed community over time in a controlled environment, in the future we want to start investigating what interactions are happening between these species using metabolomics. There is a growing number of *in silico* metabolomic interaction models of the gut microbiota (Baldini *et al.*, 2018; Sen and Orešič, 2019; Phalak and Henson, 2019). These models would greatly benefit from our multispecies tracking system as we can now validate any predicted trends. The use of these models will allow us to take a systematic approach to understanding the real metabolic interactions present. Already we are in a position where we can investigate the *in silico* biofilm model Henson and Phalak, 2017 proposed between *F. prausnitzii*, *B. thetaiotaumicron* and *E. coli*.

FISH has showed great success in oral mixed biofilms (Thurnheer, Gmür and Guggenheim, 2004; Kommerein *et al.*, 2018), our current data gives great insights into the changes happening overtime, combining this with a FISH technique would allow us to add a great deal of spatial information. We would like to establish how the biofilms are being established; are species randomly dispersed or are there dense patches of a single species? Knowing how species

are structured spatially will give information on what species are potentially interacting.

6 Population dynamics of the gut microbiota with *C. difficile*

6.1 Introduction

C. difficile infections (CDI) are the leading cause of hospital associated diarrhoea in the US, with half a million new cases each year and a repeat infection rate of 1 in 5 patients (Lessa *et al.*, 2015). Elderly people are most at risk; their diminished immune response and higher intake of antibiotics lead to the depletion of their protective gut microbiota and leaves them highly susceptible to CDI (Asempa and Nicolau, 2017). The emergence of hypervirulent strains in both North America and Europe is leading to a growing number of younger individuals being infected without exposure to antibiotics (CDC, 2005). Since the late 1970s, the main treatment against *C. difficile* has been metronidazole or oral vancomycin. The failure rate of metronidazole has become substantially higher over time, and in the 2000s vancomycin became the advocated treatment (Kelly and LaMont, 2008). Recurrences with both treatments are high as they negatively affect the gut microbiota, reducing overall diversity and abundance in species (Lewis *et al.*, 2015; Haak *et al.*, 2018; Sun *et al.*, 2019).

In 2011, Optimer Pharmaceuticals and Cubist Pharmaceuticals released a new drug, named DIFICID™, in an attempt to combat this problem. DIFICID™ uses the narrow spectrum macrocyclic antibiotic fidaxomicin, shown to have activity against specific anaerobic Gram-positive bacteria. *In vitro* trials found fidaxomicin to be ~8 times more active against *C. difficile* than vancomycin (Credito and Appelbaum, 2004; Hecht *et al.*, 2007; Louie *et al.*, 2011; Cornely *et al.*, 2012). However, Fidaxomicin's narrow spectrum is its biggest improvement over vancomycin, it has less of an impact on the gut microbiota causing far fewer alterations to the bacteria present (Tannock *et al.*, 2010; Ajami *et al.*, 2018). This reduces the risk of recurrent infections, with a recurrence rate half that of vancomycin in one trial (Cornely *et al.*, 2012). Although, when recurrence does occur in fidaxomicin treated patients, repeat treatment has the same recurrent rate as that of vancomycin (Tieu *et al.*, 2019). Fidaxomicin is accepted as the better treatment but is not used widely owing

to high cost. All three treatment approaches are suffering from a rise in resistant *C. difficile* (Peng, Jin, *et al.*, 2017; Asempa and Nicolau, 2017), this resistance is thought to be associated with biofilm formation (Đapa *et al.*, 2013; Vuotto *et al.*, 2016; Peng *et al.*, 2017).

To overcome the rise of resistant *C. difficile* hospitals are resorting to the use of faecal transplants (FMT). This involves taking the faecal matter from healthy donors and transplanting it into long-term CDI patients to restore their microbiota. The aforementioned methodology is more successful than even Fidaxomicin, with a success rate of 80-92% (Agrawal *et al.*, 2016; Hvas *et al.*, 2019). FMT comes with risks, without correct screening transfer it can easily transfer pathogenic antibiotic-resistant bacteria, with one death due to the accidental transfer of an extended-spectrum beta-lactamase (ESBL)-producing *E. coli* already reported (FDA, 2019). In argument to this, a successful well-screened sample reduces the number of antibiotic-resistant genes observed in the gut microbiota (Millan *et al.*, 2016). Dr Jonathan Sutton a leading specialist and advocate for FMT usage in hospitals spoke recently at the Microbiology Society: Anaerobe 2019 conference about the sourcing problem faced by the UK and the need for a centralised system if the treatment was to be used routinely. If we ignore the sourcing and screening problems of FMT, there is still the underlining problem that we do not fully understand the gut microbiota. A transplanted microbiota will be beneficial against *C. difficile* but can cause unforeseen problems. For example, in 2015 a patient suffering from *C. difficile* received a transplant from a healthy but overweight donor. This cured the patient's *C. difficile* infection but led to an onset of extreme unintentional weight gain (Alang and Kelly, 2015). Similar results have been found in mice with faecal donations from obese individuals (Ridaura *et al.*, 2013). Although this is just one example it serves to highlight all that we do not know about the gut microbiota and the effect transplanting it without knowledge could have.

As shown by faecal transplant work, the best defence against *C. difficile* is the colonisation resistance generated by the gut microbiota. Understanding how it prevents *C. difficile* from invading will provide knowledge on how to treat

against it, or ways to avoid disturbing crucial parts of the microbiota during future treatments. The gut microbiota contains bacteria both in planktonic and mucus associated biofilm conditions. Research into these biofilms has been limited by the invasive biopsy techniques required to obtain samples (Crowther *et al.*, 2014a). Sampling becomes especially dangerous when suffering from a disease like CDI. *C. difficile* colonisation and interaction with the mucous layer is likely to be of importance in infection, but little is known about the interaction it has with the microbiota community and the mechanisms underlying colonisation resistance. In Chapter 4, the large impact a single species (*B. dorei*) can have on *C. difficile* was discussed. Dual species studies although informative cannot accurately simulate the complex bacterial communities found in the gut (Crowther, Wilcox and Chilton, 2016). To date most microbiota–*C. difficile* investigations have been carried out using animal models (Seekatz and Young, 2014; Pérez-Cobas *et al.*, 2015), whose microbiota differ remarkably from humans (Nguyen *et al.*, 2015), and only allow for endpoint testing so any dynamics of the system are missed. *In vitro* models offer a more accessible method to study interactions occurring at the gut mucosal interface (Anonye *et al.*, 2019). The trackable community we developed in chapter 5 will be useful in these models.

Current *in vitro C. difficile*–microbiota models are limited as they rely on chemostat or fermentation setups. These models often consist of a three-stage system, in which each vessel is maintained at a different pH to simulate a different area of the gut and faecal emulsion is inoculated into the vessels (Freeman, O'Neill and Wilcox, 2003; Crowther *et al.*, 2014b; Crowther, Wilcox and Chilton, 2016; Moura *et al.*, 2018). These fermentation style models have no representative epithelial layer; consequently, ignoring any effect that the epithelial cells could have on the microbiota-*C. difficile* dynamics. Using the E-VDC model described in chapter 4 and the trackable representative microbiota generated in chapter 5 we aimed to investigate the interactions between the gut microbiota and *C. difficile* in the presence of epithelial cells.

6.2 Results

6.2.1 Microbiota interferes in *C. difficile* adherence

To study the effects of the microbiota on *C. difficile* adhesion, we tracked the formation of adherent biofilms over six hours in the presence and absence of *C. difficile*. We measured the percentage of the initial inoculum that is able to adhere to a 24-well polystyrene plate. The inoculums were prepared with individual overnight cultures diluted and mixed the following day to achieve a final concentration of 0.1 OD_{600} per species as explained in Methods 3.6.

A significant reduction in initial adhesion was observed in *C. difficile* when cultured with the microbiota compared to a monoculture control (two-way ANOVA *P*-value <0.0001) (Figure 19). Although significant, this reduction is small, with ~8% of the initial inoculum adhering when cultured alone and ~4% with the microbiota. With respect to the microbiota, we saw that when cultured alongside *C. difficile* there is a significant increase in the number of bacteria adhering (two-way ANOVA *P*-value <0.0001). A Post-hoc Sidak's test revealed significant differences for *E. coli* (*P*-value <0.0001), *B. adolescentis* (*P*-value <0.0001) and *R. gnavus* (*P*-value = 0.0016), but the trend can be seen generally across all species. *E. coli* appears to be dominating at this early stage with far more of its original inoculum adhering than any other species. *E. coli* was the only facultative species present so any lingering oxygen in the reduced media may provide it with an initial head start.

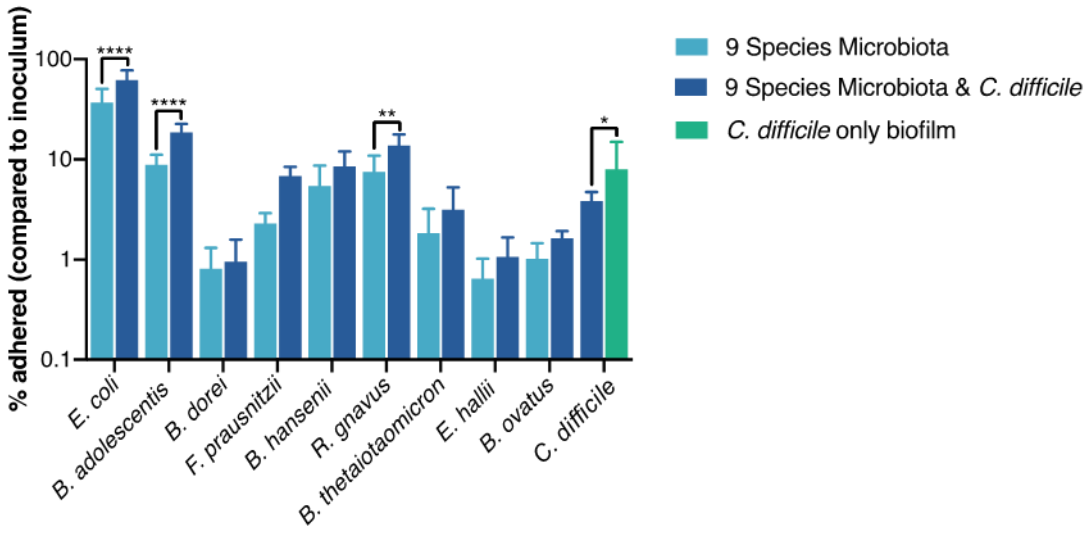

Figure 19: **The presence of *C. difficile* impacts the adhesion of several species in the adherent microbiota community.** The percentage of the inoculum which adhered after 6 hours in three conditions; a nine species microbiota community, the nine species with *C. difficile*, and a *C. difficile* control. Data shown represents the mean of three independent experiments in triplicate. Two-way ANOVA determined a significant difference between conditions (*P*-value < 0.0001). The post-hoc Sidak's test used to determine specific differences – *P*-values - **** < 0.0001, ** < 0.01, * < 0.05.

6.2.2 Reduction in *C. difficile* biofilm growth by the microbiota

We next investigated the impact on *C. difficile* during later stages of biofilm development (Figure 20). Here the microbiota impacts *C. difficile* growth, significantly reducing it at all time points when compared to a monoculture control (two-way ANOVA, *P*-value <0.0001). This impact was at its largest at 24 hours, with the microbiota causing a 10-fold drop in *C. difficile* numbers compared to the monoculture control. Given the larger inhibition seen post-adhesion, we argue that in this setup, the drop in *C. difficile* numbers is likely attributed to the microbiota negatively impacting *C. difficile* growth, rather than a reduction in *C. difficile's* ability to adhere. Unless however, the small changes in initial adhesion have a large knock-on effect.

In the presence of *C. difficile*, we tracked each of the nine species that make up the representative microbiota (Figure 21). When comparing this to a microbiota only control, we see that the presence of *C. difficile* has a neutral to positive effect, with five of the nine species having significant difference according to a two-way ANOVA: *B. dorei* (*P*-value = 0.0027), *B. ovatus* (*P*-

value = 0.0006), *E. coli* (*P*-value = 0.0054), *F. prausnitzii* (*P*-value <0.0001) and *R. gnavus* (*P*-value = 0.0332). From the post-hoc Sidak's test, we see that these differences are mainly observed at the six-hour time point. It appears although *C. difficile* increases initial binding in the microbiota, the effect is not seen long term. In both conditions, all species no matter the prior trajectory show a decrease in numbers at 72 hours. It is possible that the media is spent at this late time point and cannot support growth, furthermore, secreted bi-products could be building to toxic levels.

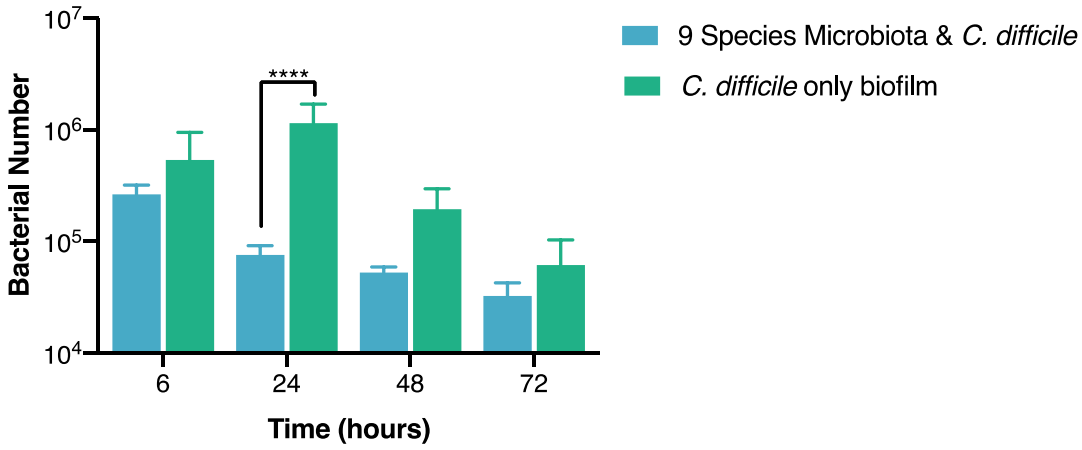

Figure 20: **The microbiota has an inhibitory effect on *C. difficile*.** *C. difficile* was cultured in monoculture biofilm and with a nine species representative microbiota. Bacterial numbers were tracked over 72 hours using PMA-qPCR. Data shown is that of three independent experiments in triplicate. A two-way ANOVA indicates a significant difference between the two conditions (*P*-value < 0.0001), with the post-hoc Sidak's test used to determine specific difference – *P*-values - **** < 0.0001.

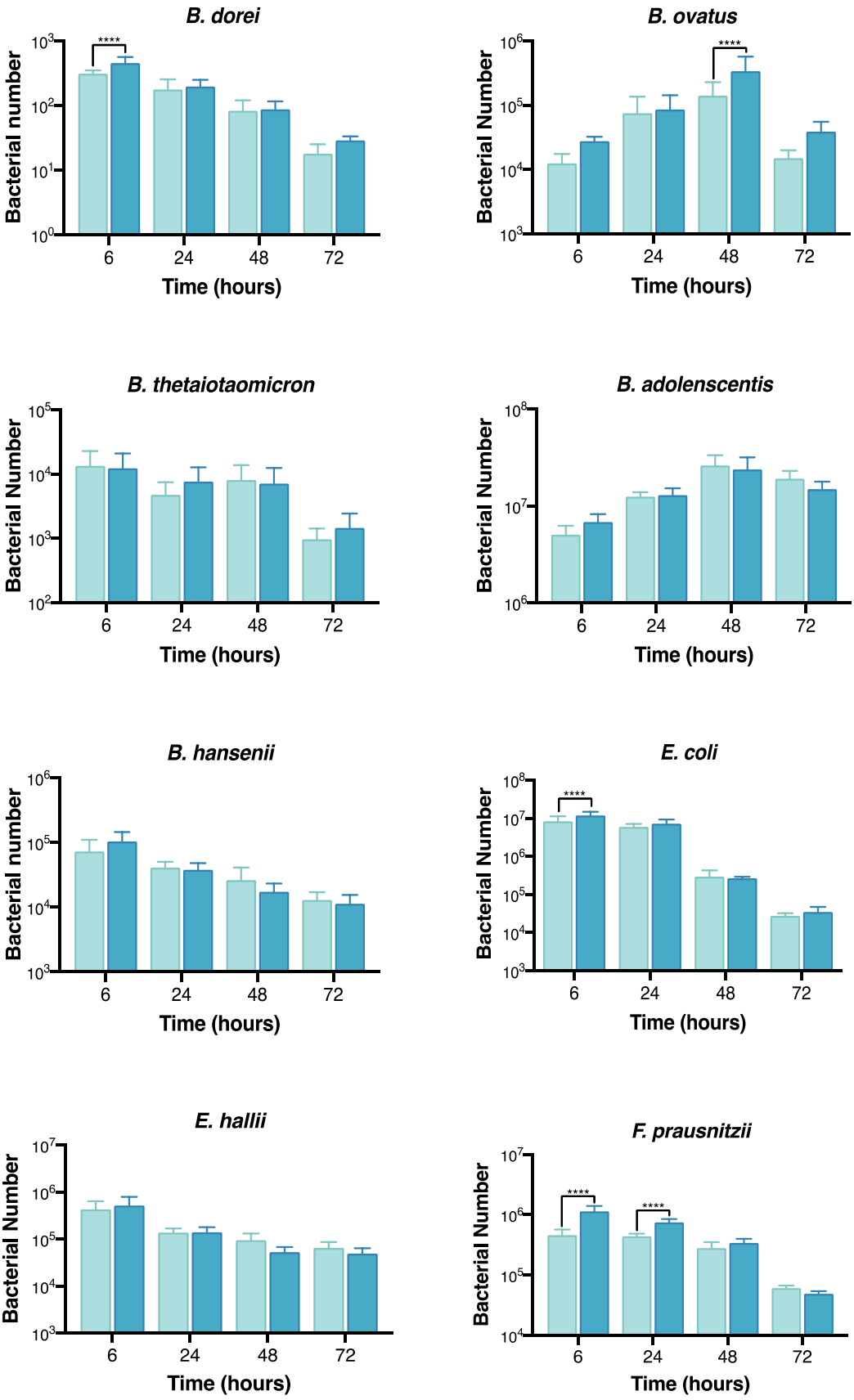
B. dorei
Bacterial number
Time (hours)
B. ovatus
Bacterial Number
Time (hours)
B. thetaiotaomicron
Bacterial Number
Time (hours)
B. adolenscentis
Bacterial Number
Time (hours)
B. hansenii
Bacterial number
Time (hours)
E. coli
Bacterial Number
Time (hours)
E. hallii
Bacterial Number
Time (hours)
F. prausnitzii
Bacterial Number
Time (hours)
****
6
24
48
72

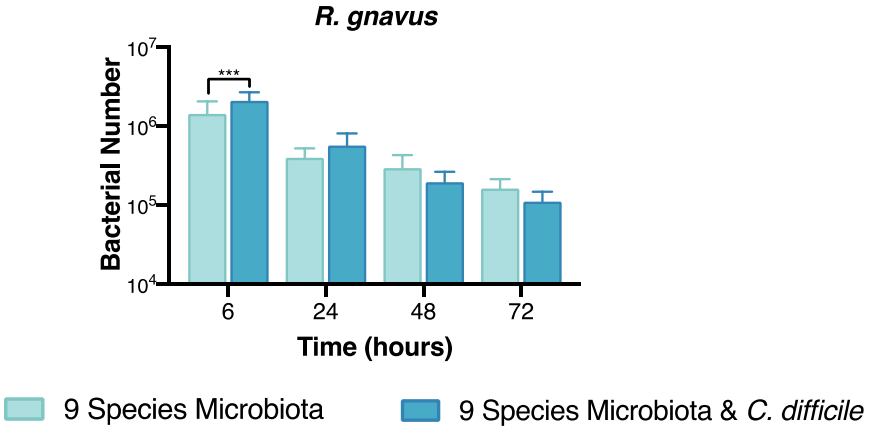

Figure 21: **Tracking the effects of *C. difficile* on a 9-species microbiota community.** Individual species within a representative microbiota and *C. difficile* biofilm were tracked over 72 hours using PMA-qPCR. A control microbiota biofilm without *C. difficile* was tracked for comparison. Data shown is that of three independent experiments in triplicate. A two-way ANOVA was used to determine significant difference between the two conditions, a post-hoc Sidak's test used to determine specific difference – *P*-values - *** < 0.001 and **** < 0.0001.

6.2.3 *C. difficile* interaction with an established microbiota biofilm

Naturally, the microbiota, when in a healthy state, would already be established before a *C. difficile* infection. To better replicate this rather than introducing *C. difficile* at the same time as the microbiota, we pre-established a microbiota for 24 hours prior to introducing *C. difficile* (Figure 22A). When comparing this to a *C. difficile* monoculture grown for the same length of time, we observed that having an established microbiota has a significant inhibitory effect on *C. difficile*, both 24 hours post-addition (*P*-value = 0.000022), and 48 hours (*P*-value = 0.000426) when tested with an unpaired student T-test. The largest difference in *C. difficile* numbers (70-fold) was seen at 24 hours post-infection. A pre-established microbiota had a significantly larger impact on *C. difficile* than when the two are seeded together (Figure 22B, unpaired Student T-test *P*-value < 0.0001).

We tracked each species in the microbiota to examine any changes in response to *C. difficile*. We expected, as the microbiota was already established, any impact that *C. difficile* had on the microbiota would be lessened compared to when seeded with *C. difficile*. However surprisingly, we found the opposite to

be true. Only three species, *B. dorei*, *B. hansenii* and *R. gnavus,* showed no significant difference in numbers when compared to a microbiota only control (Figure 23), compared to the four seen in the simultaneous addition. The other six species, when tested with an unpaired student T-test, all showed significant differences in numbers when *C. difficile* was introduced. After 24 hours with *C. difficile* (48 hours from microbiota seeding), we saw a notable positive effect for *B. thetaiotaomicron* (*P*-value = 0.015698) and *E. coli* (*P*-value < 0.000005). However, for *F. prausnitzii* (*P*-value = 0.000022) we observed fewer bacteria. 48 hours post-infection with *C. difficile* we still saw a positive effect on *E. coli* (*P*-value = 0.005211) but to a much lesser degree. An increase was also observed in *B. ovatus* (*P*-value = 0.000356) and *B. adolescentis* (*P*-value = 0.000287). However notably at 48 hours, *B. thetaiotaomicron* undergoes a drop-in numbers when compared to the microbiota control. This decrease pushes *B. thetaiotaomicron* below our detection limit; but we must note this loss could be from a qPCR error as all were run on a single plate. *E. hallii* (*P*-value = 0.000259) is also negatively impacted at 48 hours.

Interestingly, the species impacted by *C. difficile* are not similar between the two setups studied; pre-established microbiota and infected from the biofilm seeding.

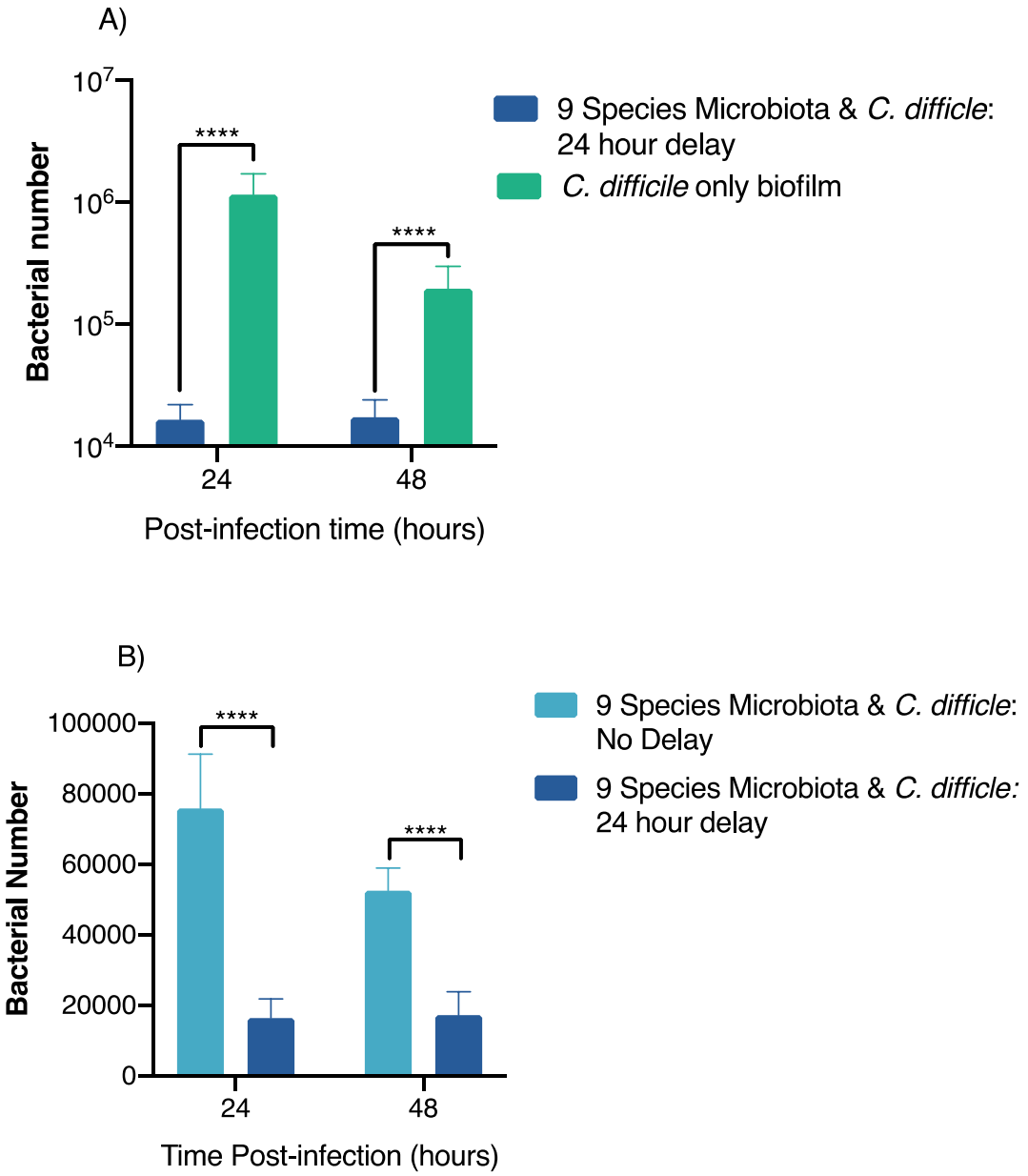

Figure 22: **A pre-established microbiota has an inhibitory effect on *C. difficile* growth within biofilms. A)** The microbiota was established for 24-hours prior to *C. difficile* infection, we compared this to a *C. difficile* only biofilm grown for the same length of time. We used our PMA-qPCR pipeline to estimate the number of bacteria. **B)** Comparing the inhibitory effect of preestablishing the microbiota (24-hour delay), with our previous experiment that contained no delay. Data shown is that of three independent experiments in triplicate. An unpaired T-test was used to test for significant difference, *P*-value < 0.0001 - ****.

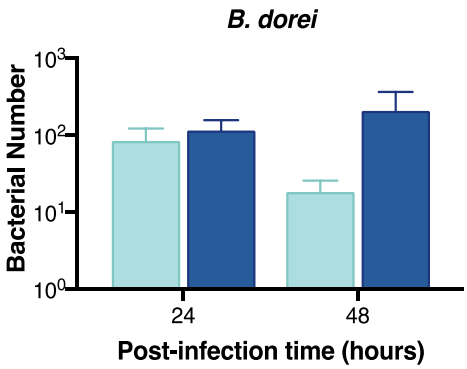
B. dorei
Bacterial Number
10^3
10^2
10^1
10^0
24
48
Post-infection time (hours)

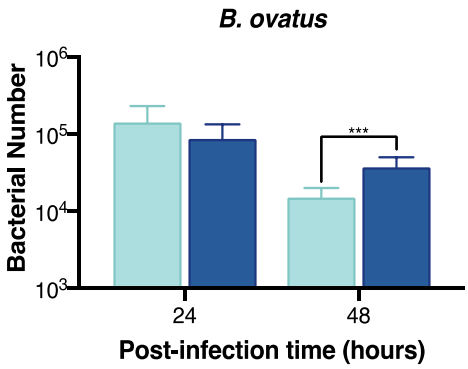
B. ovatus
Bacterial Number
10^6
10^5
10^4
10^3
***
24
48
Post-infection time (hours)

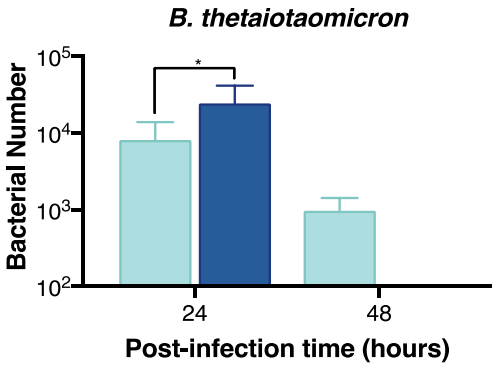
B. thetaiotaomicron
Bacterial Number
10^5
10^4
10^3
10^2
*
24
48
Post-infection time (hours)

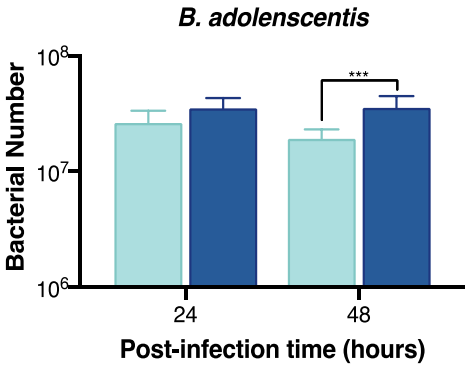
B. adolenscentis
Bacterial Number
10^8
10^7
10^6
***
24
48
Post-infection time (hours)

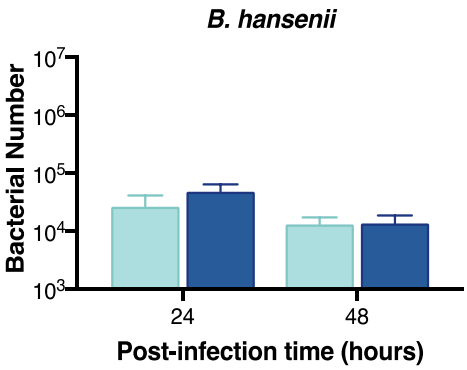
B. hansenii
Bacterial Number
10^7
10^6
10^5
10^4
10^3
24
48
Post-infection time (hours)

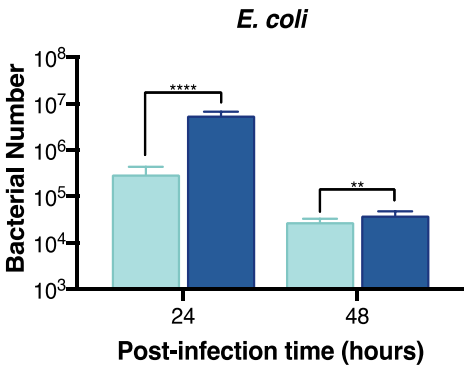
E. coli
Bacterial Number
10^8
10^7
10^6
10^5
10^4
10^3
****
**
24
48
Post-infection time (hours)

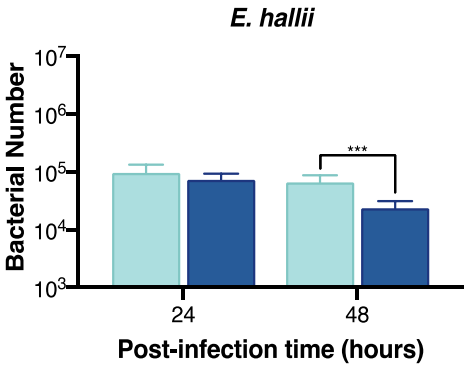
E. hallii
Bacterial Number
10^7
10^6
10^5
10^4
10^3
***
24
48
Post-infection time (hours)

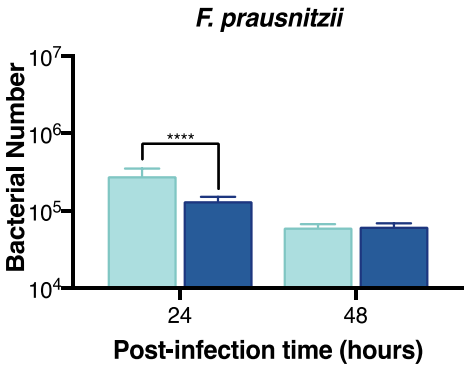
F. prausnitzii
Bacterial Number
10^7
10^6
10^5
10^4
****
24
48
Post-infection time (hours)

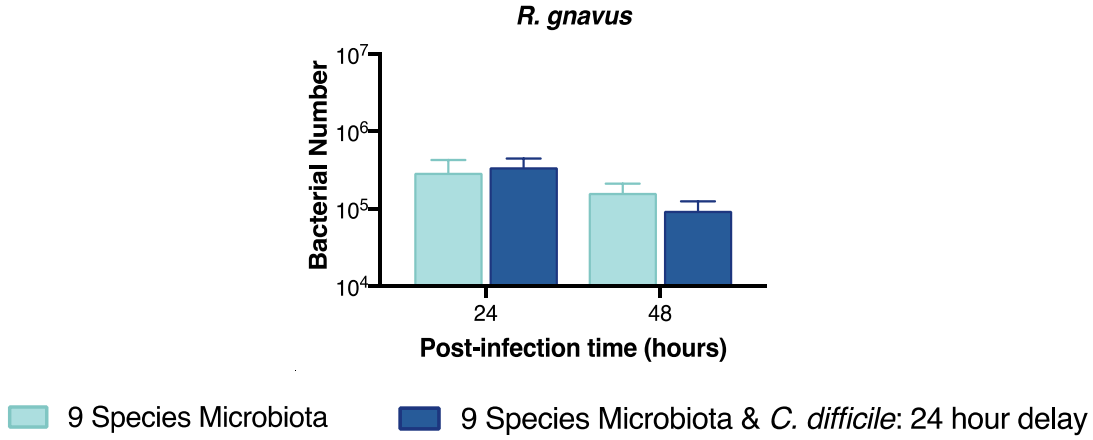

Figure 23: **Impact of *C. difficile* on a pre-established microbiota community.** We established a nine species representative microbiota biofilm 24 hours before infecting with *C. difficile*. We used PMA-qPCR to track the total number of bacteria for each species. Data shown is the mean of three independent experiments in triplicate. Unpaired student's t-tests was used to determine specific differences – *P*-values - **** < 0.0001, *** < 0.001, ** < 0.01, * < 0.05.

6.2.4 Vancomycin treatment

The next question we aimed to address was what happens when this established microbiota is disturbed? We chose antibiotic treatment as the disturbing factor, replicating the conditions ideal for a *C. difficile* infection. We treated our 24-hour pre-established microbiota with two concentrations of vancomycin; 2 μg/ml and 20 μg/ml reaching the limit prescribed to patients (Đapa *et al.*, 2013). Peláez *et al.*, 2002 tested the minimum inhibitory concentration (MIC) of 415 *C. difficile* strains and found on average for MIC50 1 μg/ml and MIC90 2 μg/ml in non-biofilm conditions. The results were contrasting to our previous work as *C. difficile* performed worse in monoculture condition rather than with the established microbiota (Figure 24). The treatment with vancomycin at either concentration had a big impact on the *C. difficile* monoculture when compared to the untreated control, especially at the earlier time point. Whereas for the microbiota plus *C. difficile* conditions we saw that adding vancomycin either mildly improved *C. difficile* numbers or had no apparent effect.

Given previous research on vancomycin and the gut microbiota, we assumed that it would detrimentally impact our nine species mix (Haak *et al.*, 2018; Sun *et al.*, 2019). We tested this assumption by tracking a nine species control group alongside the *C. difficile* experiment (Figure 25). When alone the microbiota shows no signs of instability, all species were present at both vancomycin concentrations with only a minor reduction in numbers seen between the two concentrations and our untreated control. There were minor reductions for *B. dorei*, *B. ovatus*, *B. thetaiotaomicron*, *B. hanseii*, *E. coli*, *E. hallii*, *F. prausnitzii* and *R. gnavus* when compared to the untreated control, however these were all less than 10-fold. In biofilm conditions, it seems vancomycin has less of an effect than we previously thought. With the addition of *C. difficile* alongside the antibiotic treatment, we saw some instability in *B. adolescentis* and *B. dorei* numbers as both dropped below the PMA-qPCR detection limit at 24 and 48 hours. However, this was also found to be the case in the untreated vancomycin control, implying the addition of *C. difficile* is causing this effect, not the vancomycin treatment. In the previous pre-established microbiota-*C. difficile* experiments we did not see this loss of the two species and given that the untreated control is technically the same as this previous work there should be no differences. We investigated these trend discrepancies by comparing the mixed starting inoculum of each experiment (Figure 26). We found that there are differences between the two, with our previous work generally having more bacteria. This could account for the differences between the two at later stages.

Other than these two species the addition of *C. difficile* alongside vancomycin produced an increase in microbiota bacteria numbers at 24 hours post-infection in both the 2 and 20 ug/ml when compared to their uninfected counterpart (Figure 25). This increase, likely driven by the presence of *C. difficile,* is not seen in our vancomycin untreated control, with the exception of *B. ovatus* and *B. thetaiotaumicron*. At 48 hours little difference is seen from treating with vancomycin or the addition of *C. difficile*, with all species similar to the uninfected untreated control.

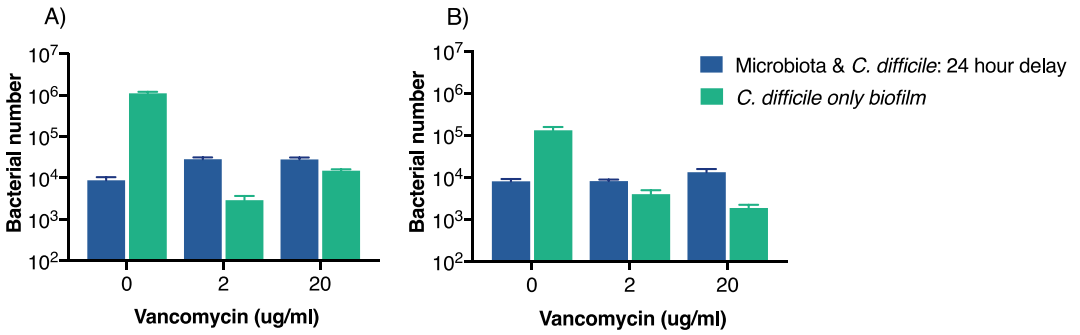

Figure 24: **Ability of *C. difficile* to establish within a disrupted microbiota.** We grew a nine species representative microbiota for 24 hours before treating with vancomycin and infecting with *C. difficile*. Two concentrations of vancomycin were used 2 and 20 μg/ml. Bacteria numbers were estimated using PMA-qPCR at **A)** 24 hours post-infection and **B)** 48 hours post-infection. The data shown is that of three biological repeats.

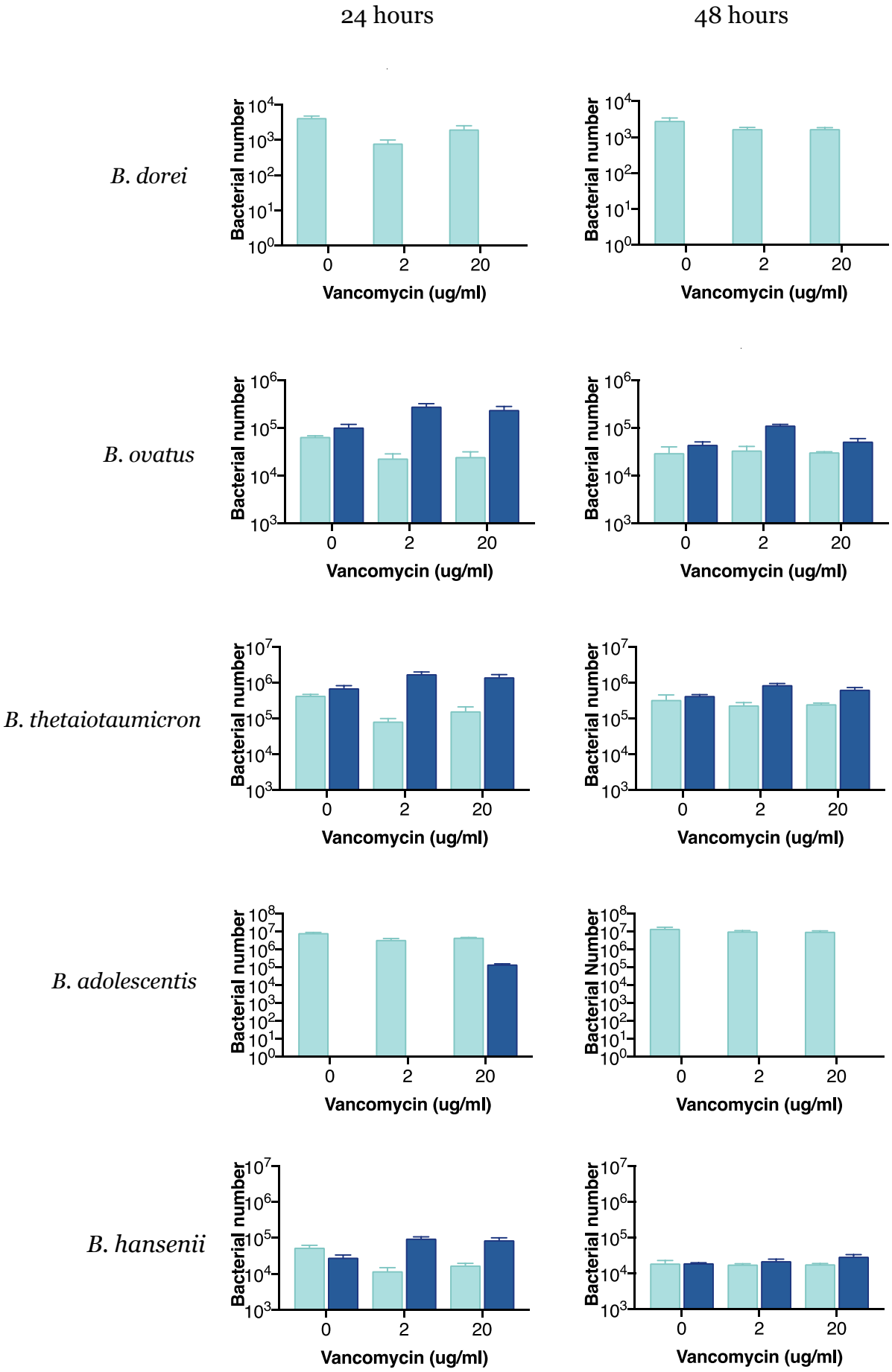
24 hours
48 hours
B. dorei
B. ovatus
B. thetaiotaumicron
B. adolescentis
B. hansenii
Bacterial number
Bacterial Number
Vancomycin (ug/ml)
0
2
20

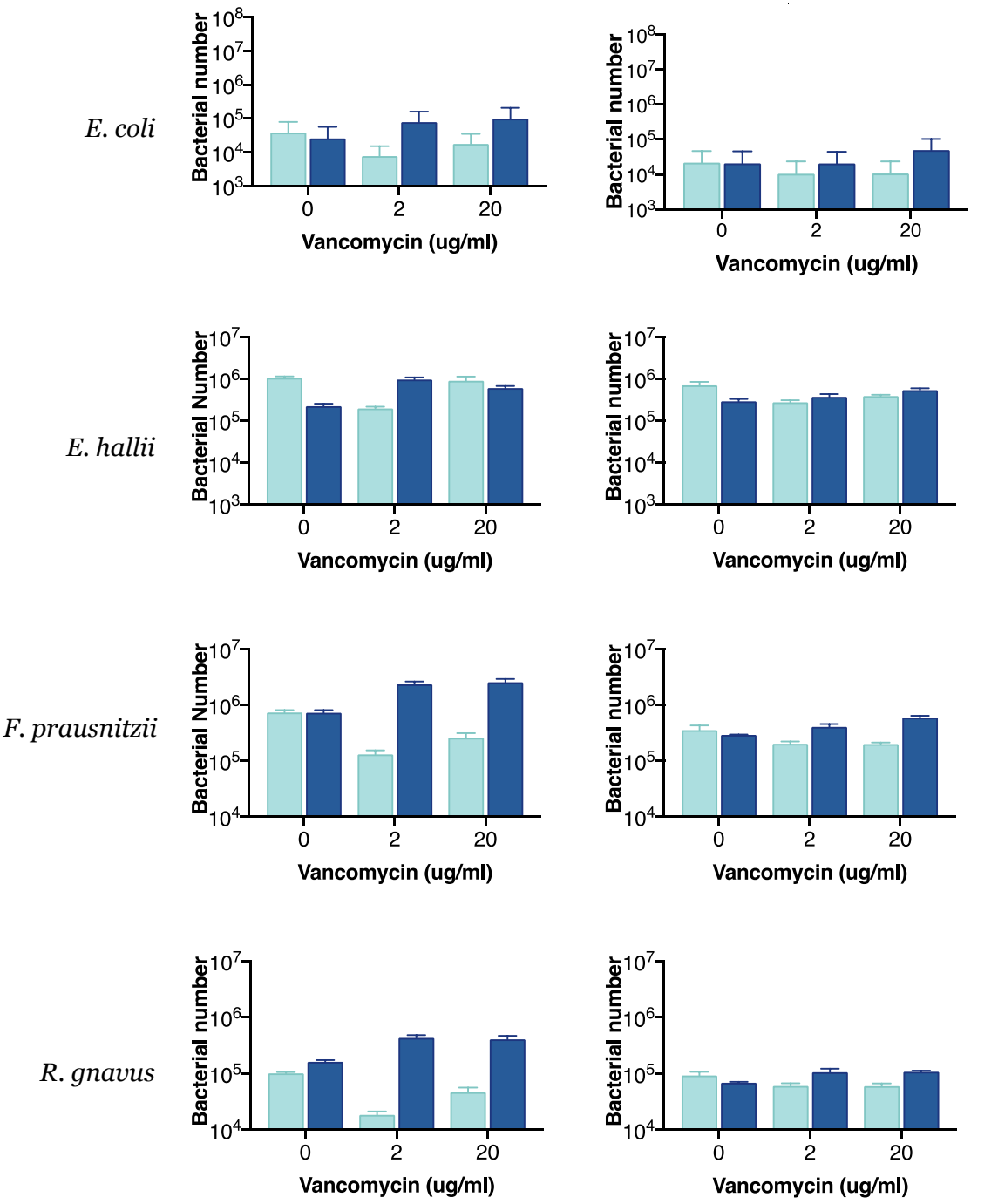

Figure 25: **Effect of vancomycin disruption on the microbiota.** A 24-hour pre-established nine species microbiota biofilm was treated with vancomycin and infected with *C. difficile*. A control without *C. difficile* was done to investigate the effect vancomycin has on the microbiota alone. Two concentrations of vancomycin were used 2 and 20 μg/ml. Bacteria numbers were estimated using PMA-qPCR. The data shown is that of three biological repeats.

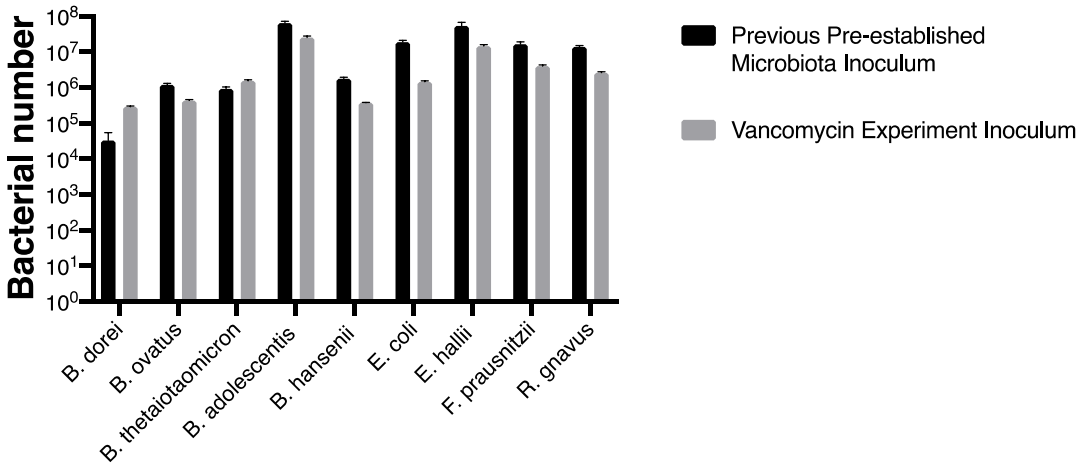

Figure 26: **Starting inoculum between microbiota experiments differ.** We compared the nine species microbiota starting inoculums of two experiments setup using the same methodology. The legend denotes which experiment; the pre-established nine species gut microbiota that was tested against *C. difficile*, and the nine species gut microbiota that was used to investigate effect of vancomycin treatments. Both at the inoculum stage should be identical.

6.2.5 Testing the microbiota within a human gut model

In a gut infection there are three main systems in play; the gut microbiota, the infecting pathogen and host cell response. Until now, we have shown the interactions between the microbiota and *C. difficile* in isolation without including any representative of human cells. The gut epithelium interacts closely with immune system and is the first barrier against pathogens. We chose to limit our model to the epithelial layer (Caco-2 and HT29-MTX) with future aims to incorporate an immune cell representative. To do this we utilized the same E-VDC system used to test the interaction between *B. dorei* and *C. difficile* in Chapter 4.

Before testing in the E-VDC we assessed the ability of all nine species to grow in DMEM-10 separately. Individual species were cultured overnight in SAB+, each species was then spun down and resuspended in DMEM-10. Cultures were diluted down to 0.1 OD (5 ml total) and grown within an anaerobic cabinet (37 °C). Each of the individual cultures showed good signs of growth after 24 hours when measured using OD_{600}.

When setting up the inoculum for the E-VDC we elected to dilute the normal 0.1 OD_{600} to 0.01 as during a pilot experiment, we found using 0.1 OD, overwhelmed the epithelial cells quickly reducing their TEER values over 6 hours (Data not shown). To fix this we tried reducing the starting concentration (0.01 OD_{600}). Three conditions were tested in the E-VDC; the nine species microbiota alone, the microbiota with *C. difficile* and a *C. difficile* only culture. In all our PMA-qPCR experiments we tested the microbiota primers against the *C. difficile* monocultures to ensure there was no cross-talk occurring and to act as a general background check, we did this for also *C. difficile* but against the microbiota only condition. Typically, there was no detection or it was above ~35 cycles and was assumed to be noise. In the E-VDC experiment (24 hour time point) we found this not to be this case with the microbiota primers reporting detection in the *C. difficile* monocultures similar to their detection of the actual nine species microbiota mix (Figure 27). This increased background could be the result of epithelial cells being present. The extra DNA in the system may have created a higher background. However, given the *E. coli* low CT value it is more likely that there is cross-talk occurring with the epithelial cells or some form of contamination happened during the experiment. *C. difficile* primers were unable to detect anything in any of the three conditions in the E-VDC at 24 hours. The use of a lower starting inoculum of *C. difficile* was likely leading to an unstable population, a higher inoculum of *C. difficile* is needed for future experiments.

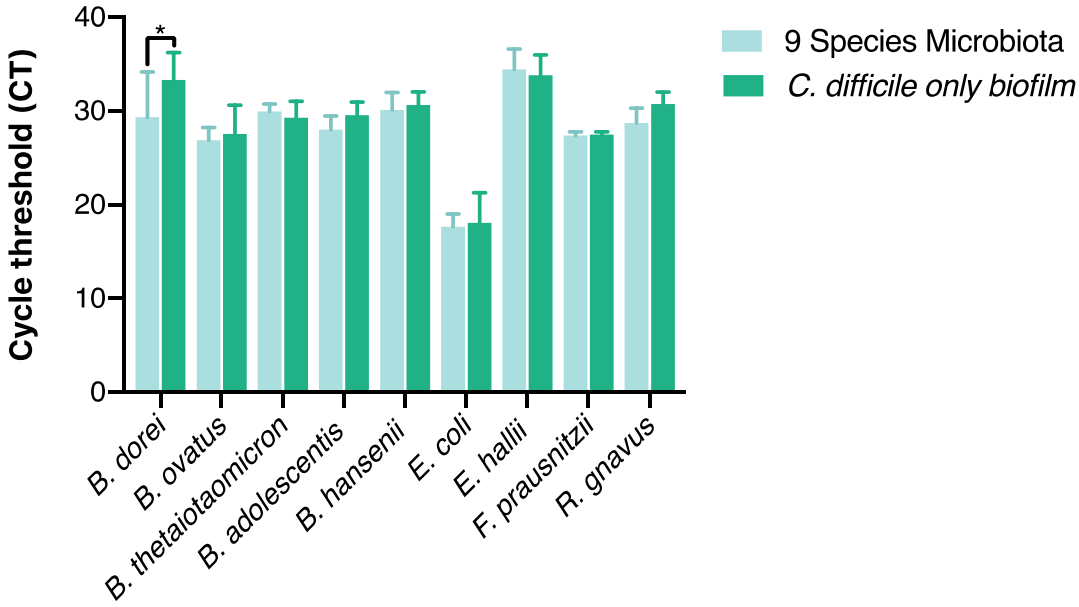

Figure 27: **Primer cross-talk in the E-VDC.** The E-VDC was inoculated with either a nine species microbiota mix or a *C. difficile* monoculture, after 24 hours DNA was extracted from the adherent populations. Each of the nine species primers were tested against the two conditions using PMA-qPCR. A student's unpaired T-tests was used to determin significant differences – *P*-values - * < 0.05.

6.3 Discussion

Using PMA-qPCR we tracked the impact a nine species gut microbiota representative had on *C. difficile*, and the reciprocal effects of *C. difficile* on the microbiota. We explored a biofilm setup seeded with both the microbiota and *C. difficile* simultaneously. Studying the initial binding over the first six hours revealed two major results. The first was that the presence of *C. difficile* caused an increase in adhesion for many of the microbiota species (Figure 19). We predict that *C. difficile* is likely either producing a metabolic bi-product that improves initial growth and binding for species in the microbiota, or detection of *C. difficile* is inducing a metabolic shift within these species. Increased biofilm formation by *Bacteroidetes* species when cultured with *C. difficile* has been previously observed (Anonye *et al.*, 2019; Slater *et al.*, 2019). Comparing the RNA expression of *B. fragilis* with and without *C. difficile* showed that *B. fragilis* is highly influenced by the presence of *C. difficile* (Slater *et al.*, 2019). Little to no research has been carried out on the effect *C. difficile* has on the initial adherent stage of a biofilm. Further studies using *C. difficile* are

necessary to establish whether soluble factors are involved in the increased adherence observed, or whether this is a metabolic effect.

The second result we saw was a reduction in the initial adhesion of *C. difficile* when cultured with the microbiota, compared with a monoculture control (Figure 19). This reduction was expected, as there is a wealth of data on the microbiota's disruptive effect on *C. difficile* colonisation (Britton and Young, 2012; Pérez-Cobas *et al.*, 2015). However, the reduction we see is small, roughly half the number of cells appear to adhere when the microbiota is present. Later time points of this experiment, on the other hand, do show a bigger influence of the microbiota (Figure 20), with *C. difficile* numbers dropping by over 10-fold. Normally an infecting *C. difficile* is competing with an established microbiota, the low levels of bacteria we saw at the initial adherent stage may not be enough to effectively inhibit *C. difficile*, but as they reached higher numbers the colonisation resistance effect could establish itself. There were no bile acids in our media, meaning any inhibition of *C. difficile* was not through the conversion of primary to secondary bile acids but via another method. The germination prevention and secondary bile acid inhibition argument for colonisation resistance appears to be only part of the mechanism.

The microbiota tracked alongside *C. difficile* showed no significant reductions when compared to a control culture without *C. difficile* (Figure 21). Instead, there was a significant increase in the numbers of; *B. dorei*, *B. ovatus*, *E. coli*, *F. prausnitzii*, and *R. gnavus*. Their improvements, although significant were only small, all below 1-order. In a successful infection, *C. difficile* is thought to control the microbiota by upregulating the production of indole. It does this through influencing the expression of tryptophanase (tnaA) in other species, as *C. difficile* itself does not contain the gene homolog required to make indole. Previous work found increased levels of indole in the faeces of patients suffering from CDI, it is believed that *C. difficile* is using indole's inhibitory effect on bacterial growth to limit the recovery of the microbiota (Darkoh *et al.*, 2019). Of our nine species; *B. ovatus*, *B. thetaiotaomicron* (Teng *et al.*, 2004), *B. adolescentis* (Aragozzini *et al.*, 1979), *E. coli* (Darkoh *et al.*, 2019)

and *F. prausnitzii* (Berstad, Raa and Valeur, 2015) are all indole producers yet no inhibitory effects were seen. Given *C. difficile* was inhibited, we theorise that it was unable to reach sufficient numbers to influence indole production. It would be interesting to see the effect of a pre-established *C. difficile* biofilms response to the addition of our microbiota, and whether indole becomes a factor. At 72 hours we saw a decrease across all species both with and without *C. difficile*, as highlighted in the last chapter we believe this was a spent media issue, which we aim to solve in the future with the use of fluidics.

As we previously highlighted, a healthy microbiota would already be well-established on the mucus/epithelial layer before a *C. difficile* infection, and so to better mimic physiological conditions we established the nine species microbiota biofilm 24 hours prior to infecting with *C. difficile*. We found that the pre-established microbiota had a more substantial impact on *C. difficile* growth (Figure 22A & B). Pre-establishing the microbiota could have numerous effects on *C. difficile* ability to adhere and grow. The increased abundance of the microbiota bacteria would likely mean any secreted inhibitory molecules would be in higher numbers, space for *C. difficile* to adhere would be far less abundant and any nutrients *C. difficile* needs could already be taken out of the media by this stage. From a microbiota perspective, after the addition of *C. difficile*, we saw an increase in *E. coli* numbers compared to an uninfected control (Figure 23). This increase is usually a characteristic of a successful *C. difficile* infection with an overabundance of *Proteobacteria* often found in CDI patients (Weingarden *et al.*, 2013; Fuentes *et al.*, 2014; Dong *et al.*, 2018). However, here we had a highly inhibited *C. difficile* still able to bring about a similar increase. In chapter 4, we outlined the inhibitory qualities of several Bacteroidetes species on *C. difficile*, and the associated loss in abundance and diversity with a successful *C. difficile* infection. We also showed how culturing *B. dorei* with *C. difficile* showed an increase in *B. dorei* numbers (Anonye *et al.*, 2019), matching similar work done with *B. fragilis* (Slater *et al.*, 2019). In both our simultaneous and pre-established microbiota-*C. difficile* experiments we saw this same increase in abundance across all the Bacteroidetes species (*B. dorei*, *B. ovatus* and *B. thetaiotaomicron*) with the addition of *C. difficile*. This dynamic between

Bacteroidetes and *C. difficile* is interesting, as without a prior microbiota disturbance *C. difficile* is unable to bring about a depletion in Bacteroidetes numbers, but instead reinforces Bacteroidetes dominance by improving growth. Other markers of a healthy gut also shared this unexpected benefit from being cultured with *C. difficile* such as *B. adolescentis* (Figure 23) and *F. prausnitzii* (Figure 21). In a healthy state, we have demonstrated that the gut microbiota representative is enough to resist a *C. difficile* infection, even without epithelial and immune cells present.

To mimic the antibiotic-induced dysbiosis state of the microbiota during a CDI, we disrupted the microbiota using vancomycin (Lewis *et al.*, 2015). We hypothesized that disrupting the microbiota would allow *C. difficile* to establish itself better and overcome the inhibition from the microbiota. We observed that *C. difficile,* in the presence of the microbiota, performed better than its monoculture counterpart (Figure 24). However, this is not because *C. difficile* was doing better with the microbiota; bacterial numbers in both concentrations of vancomycin were comparable to the untreated control. Instead, we found that the monoculture performs poorly with antibiotic treatment. This result is similar to that reported by Crowther *et al.*, 2014, where using an *in vitro* gut chemostat model they tested vancomycin against *C. difficile* and a faecal emulsion, they found that in the presence of the microbiota *C. difficile* performed better than in monoculture. They argue that the microbiota biofilm provides a safe haven for *C. difficile* and could act as a reservoir for repeat infection.

All metagenomics studies on vancomycin and the gut microbiota in humans have indicated a reduction in the diversity and overall bacterial numbers (Haak *et al.*, 2018; Bhalodi *et al.*, 2019; Khan *et al.*, 2019). The result we saw contradicted this; at both 2 and 20 μg/ml we see a stable microbiota with all nine species present (Figure 25). Metagenomic studies have focused on faecal samples, which consist primarily of bacteria from the lumen and are in a free-form or planktonic state, differing from the mucus-associated/adherent bacteria (Zoetendal *et al.*, 2002). Planktonic/free bacteria are much more susceptible compared to their biofilm counterpart. This leads us to question

the state of the microbiota attached to the mucus layer of the gut epithelium. Our results imply that the microbiota may be more intact after vancomycin treatment than was previously thought.

The addition of *C. difficile* to the vancomycin experiments caused more disturbances than in previous experiments. This was also the case for the untreated vancomycin controls too (Figure 25 , which should have mimicked our prior pre-established microbiota and *C. difficile* experiments (Figure 21). We found that our starting inoculum differed to the previous experiment, with multiple species showing higher abundance in our earlier work. This alteration in starting numbers appears to make microbiota less stable when infected with *C. difficile*. For *B. dorei* and *B. adolescentis* this led to a drop-in numbers below that of the PMA-qPCR detection limit. Time constraints meant all biological replicates for the vancomycin experiments were carried out on the same day. We believe a mistake was made with the experiment, which affected the starting inoculum on this day. With respect to the microbiota species that remained stable even after the altered inoculum, *C. difficile* yet again provided a beneficial effect for them as they increased in numbers, especially when treated with vancomycin.

The microbiota in all three conditions (simultaneous, pre-established and vancomycin treated) saw a positive effect on growth when cultured with *C. difficile*. We are left with the question, is *C. difficile* beneficial to the gut microbiota when kept in low number? There are a proportion of people who are asymptomatic carriers of *C. difficile*. Studies have put this number somewhere between 0–17.5% for healthy adults (Ozaki *et al.*, 2004; Terveer *et al.*, 2017; Schäffler and Breitrück, 2018), for these people *C. difficile* could be having a positive effect on their gut microbiota.

We took our microbiota work a step further to investigate the effect of introducing this microbiota into our epithelial gut model. Unfortunately, in our preliminary studies, we discovered what appeared to be cross-talk when we tested the microbiota primers against a negative control (*C. difficile* monoculture) (Figure 27). For the PMA-qPCR quantification to work, it relies

on the assumption that primers are specific to the species they are quantifying, any cross-talk will ruin the accuracy of the quantification. Given until now, there have been no issues we believe the cross-talk came from the gut epithelial cells or contamination across the E-VDCs. Further work needs to be performed to understand why the cross-reactivity is occurring before the microbiota can be tracked in the E-VDC.

In the future we wish to further investigate the initial binding benefit *C. difficile* provides for the microbiota. We plan to test spent cell-free media from a *C. difficile* six-hour biofilm, to see if it gives any improved growth or binding. If improvements are seen, it strengthens the idea of a purely metabolic based benefit. Metabolomics could be used to find differences between spent and fresh media to isolate what beneficial compound *C. difficile* is providing.

Our vancomycin work left several unanswered questions, given that it did not cause the dysbiosis we expected. In order to study a successful *C. difficile* infection, we could incorporate a higher dose of vancomycin; however, we would be using concentrations that would be toxic to the human body. Our solution to this is to treat at an earlier timepoint, such as 6 hours. The microbiota biofilm would not be fully formed, meaning the vancomycin treatment would likely have a more significant effect. This disturbance will allow us to investigate how *C. difficile* can colonise a compromised microbiota.

7 Discussion

The anaerobic bacteria that make up the gut microbiota are pivotal to human health. Dysbiosis of the microbiota is associated with a variety of diseases ranging from auto-immune problems to obesity and microbial infections (Ley *et al.*, 2006; Qin *et al.*, 2012; Opazo *et al.*, 2018; Leslie *et al.*, 2019). *C. difficile* is an opportunistic bacterium that is repelled by a healthy gut microbiota; a disturbance to the microbiota caused by antibiotic therapy allows *C. difficile* to colonise the gut. The prevention of *C. difficile* colonisation by the gut microbiota is referred to as colonisation resistance, and although its importance is indisputable, we still have not grasped an understanding of its mechanisms.

The first aim of this project was to investigate the interaction between *C. difficile* and an abundant member of the gut microbiota, *B. dorei*. The Bacteroidetes phylum, in general, is often highly diminished in a successful *C. difficile* infection (Hubert *et al.*, 2014; Mahnic *et al.*, 2017) and specific Bacteroidetes species, other than *B. dorei,* have been shown to inhibit *C. difficile* growth (Rea *et al.*, 2010; Yoon *et al.*, 2017; Mathur *et al.*, 2017; Slater *et al.*, 2019). Prior to our work, no studies on the interaction between *B. dorei* and *C. difficile* had been carried out. We found that *B. dorei* also imparts an inhibitory influence on *C. difficile* growth when in an adherent biofilm coculture. To investigate mechanism underlying this inhibition, we used mass-spectrometry to perform a proteomic study comparing a coculture of the two bacteria to their respective monoculture counterparts. *B. dorei* like another Bacteroides species, *B. fragilis* inhibits *C. difficile* only when in close proximity (biofilm) conditions (Slater *et al.*, 2019). Given this and their close relation, we expected to see a similar metabolic based inhibition. From the *B. dorei* proteomics, we were unable to see any of the metabolic changes found in *B. fragilis*. Generally, none of the more abundant proteins found in the coculture were able to explain the inhibition seen. Owing to time constraints only a rudimental analysis of the data was done, further pathway analyses may reveal better insights into the inhibition mechanism. However, given the poor grouping of the datasets, it likely requires more experimental repeats to obtain the full story. We believe more Bacteroidetes species should be examined for

inhibitory effects on *C. difficile*, as a common mechanism could become apparent.

We interestingly did, however, find from our proteomics data that *C. difficile* had an increased abundance in HpdB, when cultured in the presence of *B. dorei*, as compared to monoculture. This enzyme plays a role in the production of p-cresol, a bacteriostatic that has been shown to negatively affect the gut microbiota (Passmore *et al.*, 2018). However, although HpdB is present, it would be unable to produce p-cresol as the BHIS medium we used does not contain tyrosine, which is required for production (van Leeuwen *et al.*, 2016). This could explain why *B. dorei* is not inhibited by *C. difficile*, like one would expect given the metagenomics on Bacteroidetes inhibition in *C. difficile* infections (Hubert *et al.*, 2014; Mahnic *et al.*, 2017). In the future, we would want to investigate this further by supplementing BHIS medium with tyrosine.

We refined and implemented a gut epithelial infection model using the E-VDC system. We aimed to create a model that incorporates all three of the major elements in a *C. difficile* infection; the epithelial cell layer, *C. difficile* and a microbiota representative. Previous *in vitro* models of *C. difficile* have focused on two of these elements, either *C. difficile* with the epithelial cells or *C. difficile* with the microbiota. We utilized *B. dorei* as a microbiota representative, and we found that in the E-VDC, there is a reduction in the inhibitory effect of *B. dorei* on *C. difficile*. This reduction we believe is either from the presence of gut epithelial cells or the change from BHIS to DMEM-10. If the inhibition was through a nutritional competition, a change in media would impact the effect. *B. dorei* is unable to inhibit *C. difficile* in planktonic conditions this we believe implies a spatial component to the inhibition. Planktonic cultures are more spread than their biofilm counterparts. Taking this into account, the increased area from the uneven epithelial cell layer and lower densities when compared to polystyrene could impact the inhibition. Similar to a change in medium epithelial cells will have a substantial effect of the metabolites available to both the bacteria (Fletcher *et al.*, 2018). To investigate this further, we first plan to test *B. dorei* and *C. difficile* in biofilm conditions using DMEM-10 to confirm whether it has an effect on inhibition. If this is found not to be the case, we

believe it is best to focus on answering how *B. dorei* is inhibiting *C. difficile* in biofilm conditions. Once we have established this mechanism, we will be able to start then strategizing on how the gut epithelial cells could be affecting it.

The gut microbiota is a complex community consisting of over a thousand species (Almeida *et al.*, 2019). Dual species experiments like the *C. difficile-B. dorei* work are useful for discovering novel interactions, but they overlook possible community-based effects. We created a community of nine abundant gut bacteria to reflect a natural microbiota better. We chose to do this rather than employing faecal samples in order to simplify the system and to allow for individual species tracking. Our second principal aim was to implement a PMA-qPCR tracking system. PMA-qPCR had previously only been used for the tracking of species within dental biofilms and food-based pathogen contamination (Loozen *et al.*, 2011; Banihashemi, Dyke and Huck, 2012; Zeng *et al.*, 2016; Luo *et al.*, 2017). We showed that this methodology could track a nine species mixed anaerobic biofilm over 72 hours, reporting relative changes of each species. The tracking system revealed that the nine species are stable together for 72 hours. The predominant techniques used in the field for tracking species of the gut microbiota are genomics and metagenomics. Omics research provides excellent insights into what is present but gives no information on short term dynamics and underlying bacteria interactions. We believe for a small *in vitro* system in which all the species are known, PMA-qPCR is the superior technique, as it provides quicker tracking at a cheaper cost per sample. Further improvements can be made to the PMA-qPCR tracking approach to convert the relative quantification into absolute quantification if needed (Yang, Badoni and Gill, 2011; Barbau-Piednoir *et al.*, 2014).

Utilising PMA-qPCR and the representative nine species microbiota mix allowed us to achieve our final aim of tracking the effect of a *C. difficile* infection on individual species within the gut microbiota over time. We tested three biofilm-based setups; the nine species microbiota and *C. difficile* simultaneously added, the microbiota pre-established before a *C. difficile* infection and the effect of disturbing this pre-established microbiota with

vancomycin. Both simultaneous addition and pre-establishing the gut microbiota had an inhibitory effect on *C. difficile*, with the pre-established microbiota having a more significant impact. Bile acids and salts have been shown to have a considerable impact on *C. difficile* ability to colonise the gut, with the microbiota converting the primary bile acids required for *C. difficile* germination such as taurocholic acid (Wilson, 1983; Sorg and Sonenshein, 2008). The secondary bile acids they convert into can also inhibit *C. difficile* growth (Sorg and Sonenshein, 2010). However, in our medium, there are no bile acids are present, so any inhibition observed is through other mechanisms. Further work should be carried out to understand the basis of this inhibition. In the vancomycin study, for the first time in our work, we observed the microbiota providing a beneficial edge to *C. difficile*. The microbiota acts as safe haven for *C. difficile* protecting it from the antibiotic treatment that negatively impacts the *C. difficile* monocultures, similar work has also demonstrated this result (Crowther *et al.*, 2014a).

Vancomycin is commonly used to treat *C. difficile,* however, it is well documented that vancomycin causes adverse effects on the gut microbiota (Haak *et al.*, 2018). Taking this into consideration, we predicted that vancomycin treatment would disturb the microbiota; however, this was not what we observed. The gut microbiota was stable under both concentrations of the antibiotic (2 and 20 μg/ml). The mixed microbiota biofilm community may be considered to mimic the adherent population found on the mucous/epithelial layer. Previous research on the effect of vancomycin treatment on the gut microbiota has focused on screening faecal samples (Sun *et al.*, 2019; Khan *et al.*, 2019; Tieu *et al.*, 2019). The major bacterial population in faecal samples is thought to be free-form bacteria from the lumen (Herstad *et al.*, 2018; Ingala *et al.*, 2018). Given the stability of our biofilm data when treated with vancomycin, we believe the use of faecal samples may not accurately represent the adherent community. In order to progress our knowledge on the effect of vancomycin treatment on the adherent community, we would recommend a biopsy-based metagenomic approach.

We found for all three of our microbiota and *C. difficile* biofilm communities (Simultaneous, pre-established and vancomycin treated) the gut microbiota mainly benefited from the presence of *C. difficile*. We saw a boost in initial adherence for all species when simultaneously added, and significant improvement in growth at later timepoints for five of the nine species. In the pre-established microbiota, we saw improved growth for four species, which surprisingly were not all consistent with those seen in the simultaneous addition. A control in our vancomycin dissociation experiments, untreated by vancomycin, revealed that alterations in the starting inoculum could have an impact on the stability of the system when infected with *C. difficile*. This control was identical in setup to the pre-established biofilm work, however, the addition of *C. difficile* this time caused the loss of *B. adolescentis* and *B. dorei* from the microbiota. Although, the species which were able to survive the addition of *C. difficile* yet again showed improved growth, especially when treated with vancomycin. There is a population of people who have been colonised with *C. difficile* but are asymptomatic (Terveer *et al.*, 2017), could *C. difficile* be providing a benefit for the gut microbiota in these people? We suspect, at least in our biofilm setup, *C. difficile* is providing a bi-product that is beneficial to the gut microbiota. In the future, we would want to do a metabolic study on the nine species microbiota with *C. difficile* to try to establish what this is.

Current gut epithelial models under-represent the gut microbiota. During my PhD, I aimed to track the representative gut microbiota within the E-VDC system. Unfortunately, primer cross-reactivity occurred when testing against a negative control in the E-VDC. False detection prevents us from accurately quantifying species numbers using PMA-qPCR. If this had been successful, it would have provided a novel microbiota model, incorporating both host and bacterial factors, with its own species tracking tool. The uses of this model would reach far beyond the impact of pathogen invasion and antibiotic treatment that were discussed here. This model could offer a platform for research into gut disease, small molecule effects on the microbiota, how the microbiota initially establishes itself, the viability of bacteriophage treatments for gut pathogens. Further work will be carried out to understand why the

primer cross-reactivity occurred and how we might overcome this to create a reliable and highly useful model.

To conclude, we have successfully created a trackable microbiota biofilm infection model. The qPCR aspect of the tracking system means that the system could easily be expanded to incorporate other pathogens or gut microbiota species, through the addition of species-specific primers. We have demonstrated with this system the inhibitory effect of the gut microbiota on *C. difficile*, as well as the surprising beneficial effect the microbiota receives from *C. difficile*. We developed a gut epithelial model, the E-VDC, which can support the growth of epithelial cells, a gut microbiota representative (*B. dorei*) as well as *C. difficile*. Using this system, we discovered that *B. dorei* inhibits *C. difficile* growth, with epithelial cells possibly influencing the inhibition. The inhibitory effect of *B. dorei* on *C. difficile* growth was also confirmed in biofilm studies. Overall, we believe the E-VDC system can support our nine species microbiota representative, but owing to tracking problems, we were unable to confirm this successfully.

8 Bibliography

Abaci H and Shuler M L 2015 Human-on-a-chip design strategies and principles for physiologically based pharmacokinetics/pharmacodynamics modeling *Integrative Biology* **7** 383–91

Agrawal M, Aroniadis O C, Brandt L J, Kelly C, Freeman S, Surawicz C, Broussard E, Stollman N, Giovanelli A, Smith B, Yen E, Trivedi A, Hubble L, Kao D, Borody T, Finlayson S, Ray A and Smith R 2016 The Long-term Efficacy and Safety of Fecal Microbiota Transplant for Recurrent, Severe, and Complicated Clostridium difficile Infection in 146 Elderly Individuals *Journal of Clinical Gastroenterology* **50** 403–7

Ajami N, Cope J, Wong M, Petrosino J and Chesnel L 2018 Impact of Oral Fidaxomicin Administration on the Intestinal Microbiota and Susceptibility to Clostridium difficile Colonization in Mice *Antimicrob Agents Ch* **62** e02112-17

Alang N and Kelly C R 2015 Weight Gain After Fecal Microbiota Transplantation *Open Forum Infect Dis* **2** ofv004

Almeida A, Mitchell A L, Boland M, Forster S C, Gloor G B, Tarkowska A, Lawley T D and Finn R D 2019 A new genomic blueprint of the human gut microbiota. *Nature*

Ammann T, Bostanci N, Belibasakis G and Thurnheer T 2013 Validation of a quantitative real-time PCR assay and comparison with fluorescence microscopy and selective agar plate counting for species-specific quantification of an in vitro subgingival biofilm model *Journal of Periodontal Research* **48** 517–26

Amrane S, Raoult D and Lagier J-C 2018 Metagenomics, culturomics, and the human gut microbiota *Expert Review of Anti-infective Therapy* 1–3

Anderson M, Sansonetti P J and Marteyn B S 2016 Shigella Diversity and Changing Landscape: Insights for the Twenty-First Century *Front Cell Infect Mi* **6** 45

Anonye B O, Hassall J, Patient J, Detamornrat U, Aladdad A M, Schüller S, Rose F and Unnikrishnan M 2019 Probing Clostridium difficile Infection in Complex Human Gut Cellular Models *Frontiers in Microbiology* **10** 879

Asempa T E and Nicolau D P 2017 Clostridium difficile infection in the elderly: an update on management *Clin Interv Aging* **12** 1799–809

Asensio A, Bella S, Vecchio A, Grau S, Hart W M, Isidoro B, Scotto R, Petrosillo N, Watt M and Nazir J 2015 The impact of Clostridium difficile infection on resource use and costs in hospitals in Spain and Italy: a matched cohort study *Int J Infect Dis* **36** 31–8

Bäckhed F, Fraser C M, Ringel Y, Sanders M E, Sartor R, erman P, Versalovic J, Young V and Finlay B 2012 Defining a healthy human gut microbiome: current concepts, future directions, and clinical applications. *Cell host & microbe* **12** 611–22

Banihashemi A, Dyke M I and Huck P M 2012 Long-amplicon propidium monoazide-PCR enumeration assay to detect viable Campylobacter and Salmonella *J Appl Microbiol* **113** 863–73

Barbau-Piednoir E, Mahillon J, Pillyser J, Coucke W, Roosens N H and Botteldoorn

N 2014 Evaluation of viability-qPCR detection system on viable and dead Salmonella serovar Enteritidis *Journal of Microbiological Methods* **103** 131–7

Bartlett J G, Chang W T, Gurwith M, Gorbach S L and Onderdonk A B 1978 Antibiotic-Associated Pseudomembranous Colitis Due to Toxin-Producing Clostridia *New Engl J Medicine* **298** 531–4

Bartoloni A, Mantella A, Goldstein B P, Dei R, Benedetti M, Sbaragli S and Paradisi F 2013 In-Vitro Activity of Nisin Against Clinical Isolates of Clostridium difficile *J Chemotherapy* **16** 119–21

Bein A, Shin W, Jalili-Firoozinezhad S, Park M, Sontheimer-Phelps A, Tovaglieri A, Chalkiadaki A, Kim H and Ingber D 2018 Microfluidic Organ-on-a-Chip Models of Human Intestine *Cell Mol Gastroenterology Hepatology* **5** 659–68

Bellehumeur C, Boyle B, Charette S J, Harel J, L'Homme Y, Masson L and Gagnon C A 2015 Propidium monoazide (PMA) and ethidium bromide monoazide (EMA) improve DNA array and high-throughput sequencing of porcine reproductive and respiratory syndrome virus identification *Journal of Virological Methods* **222** 182–91

Berges M, Michel A-M, Lassek C, Nuss A M, Beckstette M, Dersch P, Riedel K, Sievers S, Becher D, Otto A, Maaß S, Rohde M, Eckweiler D, Acuña J M, Jahn M, Neumann-Schaal M and Jahn D 2018 Iron Regulation in Clostridioides difficile *Front Microbiol* **9** 3183

Berstad A, Raa J and Valeur J 2015 Indole – the scent of a healthy 'inner soil' *Microb Ecol Health D* **26**

Best E L, Freeman J and Wilcox M H 2012 Models for the study of Clostridium difficile infection *Gut Microbes* **3** 145–67

Bhalodi A A, van Engelen T S, Virk H S and Wiersinga J W 2019 Impact of antimicrobial therapy on the gut microbiome *J Antimicrob Chemoth* **74** i6–15

Bhatia S N and Ingber D E 2014 Microfluidic organs-on-chips *Nature Biotechnology* **32** 760–72

Bongrand C, Koch E J, Moriano-Gutierrez S, Cordero O X, McFall-Ngai M, Polz M F and Ruby E G 2016 A genomic comparison of 13 symbiotic Vibrio fischeri isolates from the perspective of their host source and colonization behavior *The ISME Journal* **10** 2907–17

Booijink C C, Zoetendal E G, Kleerebezem M and de Vos W M 2007 Microbial communities in the human small intestine: coupling diversity to metagenomics. *Future microbiology* **2** 285–95

Bratburd J R, Keller C, Vivas E, Gemperline E, Li L, Rey F E and Currie C R 2018 Gut Microbial and Metabolic Responses to Salmonella enterica Serovar Typhimurium and Candida albicans *Mbio* **9** e02032-18

Breen D M, Rasmussen B A, Côté C D, Jackson M V and Lam T 2013 Nutrient-Sensing Mechanisms in the Gut as Therapeutic Targets for Diabetes *Diabetes* **62** 3005–13

Britton R A and Young V B 2012 Interaction between the intestinal microbiota and host in Clostridium difficile colonization resistance *Trends in Microbiology* **20** 313–9

Burger-van Paassen N, Vincent A, Puiman P J, van der Sluis M, Bouma J, Boehm G, van Goudoever J B, van Seuningen I and Renes I B 2009 The regulation of intestinal mucin MUC2 expression by short-chain fatty acids: implications for epithelial protection *Biochem J* **420** 211–9

Caplin J D, Granados N G, James M R, Montazami R and Hashemi N 2015 Microfluidic Organ-on-a-Chip Technology for Advancement of Drug Development and Toxicology *Advanced Healthcare Materials* **4** 1426–50

de Cárcer D 2018 The human gut pan-microbiome presents a compositional core formed by discrete phylogenetic units *Sci Rep-uk* **8** 14069

Cash H L, Whitham C V, Behrendt C L and Hooper L V 2006 Symbiotic Bacteria Direct Expression of an Intestinal Bactericidal Lectin *Science* **313** 1126–30

CDC 2005 *Severe Clostridium difficile-associated disease in populations previously at low risk--four states, 2005.*

Chang C -W. and Lin M -H. 2018 Optimization of PMA-qPCR for Staphylococcus aureus and determination of viable bacteria in indoor air *Indoor Air* **28** 64–72

Chen J, Li Y, Tian Y, Huang C, Li D, Zhong Q and Ma X 2015 Interaction between Microbes and Host Intestinal Health: Modulation by Dietary Nutrients and Gut-Brain-Endocrine-Immune Axis *Current Protein & Peptide Science* **16** 592–603

Chen X, Katchar K, Goldsmith J D, Nanthakumar N, Cheknis A, Gerding D N and Kelly C P 2008 A Mouse Model of Clostridium difficile–Associated Disease *Gastroenterology* **135** 1984–92

Choi W, Yeruva S and Turner J R 2017 Contributions of intestinal epithelial barriers to health and disease *Exp Cell Res* **358** 71–7

Chung H, Pamp S J, Hill J A, Surana N K, Edelman S M, Troy E B, Reading N C, Villablanca E J, Wang S, Mora J R, Umesaki Y, Mathis D, Benoist C, Relman D A and Kasper D L 2012 Gut immune maturation depends on colonization with a host-specific microbiota. *Cell* **149** 1578–93

Clarke T B, vis K, Lysenko E S, Zhou A Y, Yu Y and Weiser J N 2010 Recognition of peptidoglycan from the microbiota by Nod1 enhances systemic innate immunity *Nat Med* **16** 228

Cornely O A, Crook D W, Esposito R, Poirier A, Somero M S, Weiss K, Sears P, Gorbach S and for the Group O-80-004 2012 Fidaxomicin versus vancomycin for infection with Clostridium difficile in Europe, Canada, and the USA: a double-blind, non-inferiority, randomised controlled trial *Lancet Infect Dis* **12** 281–9

Credito K L and Appelbaum P C 2004 Activity of OPT-80, a Novel Macrocycle, Compared with Those of Eight Other Agents against Selected Anaerobic Species *Antimicrob Agents Ch* **48** 4430–4

Crowther G S, Chilton C H, Todhunter S L, Nicholson S, Freeman J, Baines S D and Wilcox M H 2014a Comparison of planktonic and biofilm-associated communities of

Clostridium difficile and indigenous gut microbiota in a triple-stage chemostat gut model *Journal of Antimicrobial Chemotherapy* **69** 2137–47

Crowther G S, Chilton C H, Todhunter S L, Nicholson S, Freeman J, Baines S D and Wilcox M H 2014b Development and Validation of a Chemostat Gut Model To Study Both Planktonic and Biofilm Modes of Growth of Clostridium difficile and Human Microbiota *Plos One* **9** e88396

Crowther G S, Wilcox M H and Chilton C H 2016 Clostridium difficile, Methods and Protocols 223–34

Dabard J, Bridonneau C, Phillipe C, Anglade P, Molle D, Nardi M, Ladiré M, Girardin H, Marcille F, Gomez A and Fons M 2001 Ruminococcin A, a New Lantibiotic Produced by aRuminococcus gnavus Strain Isolated from Human Feces *Appl Environ Microb* **67** 4111–8

Đapa T, Dapa T, Leuzzi R, Ng Y K, Baban S T, Adamo R, Kuehne S A, Scarselli M, Minton N P, Serruto D and Unnikrishnan M 2013 Multiple Factors Modulate Biofilm Formation by the Anaerobic Pathogen Clostridium difficile *Journal of Bacteriology* **195** 545–55

D'Argenio V and Salvatore F 2015 The role of the gut microbiome in the healthy adult status *Clinica Chimica Acta* **451** 97–102

Darkoh C, Odo C and DuPont H L 2016 Accessory Gene Regulator-1 Locus Is Essential for Virulence and Pathogenesis of Clostridium difficile *Mbio* **7** e01237-16

Darkoh C, Plants-Paris K, Bishoff D and DuPont H L 2019 Clostridium difficile Modulates the Gut Microbiota by Inducing the Production of Indole, an Interkingdom Signaling and Antimicrobial Molecule *mSystems* **4** e00346-18

Deng H, Yang S, Zhang Y, Qian K, Zhang Z, Liu Y, Wang Y, Bai Y, Fan H, Zhao X and Zhi F 2018 Bacteroides fragilis Prevents Clostridium difficile Infection in a Mouse Model by Restoring Gut Barrier and Microbiome Regulation *Frontiers in Microbiology* **9** 2976

DePestel D D and Aronoff D M 2013 Epidemiology of Clostridium difficile Infection *Journal of Pharmacy Practice* **26** 464–75

Deplancke B and Gaskins H 2001 Microbial modulation of innate defense: goblet cells and the intestinal mucus layer. *The American journal of clinical nutrition* **73** 1131S-1141S

Desai M S, ekatz A, Koropatkin N M, Kamada N, Hickey C A, Wolter M, Pudlo N A, Kitamoto S, Terrapon N, Muller A, Young V B, Henrissat B, Wilmes P, Stappenbeck T S, Núñez G and Martens E C 2016 A Dietary Fiber-Deprived Gut Microbiota Degrades the Colonic Mucus Barrier and Enhances Pathogen Susceptibility *Cell* **167** 1339-1353.e21

Deshpande A, Pasupuleti V, Thota P, Pant C, Rolston D D K, Sferra T J, Hernandez A V and Donskey C J 2013 Community-associated Clostridium difficile infection and antibiotics: a meta-analysis *Journal of …* Online: academic.oup.com

Dethlefsen L, Huse S, Sogin M L and Relman D A 2008 The Pervasive Effects of an Antibiotic on the Human Gut Microbiota, as Revealed by Deep 16S rRNA Sequencing *Plos Biol* **6** e280

Sridevi Devaraj, Hemarajata P and Versalovic J 2013 The Human Gut Microbiome and Body Metabolism: Implications for Obesity and Diabetes *Clinical Chemistry* **59** 617–28

Dharmasena M and Jiang X 2018 Isolation of Toxigenic Clostridium difficile from Animal Manure and Composts Being Used as Biological Soil Amendments. *Applied and environmental microbiology* **84**

Diaz C, Seyboldt C and Rupnik M 2018 Non-human *C. difficile* Reservoirs and Sources: Animals, Food, Environment *Updates on Clostridium difficile in Europe, Advances in Microbiology, Infectious Diseases and Public Health Volume 8* pp 227–43

Ditommaso S, Giacomuzzi M, Ricciardi E and Zotti C M 2015 Viability-qPCR for detecting Legionella: Comparison of two assays based on different amplicon lengths *Molecular and Cellular Probes* **29** 237–43

Donaldson G P, Lee M S and Mazmanian S K 2015 Gut biogeography of the bacterial microbiota *Nature Reviews Microbiology* **14** 20–32

Drissi F, Buffet S, Raoult D and Merhej V 2015 Common occurrence of antibacterial agents in human intestinal microbiota *Front Microbiol* **6** 441

Duplantier A J and van Hoek M L 2013 The Human Cathelicidin Antimicrobial Peptide LL-37 as a Potential Treatment for Polymicrobial Infected Wounds *Front Immunol* **4** 143

Eckburg P B, Bik E M, Bernstein C N, Purdom E, Dethlefsen L, Sargent M, Gill S R, Nelson K E and Relman D A 2005 Diversity of the human intestinal microbial flora. *Science (New York, N.Y.)* **308** 1635–8

Edwards A N, Karim S T, Pascual R A, Jowhar L M, Anderson S E and McBride S M 2016 Chemical and Stress Resistances of Clostridium difficile Spores and Vegetative Cells *Frontiers in Microbiology* **7** 1698

Engevik M A, Yacyshyn M, Engevik K A, Wang J, Darien B, Hassett D J, Yacyshyn B R and Worrell R T 2014 Human Clostridium difficile infection: altered mucus production and composition. *Am J Physiology Gastrointest Liver Physiology* **308** G510-24

Falsetta M L, Klein M I, Colonne P M, Scott-Anne K, Gregoire S, Pai C-H, Gonzalez-Begne M, Watson G, Krysan D J, Bowen W H and Koo H 2014 Symbiotic Relationship between Streptococcus mutans and Candida albicans Synergizes Virulence of Plaque Biofilms In Vivo *Infect Immun* **82** 1968–81

Fang K, Jin X and Hong S 2018 Probiotic Escherichia coli inhibits biofilm formation of pathogenic *E. coli* via extracellular activity of DegP *Sci Rep-uk* **8** 4939

FDA 2019 Important Safety Alert Regarding Use of Fecal Microbiota for Transplantation and Risk of Serious Adverse Reactions Due to Transmission of Multi-Drug Resistant Organisms Online: https://www.fda.gov/vaccines-blood-biologics/safety-availability-biologics/important-safety-alert-regarding-use-fecal-microbiota-transplantation-and-risk-serious-adverse

Fetissov S O 2016 Role of the gut microbiota in host appetite control: bacterial

growth to animal feeding behaviour *Nature Reviews Endocrinology* **13** 11–25

Filippo C, Cavalieri D, Paola M, Ramazzotti M, Poullet J, Massart S, Collini S, Pieraccini G and Lionetti P 2010 Impact of diet in shaping gut microbiota revealed by a comparative study in children from Europe and rural Africa *Proc National Acad Sci* **107** 14691–6

Fittipaldi M, Nocker A and Codony F 2012 Progress in understanding preferential detection of live cells using viability dyes in combination with DNA amplification *Journal of Microbiological Methods* **91** 276–89

Flint H J, Duncan S H, Scott K P and Louis P 2007 Interactions and competition within the microbial community of the human colon: links between diet and health *Environmental Microbiology* **9** 1101–11

Flint H J, Scott K P, Duncan S H, Louis P and Forano E 2012 Microbial degradation of complex carbohydrates in the gut *Gut Microbes* **3** 289–306

Freedberg D E, Toussaint N C, Chen S P, Ratner A J, Whittier S, Wang T C, Wang H H and Abrams J A 2015 Proton Pump Inhibitors Alter Specific Taxa in the Human Gastrointestinal Microbiome: A Crossover Trial *Gastroenterology* **149** 883-885.e9

Freeman J, O'Neill F J and Wilcox M H 2003 Effects of cefotaxime and desacetylcefotaxime upon Clostridium difficile proliferation and toxin production in a triple-stage chemostat model of the human gut *J Antimicrob Chemoth* **52** 96–102

Freter R 1955 The Fatal Enteric Cholera Infection in the Guinea Pig, Achieved by Inhibition of Normal Enteric Flora *J Infect Dis* **97** 57–65

Fujimoto J, Tanigawa K, Kudo Y, Makino H and Watanabe K 2011 Identification and quantification of viable Bifidobacterium breve strain Yakult in human faeces by using strain-specific primers and propidium monoazide *J Appl Microbiol* **110** 209–17

Gaillard-Gendron S, Vignon D, Cottenceau G, Graber M, Zorn N, Dorsselaer A and Pons A 2000 Isolation, purification and partial amino acid sequence of a highly hydrophobic new microcin named microcin L produced by Escherichia coli *Fems Microbiol Lett* **193** 95–8

Garcia-Gutierrez E, Mayer M J, Cotter P D and Narbad A 2018 Gut microbiota as a source of novel antimicrobials *Gut Microbes* **10** 1–57

Gerritsen J, Smidt H, Rijkers G T and de Vos W M 2011 Intestinal microbiota in human health and disease: the impact of probiotics *Genes & Nutrition* **6** 209–40

Gevers D, Knight R, Petrosino J F, Huang K, McGuire A L, Birren B W, Nelson K E, White O, Methé B A and Huttenhower C 2012 The Human Microbiome Project: A Community Resource for the Healthy Human Microbiome *Plos Biol* **10** e1001377

Giel J L, Sorg J A, Sonenshein A L and Zhu J 2010 Metabolism of Bile Salts in Mice Influences Spore Germination in Clostridium difficile *PLoS ONE* **5** e8740

Gill S R, Pop M, DeBoy R T, Eckburg P B, Turnbaugh P J, Samuel B S, Gordon J I, Relman D A, Fraser-Liggett C M and Nelson K E 2006 Metagenomic Analysis of the Human Distal Gut Microbiome *Science* **312** 1355–9

Goodrich J K, Waters J L, Poole A C, Sutter J L, Koren O, Blekhman R, Beaumont M, Van Treuren W, Knight R, Bell J T, Spector T D, Clark A G and Ley R E 2014 Human Genetics Shape the Gut Microbiome *Cell* **159** 789–99

Grass G and Sweetana S 1988 In vitro measurement of gastrointestinal tissue permeability using a new diffusion cell. *Pharmaceutical research* **5** 372–6

Guinane C M and Cotter P D 2013 Role of the gut microbiota in health and chronic gastrointestinal disease: understanding a hidden metabolic organ *Ther Adv Gastroenter* **6** 295–308

Haak B W, Lankelma J M, Hugenholtz F, Belzer C, de Vos W M and Wiersinga J W 2018 Long-term impact of oral vancomycin, ciprofloxacin and metronidazole on the gut microbiota in healthy humans *Journal of Antimicrobial Chemotherapy* **74** 782–6

Hacquard S, Garrido-Oter R, González A, Spaepen S, Ackermann G, Lebeis S, McHardy A C, Dangl J L, Knight R, Ley R and Schulze-Lefert P 2015 Microbiota and Host Nutrition across Plant and Animal Kingdoms *Cell Host Microbe* **17** 603–16

Hall I C and O'Toole E 1935 Intestinal Flora In New-Born Infants: With A Description Of A New Pathogenic Anaerobe, Bacillus Difficilis *Am J Dis Child* **49** 390–402

Haro C, Garcia-Carpintero S, Alcala-Diaz J F, Gomez-Delgado F, Delgado-Lista J, Perez-Martinez P, Zuñiga O A, Quintana-Navarro G M, Landa B B, Clemente J C, Lopez-Miranda J, Camargo A and Perez-Jimenez F 2016 The gut microbial community in metabolic syndrome patients is modified by diet. *The Journal of nutritional biochemistry* **27** 27–31

Harris K G and Chang E B 2018 The intestinal microbiota in the pathogenesis of inflammatory bowel diseases: new insights into complex disease. *Clinical science (London, England : 1979)* **132** 2013–28

Hatayama H, Iwashita J, Kuwajima A and Abe T 2007 The short chain fatty acid, butyrate, stimulates MUC2 mucin production in the human colon cancer cell line, LS174T *Biochem Bioph Res Co* **356** 599–603

Hecht D W, Galang M A, Sambol S P, Osmolski J R, Johnson S and Gerding D N 2007 In Vitro Activities of 15 Antimicrobial Agents against 110 Toxigenic Clostridium difficile Clinical Isolates Collected from 1983 to 2004 ▿ *Antimicrob Agents Ch* **51** 2716–9

Henson M A and Phalak P 2017 Byproduct Cross Feeding and Community Stability in an In Silico Biofilm Model of the Gut Microbiome *Processes* **5** 13

Herstad K, Moen A, Gaby J, Moe L and Skancke E 2018 Characterization of the fecal and mucosa-associated microbiota in dogs with colorectal epithelial tumors *Plos One* **13** e0198342

Hertzberger R, Arents J, Dekker H L, Pridmore D R, Gysler C, Kleerebezem M and de Mattos J M 2014 H2O2 Production in Species of the Lactobacillus acidophilus Group: a Central Role for a Novel NADH-Dependent Flavin Reductase *Appl Environ Microb* **80** 2229–39

Hooper L V and Gordon J I 2001 Commensal Host-Bacterial Relationships in the

Gut *Science* **292** 1115–8

Hooper L V, Stappenbeck T S, Hong C V and Gordon J I 2003 Angiogenins: a new class of microbicidal proteins involved in innate immunity *Nat Immunol* **4** ni888

Huang R, Zhang J, Yang F X and Gregory R L 2015 PCR-Based Multiple Species Cell Counting for In Vitro Mixed Culture *PLOS ONE* **10** e0126628

hubert A, Rogers M A, Ring C, Mogle J, Petrosino J P, Young V B, Aronoff D M and Schloss P D 2014 Microbiome data distinguish patients with Clostridium difficile infection and non-*C. difficile*-associated diarrhea from healthy controls. *mBio* **5** e01021-14

Hugenholtz F and de Vos W M 2018 Mouse models for human intestinal microbiota research: a critical evaluation *Cell Mol Life Sci* **75** 149–60

Huh D, Hamilton G A and Ingber D E 2011 From 3D cell culture to organs-on-chips *Trends in Cell Biology* **21** 745–54

Huh D, Kim H, Fraser J P, Shea D E, Khan M, Bahinski A, Hamilton G A and Ingber D E 2013 Microfabrication of human organs-on-chips *Nature Protocols* **8** 2135–57

Hutton M L, Mackin K E, Chakravorty A and Lyras D 2014 Small animal models for the study of Clostridium difficile disease pathogenesis *Fems Microbiol Lett* **352** 140–9

Hvas C, Jørgensen S, Jørgensen S, Storgaard M, Lemming L, Hansen M, Erikstrup C and Dahlerup J 2019 Fecal Microbiota Transplantation is Superior to Fidaxomicin for Treatment of Recurrent Clostridium difficile Infection *Gastroenterology* **156** 1324-1332.e3

Ingala M R, Simmons N B, Wultsch C, Krampis K, Speer K A and Perkins S L 2018 Comparing Microbiome Sampling Methods in a Wild Mammal: Fecal and Intestinal Samples Record Different Signals of Host Ecology, Evolution *Front Microbiol* **9** 803

Isidro J, Mendes A L, Serrano M, O. Henriques A and Oleastro M 2017 Clostridium Difficile - A Comprehensive Overview

Jakobsson H E, Rodríguez-Piñeiro A M, Schütte A, Ermund A, Boysen P, Bemark M, Sommer F, Bäckhed F, Hansson G C and Johansson M E 2015 The composition of the gut microbiota shapes the colon mucus barrier *EMBO reports* **16** 164–77

Jalili-Firoozinezhad S, Gazzaniga F S, Calamari E L, Camacho D M, Fadel C W, Bein A, Swenor B, Nestor B, Cronce M J, Tovaglieri A, Levy O, Gregory K E, Breault D T, Cabral J, Kasper D L, Novak R and Ingber D E 2019 A complex human gut microbiome cultured in an anaerobic intestine-on-a-chip *Nature Biomedical Engineering* 1–12

Jandhyala S 2015 Role of the normal gut microbiota *World Journal of Gastroenterology* **21** 8787

Jernberg C, Löfmark S, Edlund C and journal J J 2007 Long-term ecological impacts of antibiotic administration on the human intestinal microbiota

Johansson M E, Larsson J M and Hansson G C 2011 The two mucus layers of colon are organized by the MUC2 mucin, whereas the outer layer is a legislator of host–

microbial interactions *Proceedings of the National Academy of Sciences* **108** 4659–65

Jung T-H, Park J, Jeon W-M and Han K-S 2015 Butyrate modulates bacterial adherence on LS174T human colorectal cells by stimulating mucin secretion and MAPK signaling pathway *Nutr Res Pract* **9** 343–9

Kamada N, Kim Y-G, Sham H, Vallance B A, Puente J L, Martens E C and Núñez G 2012 Regulated Virulence Controls the Ability of a Pathogen to Compete with the Gut Microbiota *Science* **336** 1325–9

Kang D-W, ams J, Coleman D M, Pollard E L, Maldonado J, nough-Means S, Caporaso G J and Krajmalnik-Brown R 2019a Long-term benefit of Microbiota Transfer Therapy on autism symptoms and gut microbiota *Scientific Reports* **9** 5821

Kang J D, Myers C J, Harris S C, Kakiyama G, Lee I-K, Yun B-S, Matsuzaki K, Furukawa M, Min H-K, Bajaj J S, Zhou H and Hylemon P B 2019b Bile Acid 7α-Dehydroxylating Gut Bacteria Secrete Antibiotics that Inhibit Clostridium difficile: Role of Secondary Bile Acids *Cell Chem Biol* **26** 27-34.e4

Karjalainen M 2009 Mechanisms of Colonisation and Colonisation Resistance of the Digestive Tract Part 2: Bacteria/Bacteria Interactions *Microb Ecol Health D* **12** 240–6

Kasendra M, Barrile R, Leuzzi R and Soriani M 2014 Clostridium difficile Toxins Facilitate Bacterial Colonization by Modulating the Fence and Gate Function of Colonic Epithelium *J Infect Dis* **209** 1095–104

Kau A L, Ahern P P, Griffin N W, Goodman A L and Gordon J I 2011 Human nutrition, the gut microbiome and the immune system *Nature* **474** 327–36

Keel K, Brazier J S, Post K W, Weese S and Songer G J 2007 Prevalence of PCR Ribotypes among Clostridium difficile Isolates from Pigs, Calves, and Other Species ▿ *J Clin Microbiol* **45** 1963–4

Kelly C P and LaMont T J 2008 Clostridium difficile — More Difficult Than Ever *New Engl J Medicine* **359** 1932–40

Khan T, Hasan M, Azhar E I and Yasir M 2019 Association of gut dysbiosis with intestinal metabolites in response to antibiotic treatment *Human Microbiome Journal*

Kim H, Huh D, Hamilton G and Ingber D E 2012 Human gut-on-a-chip inhabited by microbial flora that experiences intestinal peristalsis-like motions and flow *Lab on a Chip* **12** 2165–74

Kim H and Ingber D E 2013 Gut-on-a-Chip microenvironment induces human intestinal cells to undergo villus differentiation *Integrative Biology* **5** 1130–40

Kim H, Li H, Collins J J and Ingber D E 2016 Contributions of microbiome and mechanical deformation to intestinal bacterial overgrowth and inflammation in a human gut-on-a-chip *Proceedings of the National Academy of Sciences* **113** E7–15

van Kleef E, Green N, Goldenberg S D, Robotham J V, Cookson B, Jit M, Edmunds W J and Deeny S R 2014 Excess length of stay and mortality due to Clostridium difficile infection: a multi-state modelling approach *J Hosp Infect* **88** 213–7

Klein M, Scott-Anne K, Gregoire S, Rosalen P and Koo H 2012 Molecular approaches for viable bacterial population and transcriptional analyses in a rodent model of dental caries. *Molecular oral microbiology* **27** 350–61

Kochan T J, Foley M H, Shoshiev M S, Somers M J, Carlson P E and Hanna P C 2018 Updates to Clostridium difficile Spore Germination *J Bacteriol* **200** e00218-18

Kommerein N, Doll K, Stumpp N S and Stiesch M 2018 Development and characterization of an oral multispecies biofilm implant flow chamber model *Plos One* **13** e0196967

Krajmalnik-Brown R, Ilhan Z-E, Kang D-W and DiBaise J K 2012 Effects of Gut Microbes on Nutrient Absorption and Energy Regulation *Nutrition in Clinical Practice* **27** 201–14

Kuehne S A, Cartman S T, Heap J T, Kelly M L, Cockayne A and Minton N P 2010 The role of toxin A and toxin B in Clostridium difficile infection *Nature* **467** 711

Kuijper E, Coignard B and Tüll P 2006 Emergence of Clostridium difficile-associated disease in North America and Europe *Clin Microbiol Infec* **12** 2–18

LaFrance M E, Farrow M A, Chandrasekaran R, Sheng J, Rubin D H and Lacy B D 2015 Identification of an epithelial cell receptor responsible for Clostridium difficile TcdB-induced cytotoxicity *Proc National Acad Sci* **112** 7073–8

Lange A, Beier S, Steimle A, Autenrieth I B, Huson D H and Frick J-S 2016 Extensive Mobilome-Driven Genome Diversification in Mouse Gut-Associated Bacteroides vulgatus mpk *Genome Biol Evol* **8** 1197–207

Larson H E, Price A B, Honour P and Borriello S P 1978 Clostridium difficile and the ætiology of pseudomembranous colitis *Lancet* **311** 1063–6

Lawley T D, Clare S, Walker A W, Stares M D, Connor T R, Raisen C, Goulding D, Rad R, Schreiber F, Brandt C, Deakin L J, Pickard D J, Duncan S H, Flint H J, Clark T G, Parkhill J and Dougan G 2012 Targeted Restoration of the Intestinal Microbiota with a Simple, Defined Bacteriotherapy Resolves Relapsing Clostridium difficile Disease in Mice *PLoS Pathogens* **8** e1002995

Lawley T D, Croucher N J, Yu L, Clare S, Sebaihia M, Goulding D, Pickard D J, Parkhill J, Choudhary J and Dougan G 2009 Proteomic and Genomic Characterization of Highly Infectious Clostridium difficile 630 Spores *J Bacteriol* **191** 5377–86

Lawson P A, Citron D M, Tyrrell K L and Finegold S M 2016 Reclassification of Clostridium difficile as Clostridioides difficile (Hall and O'Toole 1935) Prévot 1938 *Anaerobe* **40** 95–9

Lee E-S, Lee M-H and Kim B-S 2015 Evaluation of propidium monoazide-quantitative PCR to detect viable Mycobacterium fortuitum after chlorine, ozone, and ultraviolet disinfection *International Journal of Food Microbiology* **210** 143–8

Lee J and Sung J 2013 Organ-on-a-chip technology and microfluidic whole-body models for pharmacokinetic drug toxicity screening *Biotechnology Journal* **8** 1258–66

van Leeuwen P T, van der Peet J M, Bikker F J, Hoogenkamp M A, Paiva A M, Kostidis S, Mayboroda O A, Smits W and Krom B P 2016 Interspecies Interactions between Clostridium difficile and Candida albicans *Msphere* **1** e00187-16

Leffler D A and Lamont J 2015 Clostridium difficile infection. *The New England journal of medicine* **372** 1539–48

Leslie J L, Vendrov K C, Jenior M L and Young V B 2019 The Gut Microbiota Is Associated with Clearance of Clostridium difficile Infection Independent of Adaptive Immunity *Msphere* **4**

Lessa F C, Mu Y, Bamberg W M, Beldavs Z G, Dumyati G K, Dunn J R, Farley M M, Holzbauer S M, Meek J I, Phipps E C, Wilson L E, Winston L G, Cohen J A, Limbago B M, Fridkin S K, Gerding D N and Mcdonald C L 2015 Burden of Clostridium difficile Infection in the United States *The New England Journal of Medicine* **372** 825–34

Lewis B B, Buffie C G, Carter R A, Leiner I, Toussaint N C, Miller L C, Gobourne A, Ling L and Pamer E G 2015 Loss of Microbiota-Mediated Colonization Resistance to Clostridium difficile Infection With Oral Vancomycin Compared With Metronidazole *The Journal of Infectious Diseases* **212** 1656–65

Ley R E, Turnbaugh P J, Klein S and Gordon J I 2006 Microbial ecology: Human gut microbes associated with obesity *Nature* **444** 1022–3

Li D, Chen B, Zhang L, Gaur U, Ma T, Jie H, Zhao G, Wu N, Xu Z, Xu H, Yao Y, Lian T, Fan X, Yang D, Yang M, Zhu Q and Trask J 2016a The musk chemical composition and microbiota of Chinese forest musk deer males *Scientific Reports* **6** 18975

Li D, Wang P, Wang P, Hu X and Chen F 2016b The gut microbiota: A treasure for human health *Biotechnology Advances* **34** 1210–24

Li J, Jia H, Cai X, Zhong H, Feng Q, Sunagawa S, Arumugam M, Kultima J, Prifti E, Nielsen T, Juncker A, Manichanh C, Chen B, Zhang W, Levenez F, Wang J, Xu X, Xiao L, Liang S, Zhang D, Zhang Z, Chen W, Zhao H, Al-Aama J, Edris S, Yang H, Wang J, Hansen T, Nielsen H, Brunak S, Kristiansen K, Guarner F, Pedersen O, Doré J, Ehrlich D S, Pons N, Chatelier E, Batto J-M, Kennedy S, Haimet F, Winogradski Y, Pelletier E, LePaslier D, Artiguenave F, Bruls T, Weissenbach J, Turner K, Parkhill J, Antolin M, Casellas F, Borruel N, Varela E, Torrejon A, Denariaz G, Derrien M, van Vlieg J E, Viega P, Oozeer R, Knoll J, Rescigno M, Brechot C, M'Rini C, Mérieux A, Yamada T, Tims S, Zoetendal E G, Kleerebezem M, de Vos W M, Cultrone A, Leclerc M, Juste C, Guedon E, Delorme C, Layec S, Khaci G, van de Guchte M, Vandemeulebrouck G, Jamet A, Dervyn R, Sanchez N, Blottière H, Maguin E, Renault P, Tap J, Mende D R, Bork P and Wang J 2014 An integrated catalog of reference genes in the human gut microbiome *Nature Biotechnology* **32** 834–41

Li M, van Esch B, Wagenaar G, Garssen J, Folkerts G and Henricks P 2018 Pro- and anti-inflammatory effects of short chain fatty acids on immune and endothelial cells *European Journal of Pharmacology* **831** 52–9

Lloyd-Price J, Abu-Ali G and Huttenhower C 2016 The healthy human microbiome *Genome Medicine* **8** 1–11

Longford S R, Campbell A H, Nielsen S, Case R J, Kjelleberg S and Steinberg P D

2019 Interactions within the microbiome alter microbial interactions with host chemical defences and affect disease in a marine holobiont *Scientific Reports* **9** 1363

Loozen G, Boon N, Pauwels M, Quirynen M and Teughels W 2011 Live/dead real-time polymerase chain reaction to assess new therapies against dental plaque-related pathologies *Mol Oral Microbiol* **26** 253–61

Louie T J, Miller M A, Mullane K M, Weiss K, Lentnek A, Golan Y, Gorbach S, Sears P, Shue Y-K and Group O-80-003 2011 Fidaxomicin versus Vancomycin for Clostridium difficile Infection *New Engl J Medicine* **364** 422–31

Lukeš J, Stensvold C, Jirků-Pomajbíková K and Parfrey L 2015 Are Human Intestinal Eukaryotes Beneficial or Commensals? *Plos Pathog* **11** e1005039

Luo Y, Bolt H L, Eggimann G A, McAuley D F, McMullan R, Curran T, Zhou M, Jahoda C A, Cobb S L and Lundy F T 2017 Peptoid Efficacy against Polymicrobial Biofilms Determined by Using Propidium Monoazide-Modified Quantitative PCR *Chembiochem* **18** 111–8

Lustri B C, Sperandio V and Moreira C G 2017 Bacterial Chat: Intestinal Metabolites and Signals in Host-Microbiota-Pathogen Interactions *Infection and Immunity* **85** e00476-17

Luu M, Weigand K, Wedi F, Breidenbend C, Leister H, Pautz S, Adhikary T and Visekruna A 2018 Regulation of the effector function of CD8+ T cells by gut microbiota-derived metabolite butyrate *Sci Rep-uk* **8** 14430

Macfarlane S and Macfarlane G T 2006 Composition and Metabolic Activities of Bacterial Biofilms Colonizing Food Residues in the Human Gut *Appl Environ Microb* **72** 6204–11

Mahida Y, Makh S, Hyde S, Gray T and Borriello S 1996 Effect of Clostridium difficile toxin A on human intestinal epithelial cells: induction of interleukin 8 production and apoptosis after cell detachment. *Gut* **38** 337

Mahnic A, Rupnik M, Breskvar M, Horvat S and Dzeroski S 2017 Evaluating the effect of Clostridium difficile conditioned medium on fecal microbiota community structure *Scientific Reports* **7** 16448

Manz W, Wagner M, Amann R and Schleifer K-H 1994 In situ characterization of the microbial consortia active in two wastewater treatment plants *Water Research* **28** 1715–23

Marchesi J R, Adams D H, Fava F, Hermes G D, Hirschfield G M, Hold G, Quraishi M N, Kinross J, Smidt H, Tuohy K M, Thomas L V, Zoetendal E G and Hart A 2016 The gut microbiota and host health: a new clinical frontier. *Gut* **65** 330–9

Marsh J W, Arora R, Schlackman J L, Shutt K A, Curry S R and Harrison L H 2012 Association of Relapse of Clostridium difficile Disease with BI/NAP1/027 *J Clin Microbiol* **50** 4078–82

Marzorati M, Vanhoecke B, Ryck T, Sadabad M, Pinheiro I, Possemiers S, den Abbeele P, Derycke L, Bracke M, Pieters J, Hennebel T, Harmsen H J, Verstraete W and de Wiele T 2014 The HMI™ module: a new tool to study the Host-Microbiota Interaction in the human gastrointestinal tract in vitro *BMC Microbiology* **14** 1–14

Maslowski K M, Vieira A T, Ng A, Kranich J, Sierro F, Yu D, Schilter H C, Rolph M S, Mackay F, Artis D, Xavier R J, Teixeira M M and Mackay C R 2009 Regulation of inflammatory responses by gut microbiota and chemoattractant receptor GPR43. *Nature* **461** 1282–6

Mathur H, Fallico V, O'Connor P M, Rea M C, Cotter P D, Hill C and Ross P R 2017 Insights into the Mode of Action of the Sactibiotic Thuricin CD *Front Microbiol* **8** 696

Mazmanian S K, Liu C H, Tzianabos A O and Kasper D L 2005 An immunomodulatory molecule of symbiotic bacteria directs maturation of the host immune system. *Cell* **122** 107–18

McFall-Ngai M J 1999 Consequences of Evolving with Bacterial Symbionts: Insights from the Squid-Vibrio Associations *Annual Review of Ecology and Systematics* **30** 235–56

McFarland L V 2005 Alternative treatments for Clostridium difficile disease: what really works? *Journal of medical microbiology* **54** 101–11

McKee R W, Aleksanyan N, Garrett E M and Tamayo R 2018 Type IV Pili Promote Clostridium difficile Adherence and Persistence in a Mouse Model of Infection *Infect Immun* **86** e00943-17

Megran D 1992 Enterococcal Endocarditis *Clin Infect Dis* **15** 63–71

Millan B, Park H, Hotte N, Mathieu O, Burguiere P, Tompkins T A, Kao D and Madsen K L 2016 Fecal Microbial Transplants Reduce Antibiotic-resistant Genes in Patients With Recurrent Clostridium difficile Infection *Clin Infect Dis* **62** 1479–86

Mills D C, Gundogdu O, Elmi A, Bajaj-Elliott M, Taylor P W, Wren B W and Dorrell N 2012 Increase in Campylobacter jejuni Invasion of Intestinal Epithelial Cells under Low-Oxygen Coculture Conditions That Reflect the In Vivo Environment *Infect Immun* **80** 1690–8

Morgan X C and Huttenhower C 2012 Chapter 12: Human Microbiome Analysis *PLoS Computational Biology* **8** e1002808

Moura I B, Buckley A M, Ewin D, Shearman S, Clark E, Wilcox M H and Chilton C H 2018 Omadacycline Gut Microbiome Exposure Does Not Induce Clostridium difficile Proliferation or Toxin Production in a Model That Simulates the Proximal, Medial, and Distal Human Colon *Antimicrob Agents Ch* **63** e01581-18

Muscogiuri G, Cantone E, Cassarano S, Tuccinardi D, Barrea L, Savastano S, Colao A and and group on behalf of the of nutrition R 2019 Gut microbiota: a new path to treat obesity *Int J Obes Suppl* **9** 10–9

McDonald J, Schroeter K, Fuentes S, Heikamp-deJong I, Khursigara C M, de Vos W M and Allen-Vercoe E 2013 Evaluation of microbial community reproducibility, stability and composition in a human distal gut chemostat model *Journal of Microbiological Methods* **95** 167–74

Nguyen T, Vieira-Silva S, Liston A and Raes J 2015 How informative is the mouse for human gut microbiota research? *Disease Models & Mechanisms* **8** 1–16

Niessen C M 2007 Tight Junctions/Adherens Junctions: Basic Structure and

Function *J Invest Dermatol* **127** 2525–32

Srinivasan B, Kolli A, Esch M, Abaci H, Shuler M L and Hickman J J 2015 TEER Measurement Techniques for In Vitro Barrier Model Systems *Journal of Laboratory Automation* **20** 107–26

Nocker A, Cheung C-Y Y and Camper A K 2006 Comparison of propidium monoazide with ethidium monoazide for differentiation of live vs. dead bacteria by selective removal of DNA from dead cells. *Journal of microbiological methods* **67** 310–20

Nocker A, Sossa-Fernandez P, Burr M D and Camper A K 2007 Use of Propidium Monoazide for Live/Dead Distinction in Microbial Ecology *Applied and Environmental Microbiology* **73** 5111–7

O'Hara A M and Shanahan F 2006 The gut flora as a forgotten organ *EMBO reports* **7** 688–93

Okumura R and Takeda K 2017 Roles of intestinal epithelial cells in the maintenance of gut homeostasis *Experimental & Molecular Medicine* **49** e338

O'Loughlin J L, Samuelson D R, Braundmeier-Fleming A G, White B A, Haldorson G J, Stone J B, Lessmann J J, Eucker T P and Konkel M E 2015 The Intestinal Microbiota Influences Campylobacter jejuni Colonization and Extraintestinal Dissemination in Mice *Appl Environ Microb* **81** 4642–50

Opazo M C, Ortega-Rocha E M, Coronado-Arrázola I, Bonifaz L C, Boudin H, Neunlist M, Bueno S M, Kalergis A M and Riedel C A 2018 Intestinal Microbiota Influences Non-intestinal Related Autoimmune Diseases *Frontiers in Microbiology* **9** 432

Ozaki E, Kato H, Kita H, Karasawa T, Maegawa T, Koino Y, Matsumoto K, Takada T, Nomoto K, Tanaka R and Nakamura S 2004 Clostridium difficile colonization in healthy adults: transient colonization and correlation with enterococcal colonization *J Med Microbiol* **53** 167–72

Passmore I J, Letertre M P, Preston M D, Bianconi I, Harrison M A, Nasher F, Kaur H, Hong H A, Baines S D, Cutting S M, Swann J R, Wren B W and Dawson L F 2018 Para-cresol production by Clostridium difficile affects microbial diversity and membrane integrity of Gram-negative bacteria *Plos Pathog* **14** e1007191

Patzer S, Baquero M, Bravo D, Moreno F and Hantke K 2003 The colicin G, H and X determinants encode microcins M and H47, which might utilize the catecholate siderophore receptors FepA, Cir, Fiu and IroN *Microbiology+* **149** 2557–70

Paulsen I, Banerjei L, Myers G, Nelson K, Seshadri R, Read T, Fouts D, Eisen J, Gill S, Heidelberg J, Tettelin H, Dodson R, Umayam L, Brinkac L, Beanan M, Daugherty S, DeBoy R, Durkin S, Kolonay J, Madupu R, Nelson W, Vamathevan J, Tran B, Upton J, Hansen T, Shetty J, Khouri H, Utterback T, Radune D, Ketchum K, Dougherty B and Fraser C 2003 Role of Mobile DNA in the Evolution of Vancomycin-Resistant Enterococcus faecalis *Science* **299** 2071–4

Peláez T, Alcalá L, Alonso R, Rodríguez-Créixems M, García-Lechuz J and Bouza E 2002 Reassessment of Clostridium difficile Susceptibility to Metronidazole and Vancomycin *Antimicrob Agents Ch* **46** 1647–50

Peng L, Li Z-R, Green R S, Holzman I R and Lin J 2009 Butyrate Enhances the Intestinal Barrier by Facilitating Tight Junction Assembly via Activation of AMP-Activated Protein Kinase in Caco-2 Cell Monolayers *J Nutrition* **139** 1619–25

Peng Z, Jin D, Kim H, Stratton C W, Wu B, Tang Y-W and Sun X 2017 Update on Antimicrobial Resistance in Clostridium difficile: Resistance Mechanisms and Antimicrobial Susceptibility Testing *Journal of Clinical Microbiology* **55** 1998–2008

Pepin J, Saheb N, Coulombe -A M, Alary -E M, Corriveau -P M, Authier S, Leblanc M, Rivard G, Bettez M, Primeau V, Nguyen M, Jacob -E C and Lanthier L 2005 Emergence of Fluoroquinolones as the Predominant Risk Factor for Clostridium difficile-Associated Diarrhea: A Cohort Study during an Epidemic in Quebec *Clin Infect Dis* **41** 1254–60

Pérez-Cobas A, Moya A, Gosalbes M and Latorre A 2015 Colonization Resistance of the Gut Microbiota against Clostridium difficile *Antibiotics* **4** 337–57

Peterfreund G L, Vandivier L E, Sinha R, Marozsan A J, Olson W C, Zhu J and Bushman F D 2012 Succession in the Gut Microbiome following Antibiotic and Antibody Therapies for Clostridium difficile *Plos One* **7** e46966

Peters B M, Jabra-Rizk M, Scheper M A, Leid J G, Costerton J and Shirtliff M E 2010 Microbial interactions and differential protein expression in Staphylococcus aureus –Candida albicans dual-species biofilms *Fems Immunol Medical Microbiol* **59** 493–503

Petrof E O, Gloor G B, Vanner S J, Weese S J, Carter D, Daigneault M C, Brown E M, Schroeter K and Allen-Vercoe E 2012 Stool substitute transplant therapy for the eradication of Clostridium difficile infection: 'RePOOPulating' the gut *Microbiome* **1** 1–12

Pilato V, Freschi G, Ringressi M, Pallecchi L, Rossolini G and Bechi P 2017 The esophageal microbiota in health and disease *Annals of the New York Academy of Sciences* **1381** 21–33

Polk B and Kasper D 1977 Bacteroides fragilis Subspecies in Clinical Isolates *Ann Intern Med* **86** 569

Poon S and Lansdorp P M 2001 Current Protocols in Cell Biology *Current protocols in cell biology / editorial board, Juan S. Bonifacino ... [et al.]* **Chapter 18** 18.4.1-18.4.21

Proctor L M 2011 The Human Microbiome Project in 2011 and Beyond *Cell Host & Microbe* **10** 287–91

Qin J, Li R, Raes J, Arumugam M, Burgdorf K, Manichanh C, Nielsen T, Pons N, Levenez F, Yamada T, Mende D R, Li J, Xu J, Li S, Li D, Cao J, Wang B, Liang H, Zheng H, Xie Y, Tap J, Lepage P, Bertalan M, Batto J-M, Hansen T, Paslier D, Linneberg A, Nielsen B H, Pelletier E, Renault P, Sicheritz-Ponten T, Turner K, Zhu H, Yu C, Li S, Jian M, Zhou Y, Li Y, Zhang X, Li S, Qin N, Yang H, Wang J, Brunak S, Doré J, Guarner F, Kristiansen K, Pedersen O, Parkhill J, Weissenbach J, Consortium M, Antolin M, Artiguenave F, Blottiere H, Borruel N, Bruls T, Casellas F, Chervaux C, Cultrone A, Delorme C, Denariaz G, Dervyn R, Forte M, Friss C, van de Guchte M, Guedon E, Haimet F, Jamet A, Juste C, Kaci G, Kleerebezem M, Knol J, Kristensen M, Layec S, Roux K, Leclerc M, Maguin E, Minardi R, Oozeer R, Rescigno

M, Sanchez N, Tims S, Torrejon T, Varela E, de Vos W, Winogradsky Y, Zoetendal E, Bork P, Ehrlich D S and Wang J 2010 A human gut microbial gene catalogue established by metagenomic sequencing *Nature* **464** 59

Qin J, Li Y, Cai Z, Li S, Zhu J, Zhang F, Liang S, Zhang W, Guan Y, Shen D, Peng Y, Zhang D, Jie Z, Wu W, Qin Y, Xue W, Li J, Han L, Lu D, Wu P, Dai Y, Sun X, Li Z, Tang A, Zhong S, Li X, Chen W, Xu R, Wang M, Feng Q, Gong M, Yu J, Zhang Y, Zhang M, Hansen T, Sanchez G, Raes J, Falony G, Okuda S, Almeida M, LeChatelier E, Renault P, Pons N, Batto J-M, Zhang Z, Chen H, Yang R, Zheng W, Li S, Yang H, Wang J, Ehrlich D S, Nielsen R, Pedersen O, Kristiansen K and Wang J 2012 A metagenome-wide association study of gut microbiota in type 2 diabetes *Nature* **490** 55–60

Ramírez E and Bouza E 2018 Updates on Clostridium difficile in Europe, Advances in Microbiology, Infectious Diseases and Public Health Volume 8 *Advances in experimental medicine and biology* **1050** 1–12

Surawicz C, Brandt L J, Binion D G, Ananthakrishnan A N, Curry S R, Gilligan P H, McFarland L V, Mellow M and Zuckerbraun B S 2013 Guidelines for Diagnosis, Treatment, and Prevention of Clostridium difficile Infections *The American Journal of Gastroenterology* **108** 478

Rea M C, Clayton E, O'Connor P M, Shanahan F, Kiely B, Ross P R and Hill C 2007 Antimicrobial activity of lacticin 3147 against clinical Clostridium difficile strains *J Med Microbiol* **56** 940–6

Rea M C, Sit C S, Clayton E, O'Connor P M, Whittal R M, Zheng J, Vederas J C, Ross P R and Hill C 2010 Thuricin CD, a posttranslationally modified bacteriocin with a narrow spectrum of activity against Clostridium difficile *Proceedings of the National Academy of Sciences* **107** 9352–7

Reading N C and Kasper D L 2011 The Starting Lineup: Key Microbial Players in Intestinal Immunity and Homeostasis *Frontiers in Microbiology* **2** 148

Reygner J, Condette C, Bruneau A, Delanaud S, Rhazi L, Depeint F, Abdennebi-Najar L, Bach V, Mayeur C and Khorsi-Cauet H 2016 Changes in Composition and Function of Human Intestinal Microbiota Exposed to Chlorpyrifos in Oil as Assessed by the SHIME® Model *Int J Environ Res Pu* **13** 1088

Ridaura V K, Faith J J, Rey F E, Cheng J, Duncan A E, Kau A L, Griffin N W, Lombard V, Henrissat B, Bain J R, Muehlbauer M J, Ilkayeva O, Semenkovich C F, Funai K, Hayashi D K, Lyle B J, Martini M C, Ursell L K, Clemente J C, Treuren W, Walters W A, Knight R, Newgard C B, Heath A C and Gordon J I 2013 Gut Microbiota from Twins Discordant for Obesity Modulate Metabolism in Mice *Science* **341** 1241214

Ridlon J M, Kang D J, Hylemon P B and Bajaj J S 2014 Bile acids and the gut microbiome *Current Opinion in Gastroenterology* **30** 332

Rinninella E, Raoul P, Cintoni M, Franceschi F, Miggiano G, Gasbarrini A and Mele M 2019 What is the Healthy Gut Microbiota Composition? A Changing Ecosystem across Age, Environment, Diet, and Diseases *Microorg* **7** 14

Rodriguez-Palacios A and LeJeune J T 2011 Moist-Heat Resistance, Spore Aging, and Superdormancy in Clostridium difficile † *Applied and Environmental Microbiology* **77** 3085–91

Roediger W 1980 Role of anaerobic bacteria in the metabolic welfare of the colonic mucosa in man. *Gut* **21** 793

Rolhion N and Chassaing B 2016 When pathogenic bacteria meet the intestinal microbiota *Phil. Trans. R. Soc. B* **371** 20150504

Rosenberg E and Zilber-Rosenberg I 2016 Microbes Drive Evolution of Animals and Plants: the Hologenome Concept *mBio* **7** e01395-15

Rothschild D, Weissbrod O, Barkan E, Kurilshikov A, Korem T, Zeevi D, Costea P I, Godneva A, Kalka I N, Bar N, Shilo S, Lador D, Vila A, Zmora N, Pevsner-Fischer M, Israeli D, Kosower N, Malka G, Wolf B, Avnit-Sagi T, Lotan-Pompan M, Weinberger A, Halpern Z, Carmi S, Fu J, Wijmenga C, Zhernakova A, Elinav E and Segal E 2018 Environment dominates over host genetics in shaping human gut microbiota *Nature* **555** 210

Round J L and Mazmanian S K 2010 Inducible Foxp3+ regulatory T-cell development by a commensal bacterium of the intestinal microbiota. *Proceedings of the National Academy of Sciences of the United States of America* **107** 12204–9

Round J L and Mazmanian S K 2009 The gut microbiota shapes intestinal immune responses during health and disease *Nature Reviews Immunology* **9** 313–23

Roussel C, Galia W, Leriche F, Chalancon S, Denis S, de Wiele V T and Blanquet-Diot S 2018 Comparison of conventional plating, PMA-qPCR, and flow cytometry for the determination of viable enterotoxigenic Escherichia coli along a gastrointestinal in vitro model *Applied Microbiology and Biotechnology* **102** 9793–802

Rupnik M, Wilcox M H and Gerding D N 2009 Clostridium difficile infection: new developments in epidemiology and pathogenesis. *Nature reviews. Microbiology* **7** 526–36

Saito K, Suzuki R, Koyanagi Y, Isogai H, Yoneyama H and Isogai E 2019 Inhibition of enterohemorrhagic Escherichia coli O157:H7 infection in a gnotobiotic mouse model with pre-colonization by Bacteroides strains *Biomed Reports* **01** 1–8

dos Santos V, Müller M and de Vos W M 2010 Systems biology of the gut: the interplay of food, microbiota and host at the mucosal interface. *Current opinion in biotechnology* **21** 539–50

Schäffler H and Breitrück A 2018 Clostridium difficile – From Colonization to Infection *Frontiers in Microbiology* **09** 646

Schauber J, Svanholm C, Termén S, Iffland K, Menzel T, Scheppach W, Melcher R, erberth, Lührs H and Gudmundsson G 2003 Expression of the cathelicidin LL-37 is modulated by short chain fatty acids in colonocytes: relevance of signalling pathways. *Gut* **52** 735–41

Schloissnig S, Arumugam M, Sunagawa S, Mitreva M, Tap J, Zhu A, Waller A, Mende D R, Kultima J R, Martin J, Kota K, Sunyaev S R, Weinstock G M and Bork P 2013 Genomic variation landscape of the human gut microbiome. *Nature* **493** 45–50

Schüller S and Phillips A D 2010 Microaerobic conditions enhance type III secretion and adherence of enterohaemorrhagic Escherichia coli to polarized human intestinal

epithelial cells *Method Enzymol* **12** 2426–35

Seekatz A M, Wolfrum E, DeWald C M, Putler R, Vendrov K C, Rao K and Young V B 2018 Presence of multiple Clostridium difficile strains at primary infection is associated with development of recurrent disease *Anaerobe* **53** 74–81

Seekatz A M and Young V B 2014 Clostridium difficile and the microbiota *Journal of Clinical Investigation* **124** 4182–9 Online: http://www.jci.org/articles/view/72336

Selimović Š, Dokmeci M R and Khademhosseini A 2013 Organs-on-a-chip for drug discovery *Current Opinion in Pharmacology* **13** 829–33

Sender R, Fuchs S and Milo R 2016 Revised Estimates for the Number of Human and Bacteria Cells in the Body *PLOS Biology* **14** e1002533

Shah P, Fritz J V, Glaab E, Desai M S, Greenhalgh K, Frachet A, Niegowska M, Estes M, Jäger C, Seguin-Devaux C, Zenhausern F and Wilmes P 2016 A microfluidics-based in vitro model of the gastrointestinal human-microbe interface *Nature Communications* **7** 11535

Shahinas D, Silverman M, Sittler T, Chiu C, Kim P, Allen-Vercoe E, Weese S, Wong A, Low D E and Pillai D R 2012 Toward an Understanding of Changes in Diversity Associated with Fecal Microbiome Transplantation Based on 16S rRNA Gene Deep Sequencing *mBio* **3** e00338-12

Sharon G, Sampson T R, Geschwind D H and Mazmanian S K 2016 The Central Nervous System and the Gut Microbiome *Cell* **167** 915–32

Shim K-Y Y, Lee D, Han J, Nguyen N-T T, Park S and Sung J H 2017 Microfluidic gut-on-a-chip with three-dimensional villi structure. *Biomedical microdevices* **19** 37

Slater R T, Frost L R, Jossi S E, Millard A D and Unnikrishnan M 2019 Clostridioides difficile LuxS mediates inter-bacterial interactions within biofilms *Scientific Reports* **9** 9903

Sommer F and Bäckhed F 2013 The gut microbiota — masters of host development and physiology *Nature Reviews Microbiology* **11** 227

Sorg J A and Sonenshein A L 2008 Bile Salts and Glycine as Cogerminants for Clostridium difficile Spores ▿ *Journal of Bacteriology* **190** 2505–12

Sorg J A and Sonenshein A L 2010 Inhibiting the Initiation of Clostridium difficile Spore Germination using Analogs of Chenodeoxycholic Acid, a Bile Acid *J Bacteriol* **192** 4983–90

Sorini C, Cardoso R F, Gagliani N and Villablanca E J 2018 Commensal Bacteria-Specific CD4+ T Cell Responses in Health and Disease *Front Immunol* **9** 2667

Sousa A, Frazão N, Ramiro R S and Gordo I 2017 Evolution of commensal bacteria in the intestinal tract of mice *Curr Opin Microbiol* **38** 114–21

Stabler R A, He M, Dawson L, Martin M, Valiente E, Corton C, Lawley T D, Sebaihia M, Quail M A, Rose G, Gerding D N, Gibert M, Popoff M R, Parkhill J, Dougan G and Wren B W 2009 Comparative genome and phenotypic analysis of Clostridium difficile 027 strains provides insight into the evolution of a hypervirulent bacterium *Genome Biol* **10** R102

Sun L, Zhang X, Zhang Y, Zheng K, Xiang Q, Chen N, Chen Z, Zhang N, Zhu J and He Q 2019 Antibiotic-Induced Disruption of Gut Microbiota Alters Local Metabolomes and Immune Responses *Front Cell Infect Mi* **9** 99

Svec D, Tichopad A, Novosadova V, Pfaffl M W and Kubista M 2015 How good is a PCR efficiency estimate: Recommendations for precise and robust qPCR efficiency assessments *Biomol Detect Quantification* **3** 9–16

Tamburini F B, Andermann T M, Tkachenko E, Senchyna F, Banaei N and Bhatt A S 2018 Precision identification of diverse bloodstream pathogens in the gut microbiome *Nat Med* **24** 1809–14

Tannock G W, Munro K, Taylor C, Lawley B, Young W, Byrne B, Emery J and Louie T 2010 A new macrocyclic antibiotic, fidaxomicin (OPT-80), causes less alteration to the bowel microbiota of Clostridium difficile-infected patients than does vancomycin *Microbiology+* **156** 3354–9

Tantikachornkiat M, Sakakibara S, Neuner M and rall D 2016 The use of propidium monoazide in conjunction with qPCR and Illumina sequencing to identify and quantify live yeasts and bacteria *International Journal of Food Microbiology* **234** 53–9

Tavernier S and Coenye T 2015 Quantification of Pseudomonas aeruginosa in multispecies biofilms using PMA-qPCR *Peerj* **3** e787

Taylor M J, Bentham R H and Ross K E 2014 Limitations of Using Propidium Monoazide with qPCR to Discriminate between Live and Dead Legionella in Biofilm Samples *Microbiology Insights* **7** 15

Teng L-J, Hsueh P-R, Huang Y-H and Tsai J-C 2004 Identification of Bacteroides thetaiotaomicron on the Basis of an Unexpected Specific Amplicon of Universal 16S Ribosomal DNA PCR *J Clin Microbiol* **42** 1727–30

Terveer E M, Crobach M J, Sanders I M, Vos M C, Verduin C M and Kuijper E J 2017 Detection of Clostridium difficile in Feces of Asymptomatic Patients Admitted to the Hospital *J Clin Microbiol* **55** 403–11

Theriot C M and Young V B 2015 Interactions Between the Gastrointestinal Microbiome and Clostridium difficile *Annu Rev Microbiol* **69** 445–61

Thompson L R, Nikolakakis K, Pan S, Reed J, Knight R and Ruby E G 2017 Transcriptional characterization of Vibrio fischeri during colonization of juvenile Euprymna scolopes *Environmental Microbiology* **19** 1845–56

Thurnheer T, Gmür R and Guggenheim B 2004 Multiplex FISH analysis of a six-species bacterial biofilm *Journal of Microbiological Methods* **56** 37–47

Tieu J D, Williams R J, Skrepnek G H and Gentry C A 2019 Clinical outcomes of fidaxomicin vs oral vancomycin in recurrent Clostridium difficile infection *Journal of Clinical Pharmacy and Therapeutics* **44** 220–8

Tramontano M, Andrejev S, Pruteanu M, Klünemann M, Kuhn M, Galardini M, Jouhten P, Zelezniak A, Zeller G, Bork P, Typas A and Patil K 2018 Nutritional preferences of human gut bacteria reveal their metabolic idiosyncrasies *Nature Microbiology* **3** 514–22

Tran S, Billoud L, Lewis S B, Phillips A D and Schüller S 2014 Shiga toxin production and translocation during microaerobic human colonic infection with Shiga toxin-producing E. coli O157:H7 and O104:H4 *Cell Microbiol* **16** 1255–66

Tran S-L, Jenkins C, Livrelli V and Schüller S 2018 Shiga toxin 2 translocation across intestinal epithelium is linked to virulence of Shiga toxin-producing Escherichia coli in humans *Microbiology+* **164** 509–16

Tremaroli V and Bäckhed F 2012 Functional interactions between the gut microbiota and host metabolism *Nature* **489** nature11552

Trzasko A, Leeds J A, Praestgaard J, LaMarche M J and McKenney D 2012 Efficacy of LFF571 in a Hamster Model of Clostridium difficile Infection *Antimicrob Agents Ch* **56** 4459–62

Turnbaugh P J, Hamady M, Yatsunenko T, Cantarel B L, Duncan A, Ley R E, Sogin M L, Jones W J, Roe B A, Affourtit J P, Egholm M, Henrissat B, Heath A C, Knight R and Gordon J I 2008 A core gut microbiome in obese and lean twins *Nature* **457** 480

Vacharaksa A and Finlay B B 2010 Gut Microbiota: Metagenomics to Study Complex Ecology *Current Biology* **20** R569–71

Valdes A M, Walter J, Segal E and Spector T D 2018 Role of the gut microbiota in nutrition and health *BMJ* **361** k2179

Van de Wiele T, Van den Abbeele P, Ossieur W, Possemiers S and Marzorati M 2015 The Simulator of the Human Intestinal Microbial Ecosystem (SHIME®) *The Impact of Food Bioactives on Health, in vitro and ex vivo models* (springer) pp 305–17

Vandeplassche E, Coenye T and Crabbé A 2017 Developing selective media for quantification of multispecies biofilms following antibiotic treatment *PLOS ONE* **12** e0187540

Venema K 2015 The TNO In Vitro Model of the Colon (TIM-2). In: Verhoeckx K. et al. (eds) The Impact of Food Bioactives on Health. *Springer* 293-304

Villenave R, Wales S Q, Hamkins-Indik T, Papafragkou E, Weaver J C, Ferrante T C, Bahinski A, Elkins C A, Kulka M and Ingber D E 2017 Human Gut-On-A-Chip Supports Polarized Infection of Coxsackie B1 Virus In Vitro *PLOS ONE* **12** e0169412

Vonberg R -P., Kuijper E, Wilcox M, Barbut F, Tüll P, Gastmeier P, Broek V P, Colville A, Coignard B, Daha T, Debast S, Duerden B, Hof V S, Kooi V T, Maarleveld H, Nagy E, Notermans D, O'Driscoll J, Patel B, Stone S and Wiuff C 2008 Infection control measures to limit the spread of Clostridium difficile *Clinical Microbiology and Infection* **14** 2–20

Vondrakova L, Turonova H, Scholtz V, Pazlarova J and Demnerova K 2018 Impact of various killing methods on EMA/PMA-qPCR efficacy *Food Control* **85** 23–8

de Vos W M 2015 Microbial biofilms and the human intestinal microbiome *npj Biofilms and Microbiomes* **1** npjbiofilms20155

Vuotto C, Moura I, Barbanti F, Donelli G and Spigaglia P 2016 Subinhibitory concentrations of metronidazole increase biofilm formation in Clostridium difficile

strains *Pathog Dis* **74** ftv114

Wang R, Li H, Yang X, Xue X, Deng L, Shen J, Zhang M, Zhao L and Zhang C 2018 Genetically Obese Human Gut Microbiota Induces Liver Steatosis in Germ-Free Mice Fed on Normal Diet *Front Microbiol* **9** 1602

Warn P, Thommes P, Sattar A, Corbett D, Flattery A, Zhang Z, Black T, Hernandez L D and Therien A G 2016 Disease Progression and Resolution in Rodent Models of Clostridium difficile Infection and Impact of Antitoxin Antibodies and Vancomycin *Antimicrob Agents Ch* **60** 6471–82

Weingarden A R, Chen C, Bobr A, Yao D, Lu Y, Nelson V M, Sadowsky M J and Khoruts A 2013 Microbiota transplantation restores normal fecal bile acid composition in recurrent Clostridium difficile infection. *American journal of physiology. Gastrointestinal and liver physiology* **306** G310-9

Wexler H M 2007 Bacteroides: the Good, the Bad, and the Nitty-Gritty *Clin Microbiol Rev* **20** 593–621

Wiegand P N, Nathwani D, Wilcox M H, Stephens J, Shelbaya A and Haider S 2012 Clinical and economic burden of Clostridium difficile infection in Europe: a systematic review of healthcare-facility-acquired infection *J Hosp Infect* **81** 1–14

Wilcox M H, Ahir H, Coia J E, Dodgson A, Hopkins S, Llewelyn M J, Settle C, Mclain-Smith S and Marcella S W 2017 Impact of recurrent Clostridium difficile infection: hospitalization and patient quality of life. *The Journal of antimicrobial chemotherapy* **72** 2647–56

Williams J, Duckworth C, Burkitt, Watson A, Campbell B and Pritchard D 2015 Epithelial Cell Shedding and Barrier Function *Veterinary Pathology* **52** 445–55

Williamson A, Singh S, Fernekorn U and Schober A 2013 The future of the patient-specific Body-on-a-chip *Lab on a Chip* **13** 3471–80

Wilson K 1983 Efficiency of various bile salt preparations for stimulation of Clostridium difficile spore germination. *J Clin Microbiol* **18** 1017–9

Wilson K and Perini F 1988 Role of competition for nutrients in suppression of Clostridium difficile by the colonic microflora. *Infection and immunity* **56** 2610–4

Wu H-J and Wu E 2012 The role of gut microbiota in immune homeostasis and autoimmunity. *Gut microbes* **3** 4–14

Wu R, Tang X, Kang X, Luo Y, Wang L, Li J, Wu X and Liu D 2019 Effect of a Chinese medical nutrition therapy diet on gut microbiota and short chain fatty acids in the simulator of the human intestinal microbial ecosystem (SHIME) *J Funct Food* **62** 103555

Xu J, Bjursell M K, Himrod J, Deng S, Carmichael L K, Chiang H C, Hooper L V and Gordon J I 2003 A Genomic View of the Human-Bacteroides thetaiotaomicron Symbiosis *Science* **299** 2074–6

Yadav M, Verma M and Chauhan N 2018 A review of metabolic potential of human gut microbiome in human nutrition *Archives of Microbiology* **200** 203–17

Yan H and Ajuwon K M 2017 Butyrate modifies intestinal barrier function in IPEC-

J2 cells through a selective upregulation of tight junction proteins and activation of the Akt signaling pathway *Plos One* **12** e0179586

Yang X, Badoni M and Gill C O 2011 Use of propidium monoazide and quantitative PCR for differentiation of viable Escherichia coli from *E. coli* killed by mild or pasteurizing heat treatments *Food Microbiology* **28** 1478–82

Yasunaga A, Yoshida A, Morikawa K, Maki K, Nakamura S, Soh I, Awano S and Ansai T 2013 Monitoring the prevalence of viable and dead cariogenic bacteria in oral specimens and in vitro biofilms by qPCR combined with propidium monoazide *BMC Microbiology* **13** 1–9

Yasutomi E, Hoshi N, Adachi S, Otsuka T, Kong L, Ku Y, Yamairi H, Inoue J, Ishida T, Watanabe D, Ooi M, Yoshida M, Tsukimi T, Fukuda S and Azuma T 2018 Proton Pump Inhibitors Increase the Susceptibility of Mice to Oral Infection with Enteropathogenic Bacteria *Digest Dis Sci* **63** 881–9

Yatsunenko T, Rey F E, Manary M J, Trehan I, Dominguez-Bello M, Contreras M, Magris M, Hidalgo G, Baldassano R N, Anokhin A P, Heath A C, Warner B, Reeder J, Kuczynski J, Caporaso G J, Lozupone C A, Lauber C, Clemente J, Knights D, Knight R and Gordon J I 2012 Human gut microbiome viewed across age and geography *Nature* **486** 222–7

Ye J, Coulouris G, Zaretskaya I, Cutcutache I, Rozen S and Madden T L 2012 Primer-BLAST: a tool to design target-specific primers for polymerase chain reaction. *BMC bioinformatics* **13** 134

Yin N, Du H, Wang P, Cai X, Chen P, Sun G and Cui Y 2017 Interindividual variability of soil arsenic metabolism by human gut microbiota using SHIME model *Chemosphere* **184** 460–6

Yissachar N, Zhou Y, Ung L, Lai N Y, Mohan J F, Ehrlicher A, Weitz D A, Kasper D L, Chiu I M, Mathis D and Benoist C 2017 An Intestinal Organ Culture System Uncovers a Role for the Nervous System in Microbe-Immune Crosstalk. *Cell* **168** 1135-1148.e12

Yoon S, Yu J, well A, Kim S, You H and Ko G 2017 Bile salt hydrolase-mediated inhibitory effect of Bacteroides ovatus on growth of Clostridium difficile *J Microbiol* **55** 892–9

Zeng D, Chen Z, Jiang Y, Xue F and Li B 2016 Advances and Challenges in Viability Detection of Foodborne Pathogens *Frontiers in Microbiology* **7** 1833

Zheng F, Fu F, Cheng Y, Wang C, Zhao Y and Gu Z 2016 Organ-on-a-Chip Systems: Microengineering to Biomimic Living Systems. *Small (Weinheim an der Bergstrasse, Germany)* **12** 2253–82

Zoetendal E G, von Wright A, Vilpponen-Salmela T, Ben-Amor K, Akkermans A D and de Vos W M 2002 Mucosa-Associated Bacteria in the Human Gastrointestinal Tract Are Uniformly Distributed along the Colon and Differ from the Community Recovered from Feces *Applied and Environmental Microbiology* **68** 3401–7

9 Appendix 1

Code used to remove and replace any “NaN” data from proteomics data.

Coding language used was R Version 3.1.0, no packages required.

```
NaNtotal = 0;
NaNcount1 = 0;
NaNcount2 = 0;
NaNcount3 = 0;
NaNtotal = 0;
NaNcount1 = 0;
NaNcount2 = 0;
NaNcount3 = 0;
deleterow <- c();
NaN_output <- data.frame();
NaN_output <- Original_data[0,];

for (i in 1:358) {
  newcount = 1;
  NaNtotal =0;
  NaNcount1 = 0;
  NaNcount2 = 0;
  NaNcount3 = 0;
  if (Original_data[i,1] == "NaN"){
    NaNcount1 = 1;
  }
  if (Original_data[i,2] == "NaN"){
    NaNcount2 = 1;
  }
  if (Original_data[i,3] == "NaN"){
    NaNcount3 = 1;
  }

  NaNtotal = NaNcount1 + NaNcount2 + NaNcount3;
  if (NaNtotal == 3){
    NaN_output = rbind(NaN_output,Original_data[i,]);
    deleterow <- c(deleterow,i);
    #Add row to table of uncomparables
    #remove row from current table
  }
  if (Original_data[i,4] == "NaN"){
    NaNcount1 = 1;
  }
  if (Original_data[i,5] == "NaN"){
    NaNcount2 = 1;
  }
  if (Original_data[i,6] == "NaN"){
    NaNcount3 = 1;
  }
  NaNtotal = NaNcount1 + NaNcount2 + NaNcount3;
  if (NaNtotal == 3){
    NaN_output = rbind(NaN_output,Original_data[i,]);
    deleterow <- c(deleterow,i);
  }
}
Countrow = length(deleterow);
currentdata <- Original_data;
currentdata <- currentdata[-deleterow,];
curlength = length(currentdata[,1]);
minglobal = min(currentdata[,c(1:6)], na.rm = TRUE );
```

```
for (k in 1:curlength){
  if ((currentdata[k,1] == "NaN") & (currentdata[k,2] == "NaN")){
  } else if ((currentdata[k,1] == "NaN") & (currentdata[k,3] ==
"NaN"))
  } else if ((currentdata[k,2] == "NaN") & (currentdata[k,3] ==
"NaN")){
  }
  else {
    if (currentdata[k,1] == "NaN"){
      currentdata[k,1] = mean(currentdata[k,2],currentdata[k,3])
    }
    if (currentdata[k,2] == "NaN"){
      currentdata[k,2] = mean(currentdata[k,1],currentdata[k,3])
    }
    if (currentdata[k,3] == "NaN"){
      currentdata[k,3] = mean(currentdata[k,2],currentdata[k,1])
    }
  }
  if ((currentdata[k,4] == "NaN") & (currentdata[k,5] == "NaN")){
  } else if ((currentdata[k,4] == "NaN") & (currentdata[k,6] ==
"NaN")){
  } else if ((currentdata[k,5] == "NaN") & (currentdata[k,6] ==
"NaN")){
  }
  else {
    if (currentdata[k,4] == "NaN"){
      currentdata[k,4] = mean(currentdata[k,5],currentdata[k,6])
    }
    if (currentdata[k,5] == "NaN"){
      currentdata[k,5] = mean(currentdata[k,4],currentdata[k,6])
    }
    if (currentdata[k,6] == "NaN"){
      currentdata[k,6] = mean(currentdata[k,5],currentdata[k,4])
    }
  }
}
for (m in 1:curlength){
  for (n in 1:6){

    if (currentdata[m,n] == "NaN") {
      currentdata[m,n] = minglobal;
    }
  }
}

write.table(currentdata, file = "amended.txt", sep = "\t", row.names
= FALSE, col.names = TRUE)
write.table(NaN_output, file = "NaNremoved.txt", sep = "\t", row.names
= FALSE, col.names = TRUE)
```

10 Appendix 2

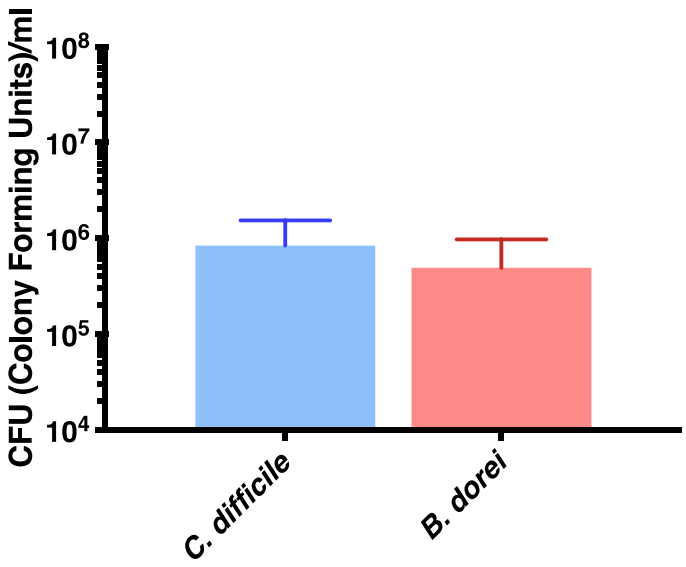

Supp Fig 1: **Inoculum of *C. difficile* and *B. dorei* used in biofilm interaction work.** Data represents the mean of three independent biological experiments in triplicate. Unpaired Student's T-test finds no significant differences between the two.

Supp Table 1 and 2 are found at:
drive.google.com/open?id=1F5D8Cee2aitd7twoX82NV-DBcipE-sCj

Captions:

Supp Table 1: **List of 486 *C. difficile* proteins found by mass-spec in monoculture and coculture conditions.** Proteins listed are those found in at least two repeats in either of the conditions. Predicted contaminant and reverse (repeat) proteins were removed prior to this.

Supp Table 2: **List of 358 *B. dorei* proteins found by mass-spec in monoculture and coculture conditions.** Proteins listed are those found in at least two repeats in either of the conditions. Predicted contaminant and reverse repeat proteins were removed prior to this.